UNIVERSITÁDEGLI STUDI DELL'INSUBRIA

DEPARTMENT OF BIOTECHNOLOGY AND LIFE SCIENCES

PhD course in Life Science and Biotechnology

A new role for HAS2-AS1 as competing endogenous RNA for miR-186-3p in a cellular model of triple-negative breast cancer.

Supervisor: Prof. Davide Vigetti

PhD Thesis by: Arianna Parnigoni

Identification number: 717501

Academic year: 2020/2021

TABLE OF CONTENTS

ABBREVIATIONS

4-MU, 4-methylumbelliferone;

AKT, protein kinase B;

AMPK, adenosine monophosphate-activated protein kinase;

AoSMC, aortic smooth muscle cells;

ATCC, American Type Culture Collection;

CCND1, cyclin D1

CD44s, CD44 standard isoform;

CD44v, CD44 variant;

CEMIP, cell migration inducing hyaluronidase 1;

ceRNA, competing endogenous RNA;

c-Src, tyrosine kinase pp60;

DMEM, Dulbecco's modified Eagle's medium;

ECM, extracellular matrix;

EMT, epithelial-to-mesenchymal transition;

ER, oestrogen receptor;

EREG, epiregulin;

ERK, extracellular signal-regulated kinases;

FAK, focal adhesion kinases;

FBS, foetal bovine serum;

GlcNAc, N-acetyl-glucosamine;

GlcUA, glucuronic acid;

HA, hyaluronan;

HABP, hyaluronan binding protein;

HAS1, 2, 3, hyaluronan synthase 1, 2, 3;

HAS2-AS1 L, exon 2 of HAS2-AS1 long isoform;

HAS2-AS1 S, exon 2 of HAS2-AS1 short isoform;

HAS2-AS1, hyaluronan synthase 2 antisense 1;

HER2, epidermal growth factor receptor 2;

HMWHA, high molecular weight hyaluronan;

HYAL, hyaluronidase;

KEGG, Kyoto Encyclopedia of Genes and Genomes;

lncRNA, long non-coding RNA;

MET, mesenchymal-to-epithelial transition;

MET, mesenchymal-to-epithelial transition;

miRNA, microRNA;

MRE, miRNA responsive element;

MTT, 3-(4,5-dimethylthiazol-2-yl)-2,5-diphenyltetrazo-lium bromide;

ncRNA, non-coding RNA;

NF-κB, nuclear factor kappa-light-chain-enhancer of activated B cells;

PBS, phosphate buffered saline;

PI3K, phosphoinositide 3-kinase;

PR, progesterone receptor;

RHAMM, receptor for HA-mediated motility;

SEM, standard error of the mean;

siRNA, silencing RNA;

TCGA, Cancer Genome Atlas;

TGFβ, transforming growth factor β;

TLR, tool-like receptor;

TNBC, triple-negative breast cancer;

TSG-6, TNF-stimulated gene 6;

TUNEL, terminal deoxynucleotidyl transferase dUTP nick end labelling;

UTR, untranslated region.

ABSTRACT

ABSTRACT

One of the most abundant constituents of the extracellular matrix is hyaluronan (HA). Being distributed almost in all vertebrates' tissues, it plays a crucial role in the regulation of cell behaviours in both physiological and pathological conditions, including cancer.
Tumour progression occurs through the crosstalk between cancer cells signalling networks and host stroma factors such as TGFβ, PDGF-BB and bFGF, all stimulating HA synthesis and creating an HA-rich stroma. Carcinoma cell-associated microenvironment is characterized by aberrant HA levels of a polydisperse size altering the composition and organization of the ECM and playing a key role in creating an environment in which enhanced inflammation and increased angiogenesis sustain cell growth, survival, and metastasis. HA influences cell behaviours through the interaction with CD44 and RHAMM, eventually triggering protein tyrosine kinases, Src, focal adhesion kinase and Erk kinases.

The most aggressive breast cancers are called triple-negative (TNBC), as they lack the expression of oestrogen, progesterone and HER2 receptors. Currently, no efficient targeted therapy is available for TNBCs. Thus, the identification of novel therapeutic targets is of critical importance.

HA and hyaluronan synthase 2 (HAS2) play a crucial role in regulating ER-negative breast cancer cells, as HAS2 silencing or HA synthesis inhibition both reduce tumour aggressiveness.
The natural antisense transcript HAS2-AS1, a long non-coding RNA, is critical to epigenetically control HAS2 transcription and HA synthesis. Since HAS2-AS1 favours cell growth, invasion, and chemotherapy resistance in several cancers, including among others brain, ovary, and lung tumours, its high expression levels generally correlate with a poor tumour prognosis. However, the role of HAS2-AS1 in breast cancers has not yet been thoroughly investigated and the results of this thesis seem to tell a different story.

First, we observed that ER-positive breast cancers had lower HAS2-AS1 expression compared to ER-negative tumours. Moreover, the survival of patients with ER-negative tumours was higher when the expression of HAS2-AS1 was elevated. Experiments with ER-negative cell lines as MDA-MB-231 and Hs 578T revealed that the overexpression of either the full-length HAS2-AS1 or its exon 2 long or short isoforms alone, strongly reduced cell viability, migration, and invasion, whereas HAS2-AS1 silencing increased cell aggressiveness. Unexpectedly, in these ER-negative cell lines, HAS2-AS1 is involved neither in the regulation of HAS2 nor in HA deposition. Transcriptome analysis revealed that HAS2-AS1 modulation affected several pathways, including apoptosis, proliferation, motility, adhesion and signalling, describing this long non-coding RNA as an important regulator of breast cancer cells aggressiveness.

In deep investigation of the molecular mechanisms driving HAS2-AS1 modulation of diverse cancer-related pathways, revealed that HAS2-AS1 can bind and sequestrate miR-186-3p, working as a competing endogenous RNA (ceRNA; sponge effect), thus altering the expression of thousand genes.

Finally, we found a strict involvement of HAS2-AS1 in modulating apoptosis in MDA-MB-231 cells, probably via miR-186-3p sponging, as its target mRNA of the P2RX7 gene was found profoundly induced upon HAS2-AS1 overexpression. Interestingly, also involvement in mesenchymal-to-epithelial transition and cell cycle regulation was suggested by some preliminary results we obtained.

These new scenarios suggest that HAS2-AS1 can be involved in a more complex network of interactions that are critical for several cellular pathways. Nowadays lncRNAs are considered pivotal factors able to alter the landscape of gene expression in many tissues and several of them

have been described to inhibit breast cancer tumorigenesis. In this light, HAS2-AS1 could be considered a new tumour suppressor specific for ER-negative breast cancer.

INTRODUCTION

BREAST CANCER

Breast cancer is a major public health issue worldwide. According to the 2020 estimates, female breast cancer has surpassed lung cancer as the most commonly diagnosed tumour, with 2.3 million new cases (11.7%) of all cancer cases, closely followed by lung (11.4%), colorectal (10.0%), prostate (7.3%), and stomach (5.6%) cancers. Moreover, accounting for 1 in 6 cancer deaths in women, breast cancer ranks first not only for incidence in the vast majority of countries (159 of 185 countries) but also for mortality in 110 countries worldwide [1].

The quite recent decrease in mortality rates both in North America and European Union can be mostly attributable to early detection and efficient systemic therapies. Indeed, after the spreading of mammographic screening, between the 1980s and 1990s it was observed a rapid and uniform increase in breast cancer incidence rates, highlighting the power of such screening method. Its combination with a reduction in the use of menopausal hormone therapy led to an important drop in female breast cancer incidence during the early 2000s [2–4]. However, even if population-wide breast cancer screening programs aim to reduce breast cancer mortality through early detection and effective treatments, establishing primary prevention programs for breast cancer remains a great challenge. Nevertheless, efforts to decrease excess body weight and alcohol consumption and to encourage physical activity and breastfeeding may have an impact in stemming the incidence of breast cancer worldwide [1].

Breast cancer is a very heterogeneous disease, consisting of different entities affecting the same anatomical organ and originating in the same anatomical structure (i.e., the terminal duct-lobular unit). Heterogeneity represents the primary challenge in treating breast cancer [5] – understanding the critical biomarkers, together with their role in carcinogenesis, drug resistance and their use for diagnosis and therapy, is crucial for an effective breast cancer treatment.

The traditional histological classification of breast carcinomas, based on the diversity of the morphological features of the tumours, has as the main drawback that about 80% of all breast cancers will eventually belong to either one of the two major histopathological classes, namely invasive ductal carcinomas, or invasive lobular carcinoma [6]. This implies that tumours having very different biological and clinical profiles are grouped, resulting in minimalised prognostic and predictive capabilities and modest clinical utility.

To compensate for the limited prognostic and predictive power of such histopathological classification of breast carcinomas, in 2000 Perou and colleagues introduced a new way of clustering breast tumours, depending on their gene expression profiles and the presence or

absence of oestrogen receptors (ER), progesterone receptors (PR), and human epidermal growth factor receptor 2 (HER2). In such a way, breast carcinomas can be classified into four main molecular subtypes: luminal A (ER^+ and/or PR^+; $HER2^-$), luminal B (ER^+ and/or PR^+; $HER2^+$), basal-like (ER^-, PR^-, and $HER2^-$) also called triple-negative breast cancer (TNBC), and HER2-enriched (ER^-, PR^-, and $HER2^+$) [7,8] (Fig. 1).

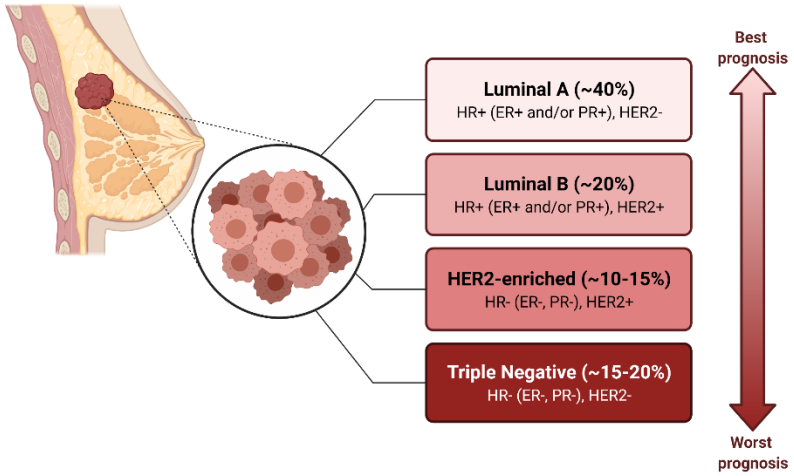

Figure 1. *Molecular subtypes of breast cancer and relative prognosis.*

While surgery is the primary treatment for breast cancer, and chemotherapy and radiation are well established adjuvant therapies, endocrine therapy has revolutionized the general management of breast cancer. Indeed, ER and HER2 are the major targets for breast cancer treatment (using for example tamoxifen and trastuzumab); otherwise, oestrogen synthesis can be blocked using aromatase inhibitors.

Due to the lack of hormone receptors, TNBCs show a more aggressive cellular phenotype and a poorer outcome in terms of survival to ER-positive tumours. Their treatment mainly relies on cytotoxic chemotherapy, which however is inadequate. Therefore, it is essential to concentrate and identify molecular targets for the development of more efficient targeted therapies against TNBC.

1 HYALURONAN

It is well accepted that tumours are not solely made by autonomous cells developing independently. On the contrary, they are cellular masses having strict and complex interactions with their microenvironment [9,10].

Apart from the cancer cells themselves, the tumour niche is composed of both stromal cells, such as fibroblasts, vascular cells, and infiltrating immune cells and of non-cellular compartments, including secreted soluble factors and solid-state structural extracellular matrix (ECM). ECM is a complex yet well-organized three-dimensional architectural network having critical structural and functional roles in many physiological as well as pathological processes [11–17]. It greatly varies among different tissues and consists of a mixture of macromolecules, including collagens, proteoglycans (PGs) and glycosaminoglycans (GAGs), elastin and elastic fibers, laminins, fibronectin, and other proteins/glycoproteins [18]. Moreover, the ECM is rich in a numerous variety of secreted molecules, including growth factors, that through binding to specific ECM molecules and membrane receptors may activate signalling pathways that control or alter cell behaviours. In such a way, the ECM can coordinate multiple inside-out or outside-in commands between cells in organs and tissues [17]. Even in the tumour microenvironment, ECM mediates the communication between cancerous cells and host stromal cells. During cancer progression, these cellular communications dramatically alter the cellular and molecular composition of the tumour niche, to sustain cancer cell proliferation, migration, invasion, and metastasis [19–21].

Hyaluronic acid (HA), a prominent component of the ECM, is an atypical unbranched GAG, as it is not covalently bound to any PG, lacks any chemical modification and is the only one produced outside the Golgi. Indeed, the enzymes involved in HA synthesis are located on the cellular membrane and directly extrude the nascent HA molecule outside of the cells, in the ECM. HA polymer is constituted by repeating disaccharide units of D-glucuronic acid (GlcUA) and N-acetyl-D-glucosamine (GlcNAc), linked together by alternating β-1,4 and β-1,3 glycosidic bonds (Fig. 2) [22].

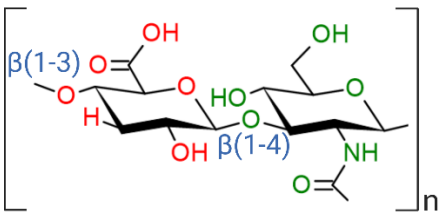

Figure 2. *HA chemical structure, highlighting the β-1,4 and β-1,3 glycosidic bonds connecting the repeating disaccharide units of GlcUA (in red) and GlcNAc (in green).*

Under homeostatic conditions, HA is synthesised as a high molecular weight polymer (HMWHA), with a mass ranging from 1 to 6 MDa. When, instead, the ECM is disrupted due to a pathological condition (i.e., cancer, inflammation, oxidative stress, tissue remodelling, etc.), HMWHA can be

quickly degraded by hyaluronidases (HYALs), cell migration-inducing and hyaluronan-binding protein (CEMIP), transmembrane protein 2 (TMEM2) and reactive oxygen species (ROS), thus generating low molecular weight HA (LMWHA), with a mass even lower than 250 kDa [23,24].

Due to its negative charge at neutral pH, HA attracts water, being capable of containing up to 10,000 times its weight of water, which contributes to the formation of loose and elastic matrices facilitating cellular migration [25]. Therefore, HA plays a key role in promoting tumorigenesis, as it can influence cell behaviours and cancer progression, not only by modulating the hydration and osmotic balance in the tumour environment but also by inducing intracellular signal transductions that can promote the malignant phenotype [14].

HA production is increased in many cancers, most notably in pancreatic carcinomas [26,27] but also in breast [28], colorectal [29], prostate [30], and brain tumours [31] and it is strongly associated with tumour aggressiveness and an unfavourable disease outcome. However, some contradictory observations made in both clinical and experimental studies, suggest that HA may regulate tumour progression in opposite ways, in a context-dependent manner. In fact, it has been observed that reduced levels of HA in patients affected by oral squamous cell carcinoma and stage I melanoma correlated with poor survival [32,33].

1.1 Hyaluronan metabolism

HA is synthesized by three transmembrane isoenzymes, called hyaluronan synthases (HAS1, 2 and 3), sharing about 60–70% identity at the amino acid level [34,35].

An important feature of all HASes is their capability of synthesising HA starting from two UDP-sugar precursors, exploiting the great energy content of the two substrates and, thus, avoiding the need for ATP [34].

Although all three HASs are found in various tumour cell types [36], and both HAS2 and HAS3 expression is correlated with malignant transformation [37], HAS2 is the most efficient HA synthesizing enzyme [38]. Itano and colleagues demonstrated the essential role exerted by both HAS2 expression and stromal HA in sustaining mammary tumour progression: high HAS2 and HA levels were shown to induce the recruitment of tumour-associated macrophages (TAMs) and tumour neovascularization [39,40]. In TNBC cell lines (i.e., MDA-MB-231 and Hs578T) HAS2 mRNA levels are significantly higher with respect to cell lines with less aggressive phenotypes (i.e., MCF-7) [41]. Furthermore, HAS2 has also a pivotal role in regulating cell motility and invasion, as its expression levels are increased in bone metastases compared to parental MDA-MB-231 cells. Finally, breast tumour biopsies showed enhanced angiogenesis and recruitment of inflammatory

cells when HAS2 expression was elevated. In support of these findings, HAS2 suppression by interfering RNA or by 4-methylubelliferone (4-MU) administration reduces tumorigenesis and progression of breast cancer cells [42–45]. These phenomena were accompanied by a reduced HAS2 expression and HA accumulation, induced HYALs activity and substantial loss of the HA receptor CD44.

HAS2 activity is tightly regulated at both transcriptional and post-transcriptional levels. First, the availability of UDP-sugar precursors (i.e., UDP-GlcUA and UDP-GlcNAc) is critical to modulate HAS2 activity and HA deposition. Indeed, 4-MU selectively inhibits HA synthesis by depleting the cytoplasmic GlcUA reservoir [46,47]. To sustain rapid cell growth and division, cancer cells metabolism is not focused on increasing ATP availability. Instead, highly proliferating cells need to focus on the synthesis of cellular building blocks, meaning macromolecules, nucleotides, proteins, lipids and glycans. So, rather than ATP, cancer cells need more carbon skeletons, nitrogen, and NADPH for anabolic reactions [48]. Because of the metabolic reprogramming that cancerous cells undergo during tumour progression (Warburg effect), glycogen metabolism is very efficient in tumour cells, rapidly converting glucose in UDP-glucose. Thanks to UDP-glucose 6-dehydrogenase (UGDH), UDP-glucose is used to finally produce UDP-GlcUA. Similarly, UDP-GlcNAc is derived from another glycolytic intermediate, glucose-6-phosphate via the Hexosamine biosynthetic pathway. These pieces of evidence could provide a possible link between high glucose uptake and excessive accumulation of HA that are observed in several tumours [49–51]

More than being solely a precursor for HA synthesis, GlcNAc is also the substrate for O-GlcNAc transferase (OGT), which has a central role in the regulation of metabolism in response to nutrient availability. OGT transfers GlcNAc moieties to serine 221 of HAS2 protein, increasing its stability in the plasma membrane (up to 5 hours) and thus HA synthesis [52]. Interestingly, O-GlcNAcylation of the NF-κB subunit p65 has a critical function in the induction of HAS2 transcription, involving HAS2-AS1 long non-coding RNA (lncRNA) as a mediator of chromatin remodelling [53].

Interestingly, HAS2 functionality also strictly depends on the energy status of the cells – indeed, adenosine monophosphate-activated protein kinase (AMPK), the sensor of cellular energy level, induces the phosphorylation of HAS2 threonine 110, blocking its enzymatic activity [54]. AMPK generally activates catabolic processes, to restore ATP levels and inhibit ATP consuming pathways (i.e., anabolism). As in tumours, anabolic pathways are preferred to catabolic ones, it is not surprising that AMPK is often found blocked in malignancies. Indeed, liver kinase B1 (LKB1), the

upstream activator of AMPK, has been found mutated in numerous malignancies, thus blocking the AMPK pathway, and favouring HA synthesis [36,55] (Fig. 3).

Other kinases like extracellular-signal-regulated kinases (ERKs) [56] and protein kinase C (PKC) [57] seem to have a role in regulating HAS2 activity. Finally, HAS2 can also form dimers or oligomers upon mono-ubiquitination K190 residue, which has a key role in its activity and, indeed, dimerization [58].

Interestingly, even numerous pro-inflammatory stimuli are involved in the regulation of HA synthesis, among which oxidized low-density lipoprotein (ox-LDL), tumour necrosis factor-alpha (TNFα) [59,60], vitamin D [61] and salicylate [62] have been proved to have a critical role. Moreover, infiltration of inflammatory cells into tumour stroma causes the release of several soluble factors including fibroblast growth factor (FGF), transforming growth factor β (TGFβ), Platelet-Derived Growth Factor-BB (PDGF-BB), hepatocyte growth factor (HGF) that all induce HAS2 expression and, consequently, HA deposition [63].

Notably, in vascular endothelial cells, HAS2 can be degraded via autophagy evoked by nutrient deprivation or mammalian target of rapamycin (mTOR) inhibition [64].

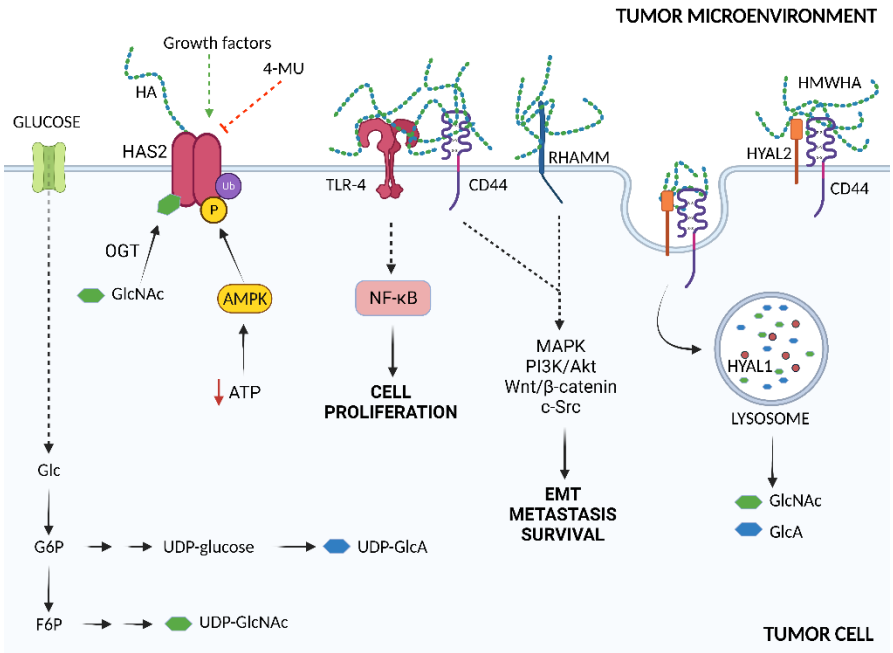

Figure 3. *Overview of HA metabolism and interaction with membrane receptors. Glc, glucose; G6P, glucose-6-phosphate; F6P, Fructose-6-phosphate.*

1.2 Hyaluronan catabolism

The length of HA polymers can vary from the disaccharide unit to thousands of disaccharides [24,65]. This polydisperse sizing of HA mainly depends on the catalytic abilities of HYALs, which are hydrolases that cleave the β-(1,4) linkage between GlcNAc and GlcUA. There are six known HYALs in humans: HYALs 1-4, HYALP and PH-20 [66]. HYALs' degrading activity is not only related to HA - HYAL4, for example, is able to cleave chondroitin sulphate, with no evidence of HA catabolic activity. Among all HYALs, HYAL1 and HYAL2 are the predominant isoforms to cleave HA [67]. At the plasma membrane, HYAL2 chops HMWHA into small fragments that are soon after internalised into the cells via endocytosis and further degrade in the lysosomes by HYAL1. Inside the cells, the complete degradation of HA is completed by the coordinate action of HYALs, β-glucuronidase and hexosaminidase, leading to free GlcUA and GlcNAc [67,68] (Fig. 3). Eventually, GlcUA is converted into xylulose-5-phosphate, which sustains the hexose monophosphate pathway for the synthesis of NADPH and ribose.
Recently, other HA degrading enzymes have been described to have hyaluronidase activity: the hyaluronan binding protein involved in hyaluronan depolymerization (HYBID) and TMEM2 [69,70].

HA catabolism results in the generation of bioactive fragments having contrasting size-dependent functions [71,72]. For instance, HMWHA is known to have anti-angiogenic, anti-proliferative and immunosuppressive features. On the other hand, LMWHA induces inflammation, angiogenesis, had immune-stimulatory functions and induces tissues reparative processes as described in wound healing [24,73]. As proof, naked mole-rat, have been proved to possess HA chains longer than 12 million Da. As a consequence, these animals have an unusually long life, about ten times longer than other rodents, and an incredible resistance to tumour development and spreading, when cancer cells are injected into the dermis [74]. Recently, it was demonstrated that these animals also express very low levels of HYAL1 and HYAL3 [75].

Contrary to what happens in the naked mole rat, tumours typically express high levels of HYALs. Via actively degrading HA, HYALs also contribute to sustaining cancer metabolism and metabolic reprogramming, both providing support to the pentose pathway to obtain reducing equivalents and ribose for anabolism and increasing the glycolytic rate to produce ATP [76].
Combined overexpression of HAS and either HYAL1 [77] or HYAL2 [78] is characteristic of the invasive front of human breast cancer. Similarly, high expression of HYAL2 is significantly increased in premalignant and malignant melanomas [79].

1.3 HA receptors and interactors

The multiple and even contradictory effects that HA polymers of different sizes have can be ascribed by the presence of several HA receptors on the cell surface, that can trigger specific and differential signalling cascades. These receptors are CD44, receptor for hyaluronan-mediated motility (RHAMM), lymphatic vessel endothelial receptor 1 (LYVE-1), HA receptor for endocytosis (HARE), and Toll-like receptors 2 and 4 (TLR2 and 4) [80]. The engagement of these binding partners explains the perturbation of the tissue homeostasis observed during pathological situations, as it derives unbalanced cell motility, proliferation, apoptosis, and tissue remodelling.

The most prominent and almost ubiquitous HA receptor is CD44, which is particularly abundant on inflammatory and cancer cells [81]. CD44 is a single-span transmembrane glycoprotein involved not only in mediating both cell-cell and cell-matrix interactions but is also a key player in transmitting HA signalling in tumour progression [82].

In humans, CD44 is encoded by a single gene that contains 20 exons and generates about 20 variants (CD44v) and possesses different levels of glycosylation. The standard isoform of CD44 (CD44s) is ubiquitously expressed, whereas CD44v are expressed mainly during inflammation and cancer [83] – CD44v6 is highly expressed in lung, breast, ovarian and colon cancer [84–87]. Notably, the switching between CD44s to CD44v exerts a key role in regulating epithelial to mesenchymal transition (EMT) and plasticity of cancer cells [88].

Different breast cancer subtypes express peculiar CD44v – this diversity in CD44v expression has been ascribed to specific clinical markers (i.e., HER2, ER, PR), suggesting the involvement of CD44v in specific oncogenic signalling pathways [89]. Moreover, $CD44^{+}/CD24^{-}$ breast cancer cells subpopulation, typically identified as cancer stem cells, is associated with invasive properties and poor prognosis [90]. In fact, HA/CD44 interaction promotes cytoskeletal remodelling, thus favouring cell growth, survival, invasion and metastasis.

HA/CD44 interaction involves the BX7B HA-binding motif on the N-terminal region of the CD44 receptor which is common to other HA-binding proteins, including RHAMM. HA interaction with CD44 triggers receptor clustering and interaction with other transmembrane proteins, including receptor tyrosine kinases, serine/threonine kinase receptors, tumour necrosis factor receptor (TNFR)-like receptors, G-protein coupled receptors, the Wnt receptor LRP5/6, CD147, and ATP-binding cassette transporters [88,91]. In such a way, the CD44 cytoplasmic domain could be phosphorylated to transduce signals when the ligand binds the extracellular domain. The signalling cascade triggered by HA/CD44 interaction mainly stimulates phosphoinositide 3-kinase/

phosphoinositide-dependent kinase-1/ protein kinase B (PI3K/PDK1/Akt) pathway, Ras phosphorylation cascade involving RAF1, mitogen-activated protein kinase kinase (MEK) and ERK1/2, as well as Wnt/b-catenin and focal adhesion kinases (FAK). Consequently, HA/CD44 interaction stimulates several oncogenic pathways and microRNA (miRNA) functions related mainly to cell adhesiveness, migration, and infiltration [92].

CD44 intracellular domain (CD44ICD) can undergo cleavage and then translocate into the nucleus, acting, at least in part, as a transcriptional regulator [93,94]. In breast cancer, CD44ICD induces the transcription of stemness factors such as Nanog, Sox2 and Oct-4, thus contributing to breast cancer aggressiveness and tumorigenesis [95].

The second most important HA receptor is RHAMM (also known as CD168), a coiled-coil protein that can be found on cell membranes, in the cytoplasm, nucleus or extracellular space. High RHAMM expression has been reported in several tumours, including breast, colon, brain, prostate, and endometrial [96–99]. When binding HA, RHAMM can interact with other receptors such as PDGF receptor (PDGFR), TGFβ receptor I (TGFβRI), and CD44 [83]. As a result, several pathways are induced, including Ras, FAK, ERK1/2, PKC, tyrosine kinase pp60 (c-Src), NF-κB, and PI3K, eventually leading to cell migration, wound healing, tumorigenesis, and EMT [100,101].

A large body of evidence supports the role of TLR2 and 4 in HA signalling. TLRs are membrane receptors typical of the immune system, that are mainly related to inflammation during viral infection and tumorigenesis [102–104]. Recently, it has been demonstrated that HA interaction with both CD44 and TLR4 sustains colon tumorigenesis, via promoting tumour growth in mice [105]. Similarly, HA/TLR4 interaction in glioblastoma provoked cell differentiation via activating NF-κB [106].

Another interesting HA-binding protein is TNF-stimulated gene 6 (TSG-6), which yields the formation of cross-links between HA and the heavy chains of the serine protease inhibitor inter-alpha-inhibitor (IαI), thus stabilizing the structural integrity of ECM. In general, TSG-6 is not a constitutively expressed protein in normal adult tissues, but its expression is upregulated during inflammation and cancer progression [107,108].

In breast cancer, HA TSG-6–crosslinked levels are significantly decreased and associated with tumour malignancy [109]. Moreover, the interaction between HMWHA and TSG-6 affects monocytes/macrophages angiogenic behaviours [108].

2 NON-CODING RNAs

The transcriptional landscape of all organisms is far more complex than what was thought – only 2% of the total 80% transcribed genome is effectively translated into proteins [110]. All the remaining non-translated portion of the genome, the once so-called "junk-DNA", has now been proved to represent the class of non-coding RNAs (ncRNAs), including housekeeping ncRNAs and regulatory RNAs. Depending on their sizes, regulatory ncRNAs can be clustered into small ncRNAs, with less than 200 bp, and lncRNAs, with a length comprised between 200 bp and ~100 kb [111,112] (Fig. 4).

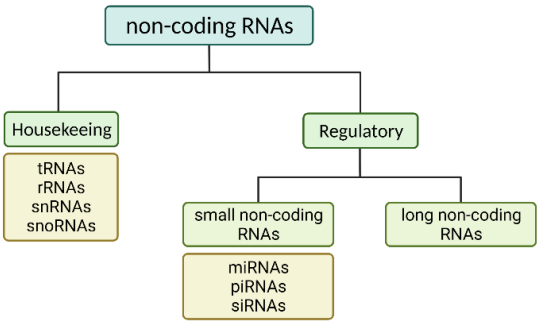

Figure 4. *Classification of non-coding RNAs.*

2.1 MicroRNAs

miRNAs are small ncRNAs, with a length comprised between 19 and 25 nucleotides, which are involved in the regulation of a plethora of target genes/mRNAs. They are involved in almost all biological processes, including those that are essential for cancer progression (i.e., proliferation, differentiation, apoptosis, energetic metabolism, immune response) [113].

miRNA biogenesis begins with the transcription of long primary transcripts (pri-miRNA, up to several kilobases) by polymerase II. pri-miRNAs are subsequently processed in the nucleus by type III RNase Drosha, into shorter stem-loop precursors (pre-miRNA, ~80nt). After being exported from the nucleus into the cytoplasm by Ran/GTP/exportin 5 complex, pre-miRNAs are processed by another RNase III enzyme, called DICER, generating a 20-22nt miRNA/miRNA duplex. At this point, the duplex is unwound into single strands by the action of helicase. Thus, two different miRNAs are generated, called either miR-3p or miR-5p, depending on which pre-miRNA strand they came from. Even if historically miR-5p has been considered the one invested with the mRNA-degrading task, in the last few years more and some miR-3p sequences were reported as guide miRNAs with abundant expression [114–117]. Indeed, the RNA strand with lower stability at the

5'-end will be integrated into the RNA-induced silencing complex (RISC), eventually becoming a mature miRNA. Conversely, the strand having higher stability at the 5'-end is normally degraded. As a final result, the mature miRNA-RISC complex binds to the 3-untranslated region (UTR) of the target mRNA, thus inhibiting its translation [118,119] (Fig. 5).

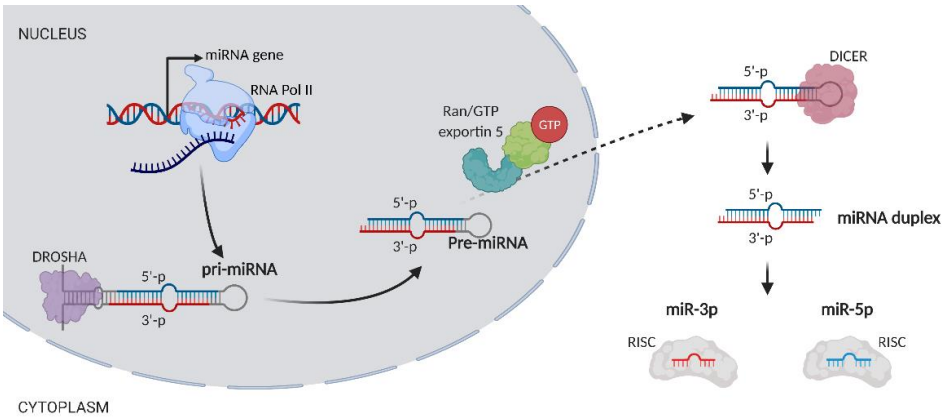

Figure 5. *schematic representation of miRNA biogenesis.*

miRNAs are crucial for normal animal development and, indeed, are involved in a variety of biological processes. Altered miRNA expression is associated with many human diseases, including cancer [120]. As miRNAs are also secreted into extracellular fluids, they have been widely reported as potential biomarkers for cancer types [121,122].

The first evidence of miRNA involvement in human cancer was provided by Croce's group – they found that miR-15a and miR-16-1 were deleted or downregulated in the majority of chronic lymphocytic leukaemias [123]. Further investigations revealed that miR-15 and miR-16-1 act as tumour suppressors to induce apoptosis by repressing Bcl-2, an anti-apoptotic protein overexpressed in malignant non-dividing B cells and other solid tumours [124,125].

Interestingly, the HA/HAS2/CD44 axis has been reported to be involved in the regulation of different miRNAs, thus influencing tumour progression and disease prognosis. As an example, HA/CD44 interaction upregulates miR-21 expression, which, in turn, is found upregulated in diverse cancer types and is currently considered officially an oncogene [126]. Similarly, HA/CD44 interaction has a role in regulating the expression levels of several other miRNAs, including miR-10b and miR-302, finally tunning important oncogenic pathways as chemotherapy resistance, apoptosis, migration, invasion, and metastasis [127].

Notably, an emerging body of evidence highlights the involvement of miRNAs in ECM synthesis – the list includes miR-21, miR-10b, miR-23 and many others [128].

2.2 Long non-coding RNAs

lncRNAs share many features with mRNAs: they are transcribed by polymerase II from genomic loci with similar chromatin state and their transcription require the canonical factors of the transcription machinery; they can have a multi-exonic composition and undergo alternative splicing (although they contain fewer exons compared to mRNA); are capped at the 5' end and polyadenylated [129,130]. However, differently from mRNAs, lncRNAs generally contain fewer but significantly longer codons [131] and lack significant and classical open reading frames (ORFs), initiation and termination codons and 3'-UTR. However, recent advanced technologies have revealed that several lncRNAs encode small peptides (<100 amino acids), which are now becoming appreciated as a new class of functional molecules contributing to multiple cellular processes, and deregulated in different diseases, including breast cancer [132–134].

lncRNAs are less evolutionary conserved compared to mRNAs – indeed, their primary structure seems to be less important when considering their secondary and tertiary structures, instead [135]. Notably, even if lncRNAs are much less expressed than mRNAs, they are more tissue-specific, and their promoters undergo a massive selective pressure [136,137].
According to their location with respect to the nearest protein-coding sequence, lncRNAs can be classified into five subgroups: sense, antisense, bidirectional, intronic and intergenic (Fig. 6).

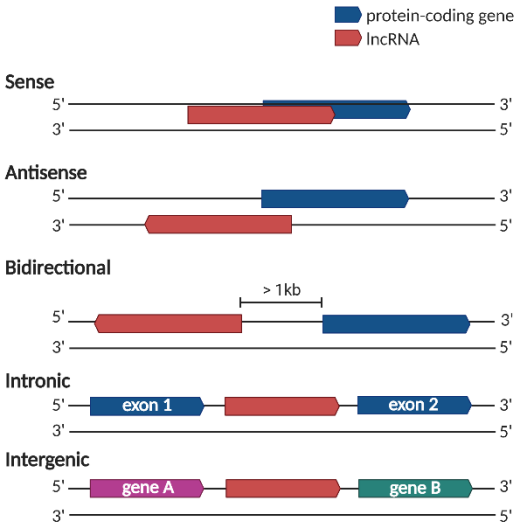

Figure 6. *Schematic representation of lncRNAs classification according to their genomic position relative to a protein-coding gene. Arrows indicate transcription direction.*

The function of lncRNAs is strictly related to their subcellular localization, mostly being situated in the nucleus (in part due to inefficient splicing and polyadenylation) or cytoplasm, but some have been found also in mitochondria and extracellular vesicles [138].

Intriguingly, in the last years, an increasing number of publications is describing that lncRNAs functioning is related to the synthesis and degradation of many components of the ECM (i.e., collagen, integrins, laminins, metalloproteases and others), being key regulators of cell proliferation, invasion and metastasis in lung and breast tumours, and squamous cell carcinomas. [139–142]. Numerous studies underline that lncRNAs can regulate gene expression at different levels (Fig. 7), starting from epigenetics and chromatin structure, transcriptional modifications, and even at translational and post-translation levels [130,143].

As a consequence, their overexpression or deficiency has a direct impact on the physiology of tissues and organs, determining cellular state, differentiation and development, thus being involved in the onset of different pathologies, including cancer [144,145]. When considering breast cancer, several lncRNAs show different expression patterns in cancer tissue compared to the normal breast tissue. Moreover, differential expression patterns are observed within different breast cancer subtypes – some are associated with ER signalling [146], others to triple-negative status [147,148].

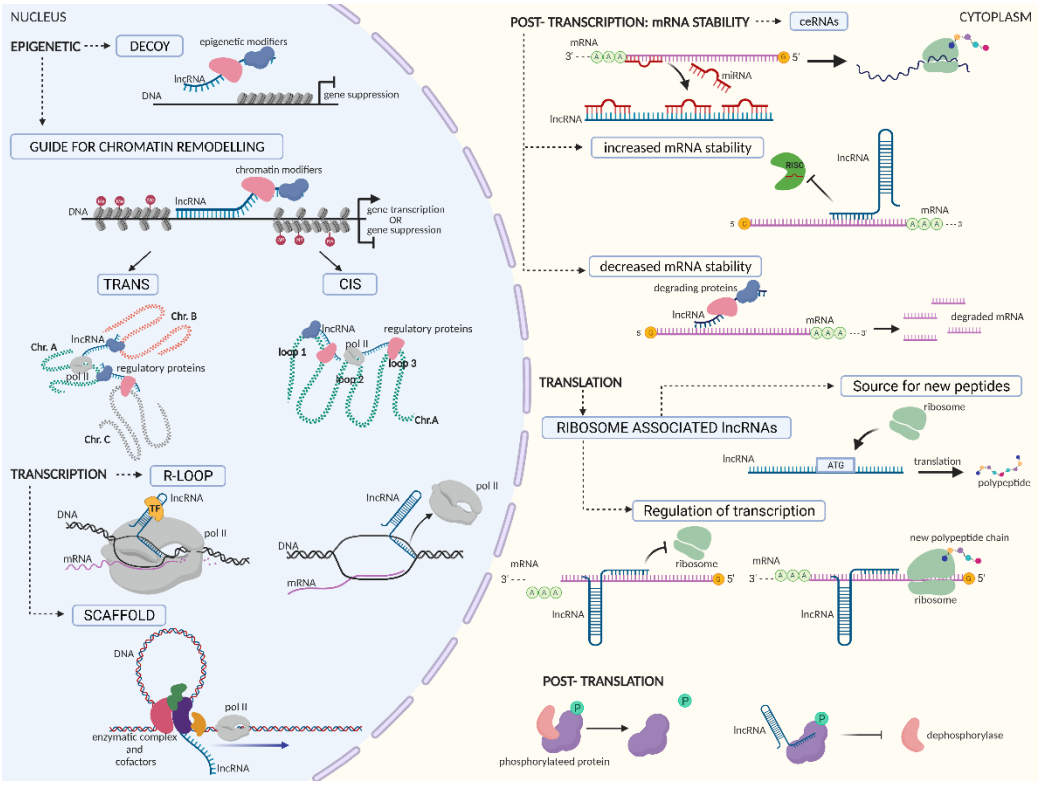

Figure 7. *Nuclear vs cytoplasmic regulatory mechanisms associated with lncRNAs.*

2.2.1 HAS2-AS1

The lncRNA hyaluronan synthase 2 antisense 1 (HAS2-AS1) was first described by Chao and Spicer in 2005 as the natural antisense of HAS2 sequence, as it is located on chromosome 8q24.13 and transcribed from the opposite strand of HAS2 gene locus. HAS2-AS1 transcript consists of four exons, flanked by a consensus splice acceptor and donor sequences. The four exons are distributed as follows with respect to HAS2 gene structure: exon 1 is encoded by sequences located within intron 1 of HAS2, exon 2 is complementary to a portion of HAS2 exon 1 and exons 3 and 4 are encoded by sequences within HAS2 proximal promoter [43] (Fig. 8).

HAS2-AS1 exon 2 contains a splicing site, which allows the generation of two splicing variants, called long (L) and short (S) depending on their nucleotide length, of 257nt and 174nt respectively (Fig. 8). These two isoforms show perfect complementarity with a region starting about 70 bp from the presumed transcription initiation site of human HAS2, allowing HAS2 mRNA and HAS2-AS1 natural antisense to form an RNA/RNA heteroduplex at the cytoplasmic level which stabilises HAS2 transcript. In 2011, Michael and colleagues proved for the first time that under the

stimulation of interleukin-1 β (IL-1β) and TGFβ, HAS2 mRNA physically interacts with HAS2-AS1 in proximal tubular epithelial cells, finally stabilising and promoting HAS2 expression [149].

Remarkably, the HAS2-AS1 effect seems to be different and specific depending on the cell type. Indeed, HAS2-AS1 overexpression in osteosarcoma cells reduces HAS2 transcript [43], while its overexpression in oral squamous cell carcinoma is crucial for HAS2 stabilisation and transcription and hypoxia-induced invasiveness [150].

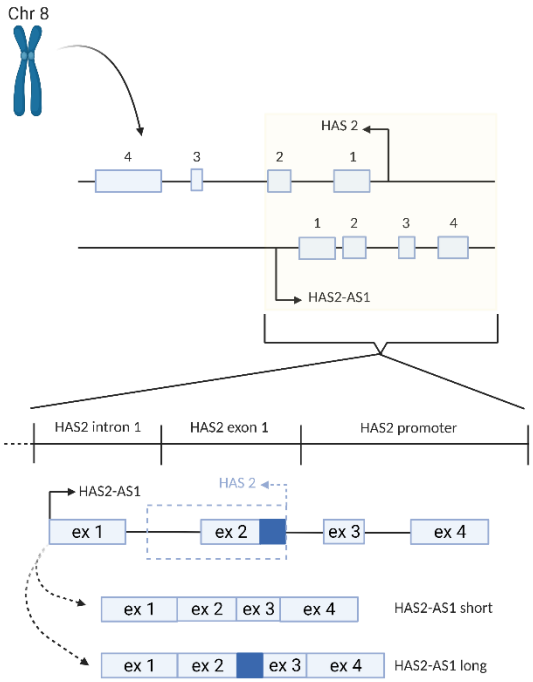

Figure 8. *Schematic representation of the genomic organization of human HAS2 and HAS2-AS1 loci on chromosome 8.*

lncRNAs functions greatly depend on their subcellular localization. As regards HAS2-AS1, it can be located either in the nucleus or in the cytoplasm [151]. In 2014, Vigetti and colleagues demonstrated that in aortic smooth muscle cells (AoSMCs) nuclear HAS2-AS1 works as a cis epigenetic regulator of HAS2, being essential to induce HAS2 transcription by facilitating chromatin remodelling and opening around HAS2 promoter [53] (Fig. 9). Interestingly, in AoSMCs the same NF-κB/HAS2-AS1/HAS2 pathway is also involved in Sirtuin 1 (SIRT1) response to inflammatory stimuli (i.e., TNFα). In particular, the activation of SIRT1 prevents NF-κB/p65 acetylation and, consequently, its nuclear translocation. As a result, there is a decrease in HAS2-AS1 transcription, which in turn regulates HAS2 and HA deposition [60] (Fig. 9).

An interesting aspect of HAS2-AS1 is its connection with hypoxia - an aberrant expression of HAS2-AS1 was observed in squamous cell carcinomas under hypoxic conditions. HAS2 expression and HA deposition are both stimulated under hypoxic conditions, since HAS2-AS1 responds to hypoxia-inducible factor-1α (HIF-1α) via the hypoxia-responsive element (HRE) included in its promoter [152] (Fig. 9).

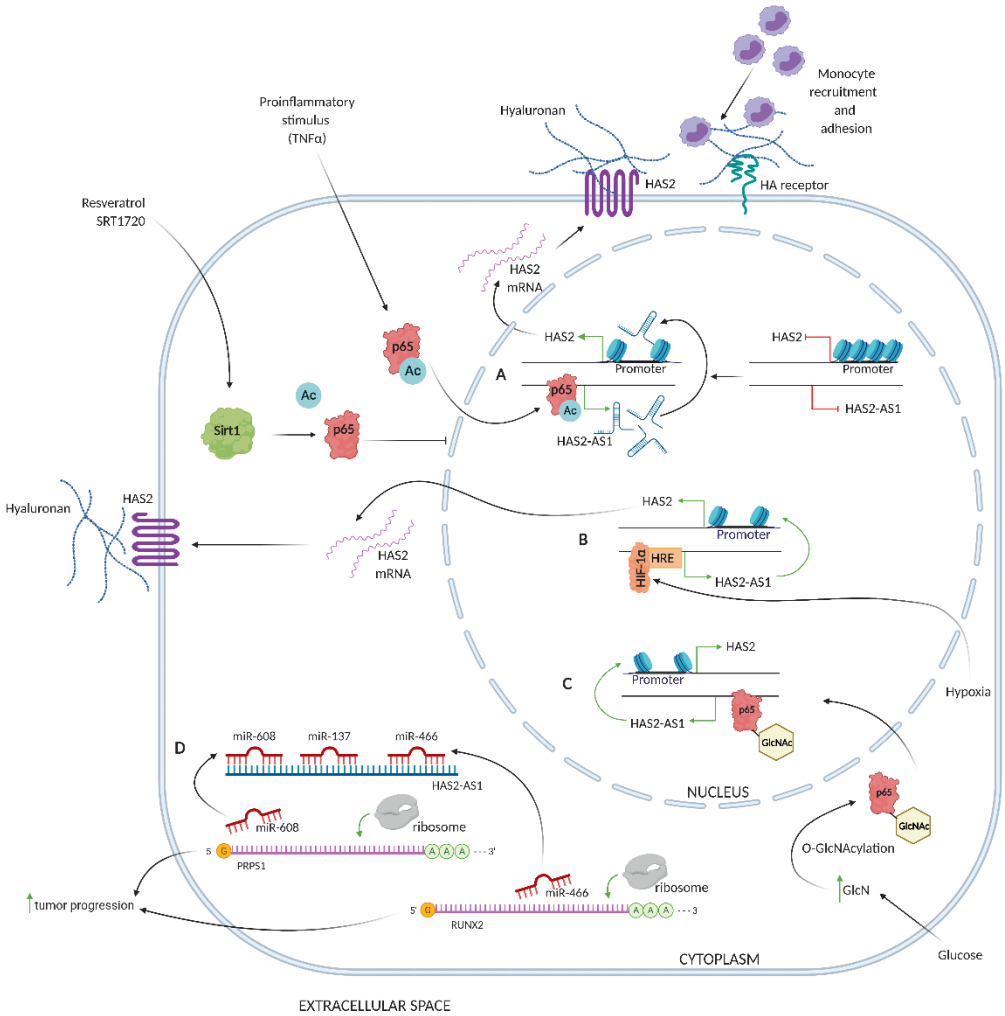

Figure 9. *Schematic illustration of HAS2-AS1 functions in cells.*

More than being solely an epigenetic regulator for the HAS2 gene, HAS2-AS1 can also be found in the cytoplasm. Different studies reported the intriguing ability of HAS2-AS1 to interact with other RNAs, which is acting as competing endogenous RNAs (ceRNAs) for miRNAs (sponge effect) (Fig. 9). An increasing number of studies report that HAS2-AS1/miRNAs interaction is functional mainly in cancer. As an example, high levels of HAS2-AS1 have been reported in glioma, where it sponges

miR-137 and eventually correlates with a lower overall survival rate [153]. Similarly, HAS2-AS1 can function as an oncogene sponging miR-608 and propelling invasion and proliferation of glioblastoma multiforme cells [154]. Finally, HAS2-AS1 has been associated with increased cell proliferation and invasion in ovarian cancer, via sequestrating miR-466 and reliving RUNX2 function [155].

As miRNAs landscape is very different between different tissues and cells, it would not be surprising if the effects of HAS2-AS1 are specific and restricted to a particular cell type or cancer histotype. Accordingly, HAS2-AS1 could be considered a potential pharmacological target to modulate not only HAS2 expression without altering the other HASes but also other malignant phenotypes, including EMT, proliferation and invasion.

3 HYALURONAN AND ITS IMPLICATION IN CANCER HALLMARKS

According to Hanahan and Weinberg, tumorigenesis consists of a multistep process reflecting the numerous genetic alterations that normal cells progressively accumulate, thus evolving into highly malignant cells. As a result, cells acquire a set of distinct characteristics that enable tumour growth and metastatic dissemination, that Hanahan and Weinberg summarized in eight distinct hallmarks: self-sufficiency in growth signals, insensitivity to anti-growth signals, evading apoptosis, limitless replicative potential, sustained angiogenesis, tissue invasion and metastasis, reprogramming of energy metabolism and evading the immune response [156].

In the last years became clear that the biology of tumours can no longer be understood simply by investigating the traits of cancer cells – instead, it is essential to focus also on the tumour microenvironment and, thus, the contribution of ECM to tumorigenesis and cancer progression.

3.1 Sustaining proliferative signalling

One of the most important mechanisms by which cells undergo tumour transformation and sustain cancer progression is their ability to escape growth regulation. Tumour cells establish their de-regulated ability to proliferate via two processes: by enhancing cell proliferation itself or by inhibiting the suppressive regulation of the surrounding environment on cell proliferation. ECM plays a key role in this context, as it modulates the presentation or sequestration of growth factors to receptors, thus contributing to the regulation of cell fate.

Notably, CD44/HA interaction activates the Rho GTPase signalling, which eventually yields to the reorganisation of the cytoskeleton, chemoresistance, cell growth and proliferation, via induction of the PI3K/Akt pathway [157]. Similarly, PI3K/Akt also activates mTOR, which is known to promote cell proliferation and metabolism [158]. In breast cancer it has been observed that Akt is constantly activated by CD44, via a positive feedback loop involving HAS2 and HA production, finally sustaining cell survival [159].

Interestingly, also RHAMM has been described to boost cancer cell proliferation [160]. Its expression increases during G2/M progression, and contributes to the formation of the mitotic spindle, the regulation of proper chromosomal segregation and genomic stability [161].

In the last years, the interest in ncRNAs involvement in tumorigenesis and cancer progression is significantly increasing, as demonstrated by the crescent number of papers published on the topic [162]. As an example, in ovarian cancer cells, HOTAIR increases the expression of cyclin D1 (CCND1) and cyclin D2 (CCND2) via sponging miR-206 [163]. Similarly, the oncogenic lncRNA MALAT1 regulates cell cycle progression at G1 phase through the regulation of p53, p16, p21 and p27 cell cycle inhibitors [164].

3.2 Tissue invasion and metastasis

Invasion and metastasis of tumour cells are processes closely related to poor prognosis. Plenty of studies demonstrated the active role of ECM in affecting primary tumour cells adhesion and penetration to metastasise target tissues [165].

Regarding breast cancer, two major models are explaining how metastasis happens: the first suggests that only cancer stem cells can metastasise and form a new tumour into a distant organ; according to the second model, instead, primary tumour cells can undergo multiple changes due to increased genomic instability and eventually acquire the ability to invade and metastasise to distant organs [166,167]. This second theory is strictly based on the EMT pathway that allows tumour cells to delaminate from the primary tumour mass.

During EMT, the epithelial-like cancer cells lose contact with each other due to a progressive loss of adherence junction proteins, such as E-cadherin, and a concomitant gain of mesenchymal markers, as N-cadherin, thus acquiring a mesenchymal migratory phenotype [63].

EMT and its reverse process, called mesenchymal-to-epithelial transition (MET), allow the transit of cells between mesenchymal and epithelial states, representing vital processes involved not only in cancer metastasis but also in physiological processes like embryogenesis and development.

Thus, it is not surprising the high intra-species conservation of EMT-MET associated pathways, like Snail/Slug, Twist, Six1, TGFβ, and Wnt/β-catenin [168].

A lot of evidence demonstrates that HA, CD44 and HAS2 are master regulators of EMT pathways. In breast tumours, high HA levels and their interaction with CD44s support EMT boosting zinc finger E-box-binding homeobox 1 (ZEB1) expression levels in an autocrine manner [169]. Instead, HAS2 depletion in murine mammary epithelial cells significantly inhibited the TGFβ-induced EMT via decreasing the expression of fibronectin, Snai1 and ZEB1 [170]. Similarly, HAS2-AS1 has a key role in TGFβ- and HAS2-induced breast cancer EMT, migration and acquisition of stemness, as it was demonstrated that its abrogation suppressed TGFβ induction of EMT markers, including Snai1, Hmga2 and fibronectin [151].
Remarkably, in breast cancer cells there is a switch in the expression of CD44v isoforms to the CD44s isoform due to inhibition of splicing activity when cells acquire a mesenchymal phenotype and undergo EMT, highlighted by a decrease in E-cadherin via activated PI3K/Akt pathway [171]. Moreover, in hepatocellular carcinoma CD44s but, not CD44v, has a key role in regulating TGFβ-mediated mesenchymal phenotype, regulating vimentin expression, mesenchymal spindle-like morphology, and eventually tumour invasiveness [172].

Notably, in the first stages of growth, tumours cells proliferate at such a high rate, that vasculature is not able to sustain the growth itself. So, tumour cells find themselves in a tumour niche that is depleted of oxygen and start to undergo a switch to anaerobic metabolism, promote angiogenesis, activate invasive growth and EMT pathways. Therefore, it can be assumed that HIF-1α/HAS2-AS1/HAS2 pathway plays an important role in promoting EMT.

3.3 Evading apoptosis

Cancer cells accomplish their uncontrolled growth not only by boosting their proliferative abilities but also by escaping apoptosis.

Depending on the type and origin of pro-apoptotic signals (i.e., intracellular, or extracellular signals), apoptosis can be induced via two different pathways, called intrinsic and extrinsic pathways, or mitochondrial and death receptor pathways, respectively (Fig. 10). Caspases are the key players in apoptosis, as being cysteine aspartyl-specific proteases, they can cleave hundreds of different proteins. They are typically classified into initiator (caspases-2, -8, -9 and -10) and executioner caspases (caspase-3, -6, and -7). The latter, are the ones that directly cleave target proteins, thus yielding cell death [173].

Typically, in cancer cells is inhibited the intrinsic pathways. Blockade of apoptotic pathways allows cancer cells to survive longer, thus favouring the accumulation of mutations which can eventually increase invasiveness during tumour progression, stimulate angiogenesis, deregulate cell proliferation, and interfere with differentiation [174]. In this light, HA appears to be a suitable candidate for the regulation of apoptosis. As an example, HA/CD44 interaction up-regulates miR-21 which, in turn, leads to the production of Bcl-2 anti-apoptotic protein, up-regulation of survival proteins, and doxorubicin chemoresistance [175].

By targeting CD44/RHAMM lung cancer cell growth is inhibited both in vitro and in vivo [176]. Evidence also depicts HA as a regulator of mitochondrial apoptosis through the p53 pathway, both in normal chondrocytes [177] and pancreatic cancer cells [178].
An interesting observation derives from a study by Vigetti et al., demonstrating that upon HA depletion via 4-MU administration, AoSMCs undergo apoptosis [179]. Supporting this finding, 4-MU treatment enhanced apoptosis and eventually decreased malignancy in peripheral nerve sheath tumours [180], pancreatic [181] and bladder cancer [182], enhancing cell apoptosis.

With regards to ncRNAs, there is a growing interest in investigating miRNAs and lncRNAs roles in tumorigenesis and tumour progression. As an example, miR-466 is significantly downregulated in osteosarcomas and negatively correlated with osteosarcoma severity. On the contrary, its overexpression inhibited cell proliferation and induced cellular apoptosis [183]. In prostate cancer, instead, PlncRNA-1 lncRNA silencing yielded apoptosis by increasing Poly(ADP-ribose) polymerase 1 (PARP-1) expression, which is a key element of the DNA damage response [184]. Lastly, overexpression of TUG1 lncRNAs in glioma cells induced intrinsic apoptosis, by regulating caspase-3 and -9 and Bcl-2-mediated anti-apoptotic pathways [185].

Intriguingly, HAS2 is targeted and negatively regulated by miR-26b, resulting in the stimulation of apoptosis mediated by caspase-3 and CD44 [186].

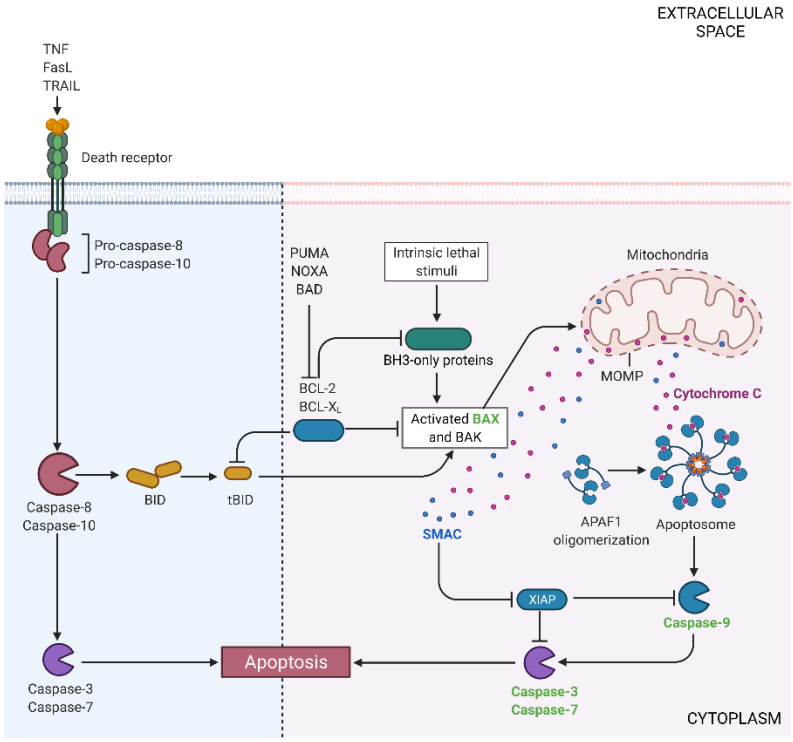

Figure 10. *Diagram depicting the intrinsic and extrinsic pathways of apoptosis.*

AIM OF THE WORK

This thesis project is fitted in a bigger framework that aims at studying the role of HA, HAS2 and HAS2-AS1 in breast tumorigenesis and aggressiveness since both HA deposition and HAS2 expression are generally found dysregulated in numerous malignancies.

In particular, previous experiments conducted in our laboratory demonstrated that HAS2-AS2 overexpression modulates cell viability, motility and invasion in TNBC cells (i.e., MDA-MB-231) but not in ER+/PR+/HER2+ cell line (i.e., MCF-7), suggesting that HAS2-AS1 could have a role in decreasing TNBC aggressiveness.

As it is well known that HAS2-AS1 lncRNA has a role in epigenetically regulating HAS2 expression at least in AoSMCs and since Heldin and colleagues already demonstrated that HAS2-AS1 expression is elevated in aggressive breast cancers, this work aimed at understanding the molecular mechanism by which HAS2-AS1 overexpression regulates TNBC cell lines aggressiveness.

In particular, a new cytoplasmic regulatory function has been proposed for HAS2-AS1, as ceRNA for miR-186-3p.

Moreover, thanks to the production of TNBC derived cellular models ectopically overexpressing HAS2-AS1, it was possible to perform a microarray analysis to better investigate the pathways that were altered upon HAS2-AS1 overexpression. Thus, further functional analyses were done to investigate some of these pathways (i.e., apoptosis and EMT).

MATHERIALS AND METHODS

1 Cell culture

MDA-MB-231, Hs 578T, BT-549 (high metastatic, TNBC cell lines) and HBL 100 cell lines (not diseased breast cells) were purchased by American Type Culture Collection (ATCC), grown, and maintained in complete Dulbecco's Modified Eagle Medium (DMEM) medium supplemented with 10% of fetal bovine serum (FBS). SUM149 (high metastatic, TNBC cell lines) were purchased by ATCC, grown, and maintained in complete F-12 Nutrient Medium (Ham's F12) supplemented with 5% of heat-inactivated FBS, 10 mM HEPES, 1 µg/ml Hydrocortisone and 5 µg/ml Insulin. BT-474 (low metastatic, ER-positive) were purchased by ATCC, grown, and maintained in complete DMEM:Ham's F12 (1:1 mixture) medium supplemented with 5% of FBS and 5 µg/ml Insulin. MCF-7 and T-47D (low metastatic, ER-positive) breast cancer cell lines were obtained from ATCC and grown in complete Roswell Park Memorial Institute (RPMI) 1640 medium with 10% FBS. All cell lines were routinely harvested in a humidified 95% air/5% CO_2 incubator, at 37°C.

2 Absolute HAS2-AS1 quantification via RT-qPCR

For the generation of the standard curve, pcDNA3-HAS2-AS1 L construct was obtained using ZymoPURE II Plasmid Kits (#D4200, Zymo Research). A ten-fold dilution series over nine points were prepared from the plasmid DNA, starting from a dilution of 1.000.000 copies/µl to 1 copy/µl; then each dilution was used as a template for RT-qPCR, and amplified using HAS2-AS1 TaqMan gene expression assays from Thermo Fisher Scientific (Table 1). Each point was performed in triplicate. The standard curve was constructed by plotting Cq values against the logarithmic concentration of the calibrator plasmid.

Total RNAs were extracted from the breast cancer cell lines and retrotranscribed as described below (see "RNA extraction and gene expression analysis"). The cDNA was analyzed for HAS2-AS1 expression via Taq Man gene expression assays from Thermo Fisher Scientific (Table 1) on Quantstudio 5 instrument (Applied Biosystems). The copies of HAS2-AS1 RNA molecules/µg of total RNA in the cell lines were obtained by interpolating the Cq values in the standard curve.

3 Bioinformatics Analysis of HAS2-AS1 expression in breast cancer patients

Breast cancer data was extracted from the Cancer Genome Atlas (TCGA) Research Network (https://www.cancer.gov/tcga) on 11th March 2021. Kaplan Meier survival analysis was conducted using SPSS version 22.0 (IBM Corp., Armonk, NY, USA). Eight of the 1,085 female patient datasets were excluded from the analysis as the HAS2-AS1 expression data was not available.

4 Cell transfection

Cells were plated in a 6-well plate and transfected with Lipofectamine 2000 Transfection Reagent (#11668027, ThermoFisher Scientific) following the manufacturer's instructions. Briefly, to transiently silence HAS2-AS1 expression, cells were transfected with 50 nM siRNA against HAS2-AS1 (Silencer® Select HAS2-AS1, #N265529, ThermoFisher Scientific), HAS2 (Silencer Pre-designed siRNA, #AM16708, ThermoFisher Scientific) or a scrambled siRNA (Silencer Negative Control #1, #AM4611, Thermo Fisher Scientific). For subsequent determinations, 24-48 hours after the transfections, cells were tested for silencing efficiency through RT-qPCR, and only cells with a residual expression of the target genes lower than 25%, were used. To transiently overexpress the exon 2 L or S isoforms of HAS2-AS1, 2 μg of a pcDNA3-HAS2-AS1 S or pcDNA3-HAS2-AS1 L [53] were transfected. As a control, the same amount of a pcDNA3 empty vector was transfected. Cells were used for subsequent determination 24-48 hours after overexpression.

5 Cell viability assay

To study cell viability upon HAS2-AS1 silencing or overexpression, a 3-(4,5-dimethylthiazol-2-yl)-2,5-diphenyltetrazolium bromide (MTT) assay (#20395, SERVA) was performed. Briefly, $9x10^3$ cells were plated in a 96-well plate and transfected with lipofectamine following the manufacturer's instructions. 48 hours after the transfection, the cell culture medium was replaced with fresh medium supplemented with 50μl of 5 mg/ml MTT and incubated at 37 °C for 5 h. The reaction was stopped by adding 200μl of DMSO and 25μl of Sorensen glycine buffer per well. The plate was read at 570 nm.

6 Wound healing assay

To determine cell migration via bi-dimensional support, a wound-healing assay (also known as scratch assay) was performed. Twenty-four hours after the transfection, three scratches per well were done with a 20 μl pipette tip. Cells were washed twice with phosphate buffered saline (PBS) and fresh medium with 0.1% FBS was added to each well, to minimize the proliferation component of cell migration. Pictures were taken at 0 and 24 hours through light microscopy and analyzed by the TScratch software [187]. Results are presented as a percentage of wound closure.

7 Determination of cellular shape and polarity

Cells were stained with 5 μM 1,1′-Dioctadecyl-3,3,3′,3′-tetramethylindocarbocyanine perchlorate (DiI; #468495, SIGMA), kept 10 minutes at 37 °C, and finally 5 minutes at 4 °C. Subsequently, after

washing the wells 5 times with PBS, pictures of the cells were taken through light microscopy and cell morphology was evaluated by measuring the long axis:short axis ratio of the cells by using Image J software [188].

8 HA pericellular coating quantification

Cell surface HA was determined by cytofluorimetric analysis as described by Vitale et al [108]. Briefly, 24 hours after the transfection cells were detached and counted. $5x10^5$ cells were washed three times in PBS and incubated with 5 µg of biotinylated hyaluronan binding protein (bHABP, #BC41, Hokudo) in 100µl of cold PBS for 1 hour at 4˚C. Cells were then washed three times with 1 ml of PBS and centrifuged 5 minutes at 0.8g at 4˚C. The supernatant was discarded, and cells were incubated with 1:100 FITC-streptavidin (#405202, Biolegend Campoverde) in cold PBS for 45 minutes at 4˚C. After three washes, MDA-MB-231 were resuspended in 400 µl of PBS and analyzed by flow cytometry.

HA pericellular coat was also evaluated via a particle exclusion assay. Briefly, 48 hours after cells seeding, $1x10^6$ fixed human red blood cells were washed in PBS and added to each well. After an incubation time of 30 minutes, cells were examined by contrast microscopy and 10 pictures per well were taken. As a control, cells were treated with 2U/ml of Hyaluronidase from *Streptomyces hyalurolyticus* (#H1136, SIGMA) or were transiently transfected with 50 nM siRNA against HAS2. The analysis of the images and the relative quantification was performed using the image analysis software ImageJ [188].

9 RNA extraction and gene expression analysis

Total RNA was extracted by NucleoSpin RNA (#740955, MACHEREY-NAGEL), an RNA isolation kit containing a DNA digestion step. RNA samples were quantified with a NanoDrop (ThermoFisher, Life Technologies) and run on an agarose gel for quality control. Two µg of total RNA were then retrotranscribed using the High Capacity cDNA synthesis kit (#4368814, Applied Biosystems) and amplified on QuantStudio 3 Real-Time PCR Instrument (Applied Biosystems). The cDNA was then analyzed using the Taq Man gene expression assays from Thermo Fisher Scientific reported in Table 1. For stable clones screening, the SYBR Green PCR Master Mix (#4309155, Thermo Fisher Scientific) was used. The expression levels of target genes were analysed using primer pairs reported in Table 2. In both TaqMan and SYBR Green assays, the expression of target genes was normalized to the expression levels of the GAPDH reference gene and relative normalized expression was calculated based on the $\Delta\Delta C_t$ method.

Table 1. *Taqman assays used for quantitative RT-PCR*

Gene/miRNA	ASSAY ID
CD44s	Hs01081473_m1
GAPDH	Hs99999905_m1
HAS2	Hs00193435_m1
HAS2-AS1	Hs03309447_m1
HAS3	Hs00193436_m1
p21	Hs00355782_m1
P2RX7	Hs00175721_m1
TGFBR3	Hs00234259_m1
hsa-miR-186-3p	002105
hsa-miR-186-5p	002285
U6 snRNA	001973

Table 2. *Sybr green assays used for quantitative RT-PCR*

TARGET GENE	FORWARD PRIMER	REVERSE PRIMER
AKT1	CCATGGACAGGGAGAGCAAA	TGGCCACAGCCTCTGATG
BAX	CCAAGGTGCCGGAACTGA	CCCGGAGGAAGTCCAATGT
Bcl-2	TGCGGCCTCTGTTTGATTTC	GGGCCAAACTGAGCAGAGTCT
CCND1	ATCAAGTGTGACCCGGACTG	CTTGGGGTCCATGTTCTGCT
E-cadherin	GAAAACAGCAAAGGGCTTGGA	TGGGGGCTTCATTCACATCC
EREG	ACAACTGTGATTCCATCATGTATCC	CTACACTTTGTTATTGACACTTGAGC
Fibronectin	ACCGTGGGCAACTCTGTCAA	CCCACTCATCTCCAACGGCA
GAPDH	CGTATTGGGCGCCTGGTCAC	ATGATGACCCTTTTGGCTCC
HAS2-AS1 exon 2 L	TCTTGACTTCTCCTTCCCCG	AAGTTGGAGGAGGCAGAAGG
HAS2-AS1 mutagenesis	CTGGCTTCGAGCAGATGTTTGAACC AGAGACTTGAAACAGCCCC	GGGGCTGTTTCAAGTCTCTGGTTCAA ACATCTGCTCGAAGCCAG
NOXA	GAGCTGGAAGTCGAGTGTGCTA	TGCCGGAAGTTCAGTTTGTCT
PUMA	TGGAGGGTCCTGTACAATCTCA	TCTGTGGCCCCTGGGTAA
SNAI1	CCCGACAAGTGACAGCCATT	CGAGCCCAGGCAGCTATTTC
Vimentin	TCGCAGAAAGGCACTTGAAAGC	TCAGCATCACGATGACCTTGAA
XIAP	TGGCATTTCCAGATTGGGGC	TGTCCACCTTTTCGCGCC
ZO-1	GATGATGCCTCGTTCTAC	GTGTTGTGGATACCTTGT

10 Western immunoblot analysis.

Cells were lysed in RIPA buffer (50 mM Tris-HCl, pH 8.0, 150 mM NaCl, 1% NP-40, 0.1% sodium dodecyl sulfate, 0.5% sodium deoxycholate), supplemented with Protease/Phopsphatase inhibitor (#5872, Cell Signaling Technology) and protein concentration was measured by Quantum Protein BCA assay (#EMP014500, Euroclone). Equal amounts of protein samples were subjected to SDS-polyacrylamide gel electrophoresis, followed by semi-dry transfer to nitrocellulose membrane using Trans-Blot Turbo Transfer System (Biorad) and blocking in 4% bovine serum albumin in Tris-buffered saline, supplemented with 0.1% Tween-20. Subsequently, the membranes were incubated with primary antibodies (Table 3) at 4 °C overnight, followed by incubation with anti-horseradish peroxidase-conjugated specific secondary antibodies (1:10,000; Santa Cruz Biotechnology) for 1 h at room temperature. The antibody/substrate complex was visualized by chemiluminescence using a chemiluminescence kit (LiteAblot TURBO, #EMP012001, Euroclone). Images were taken by Alliance Q9 Mini instrument (Uvitec) and signal intensity was evaluated using NineAlliance software (Uvitec). Tubulin or GAPDH were used as the protein loading control.

Table 3. *Primary and secondary antibodies used for immunoblotting (IB) and immunofluorescence (IF)*

TARGET	USE	SUPPLIER	DESIGNATION	DILUTION
Cleaved caspase-3	IB	Cell Signaling Technology	9661	1:1000
Cleaved caspase-8	IB	Cell Signaling Technology	9746	1:1000
Cleaved caspase-9	IB	Cell Signaling Technology	9502	1:1000
Fibronectin	IF	Sigma-Aldrich	F3648	1:1000
GAPDH	IB	Santa Cruz Biotechnology	20357	1:1000
HAS2	IB	Santa Cruz Biotechnology	34067	1:700
HDAC2	IB	Santa Cruz Biotechnology	7899	1:1000
Zo-1	IF	Life Technologies	33-9100	1:200
α-Tubulin	IB	Santa Cruz Biotechnology	135659	1:1000

11 Stable cell lines generation

MDA-MB-231 cells were plated onto 12-well plates and cultured for 24 hours at a final confluence of 85%. On the next day, cells were transfected using Lipofectamine 2000 Transfection Reagent (#11668027, Thermo Fisher Scientific) with 2 µg of pcDNA3-HAS2-AS1 L or pcDNA3 empty vector. Twenty-four hours after transfection, cells were split into five 96-well plates at a concentration of

0,4 cells/well, selected in 800 µg/ml G-418 (#G8168, Sigma-Aldrich) and expanded. Clones were then screened for their exon 2 of HAS2-AS1 L isoform expression levels, via RT-qPCR (see "RNA extraction and gene expression analysis" for details).

12 Colony formation assay

MDA-MB-231 stable clones overexpressing exon 2 of HAS2-AS1 L isoform or pcDNA3 empty vector were seeded in 60 mm plates (500 cells/well) and cultured for 10 days. The culture medium was replaced with fresh medium every 3 days. The colonies were fixed and stained with 0,1% crystal violet, washed extensively to remove excess dye, and imaged.

13 Anchorage-independent colony formation assay in soft agar

Soft agar plates were prepared by pouring in a 12 multi-well plate a feeding underlay layer and a growth overlay. To prepare the underlay, complete DMEM added with 20% FBS and 800 µg/ml G418 was mixed with Difco Noble Agar (#214230, BD Bioscience) at a final concentration of 0,6%. The plate was kept for 1 hour at room temperature and then overnight at 37 °C to solidify and equilibrate. The day after, 10^3 cells/well were resuspended in complete DMEM added with 20% FBS and 800 µg/ml G418 (#G8168, Sigma-Aldrich) and mixed with Noble Agar, at a final concentration of 0,3%. The plate was kept for 1 hour at room temperature and then overnight at 37 °C to solidify and equilibrate. Cells were let grow for 20 days, and then images of colonies were taken under a light microscope (Olympus) at 400X magnification. Colonies areas were measured with ImageJ software [188].

14 Growth curve

The growth curve was characterized by measuring the number of cells for 7 consecutive days at 24 hours intervals. MDA-MB-231 stable clones overexpressing exon 2 of HAS2-AS1 L isoform or pcDNA3 empty vector were seeded in a 6-well plate at an initial concentration of $5x10^4$ cells/well and cultured in complete DMEM with 10% FBS and 800 µg/ml G418 (#G8168, Sigma-Aldrich). The culture medium was replaced with fresh one every day. Every 24 hours, cells were harvested using 0,5% trypsin, diluted with a 0,4% trypan blue working solution and counted with a Bürker counting chamber. Each sample was measured three times, in triplicates. Cell-growth curves were drawn from living cells numbers. Population doublings was also estimated according to the following formula: $PDL = \frac{logY - logX}{log2}$, where X is the number of cells seeded at day 0, and Y is the number of confluent cells at day 7.

15 Immunofluorescence staining

For immunofluorescence staining, MDA-MB-231 stable clones overexpressing exon 2 of HAS2-AS1 L isoform or pcDNA3 empty vector were seeded in a 12-well plate upon glass microscopy dishes and allowed to settle for 24 h at 37°C. Then, cells were fixed for 30 min in 4% paraformaldehyde, followed by 15 min permeabilization in 0.1% Triton X-100, blocking for 60 min in 1% BSA in PBS, and incubation overnight at 4 °C with the primary antibodies against ZO-1 or Fibronectin (Table 3).

Then cells were incubated with secondary FITC-conjugated antibodies (1:1000) for 1 h at room temperature in the dark. Extensive washes with 1% BSA in PBS were performed between the afore-mentioned steps. Subsequently, coverslips were set onto glass slides and mounted by using 10 µl of VectaShield HardSet mounting medium containing 4′,6′-diamidino-2-phenylindole (DAPI, Vector Labora-tories, Burlingame, CA) for nuclear visualization. Finally, images were taken at 630x magnification using a confocal microscope.

16 Transcriptome analysis of stable MDA-MB-231 cells overexpressing HAS2-AS1 exon 2 L isoform

Total RNA was extracted from cultured cells using the Direct-zol RNA Kit (Zymo Research Corporation, Irvine, CA, USA) and processed for hybridization to the Affymetrix Clariom S Human Arrays (Affymetrix., Santa Clara, CA., USA) according to the respective manufacturers' instructions. The CEL files were analyzed using the Transcriptome Analysis Console 4.0 Software (Affymetrix). After Robust Multiarray Average (RMA) normalization, differentially expressed genes with 4-fold or greater changes were identified with statistical significance defined by a false discovery rate (FDR) adjusted p-value of below 0.05. The list of genes was further analyzed using DAVID v6.8 and classified into associated functional groups and KEGG pathways.

17 Nucleus-Cytoplasm Separation Assay

The nucleus and cytoplasm RNA fractions of MDA-MB-231 cells were separated by using the RNA and protein isolation (PARIS) Kit (#AM1921, Invitrogen). The RNA and protein in the nucleus and cytoplasm were extracted according to the manufacturer's instructions. Further, HAS2-AS1 mRNA was detected by RT-qPCR. HDAC2 and GAPDH proteins detection via Westernblot were used as the nucleus and cytoplasm controls, respectively.

18 Bioinformatic prediction of miRNA binding sites on HAS2-AS1

To determine predicted miR-186-3p binding sites on HAS2-AS1, we used RNA hybrid bioinformatics tool (https://bibiserv2.cebitec.uni-bielefeld.de/rnahybrid) [189], miRanda (www.microrna.org) [190,191] and DIANA-microT-CDS (http://diana.imis.athena-innovation.gr) [192].

19 Dual-luciferase reporter assays

The wild-type (WT) or mutant (MUT) binding sites sequences for miR-186-3p from HAS2-AS1 exon 2 L or S isoforms was cloned into the pMIR-GLO plasmid (#E1330, Promega). To establish the 3'-UTR of MUT HAS2-AS1 L, the binding sites were mutated via QuikChange Lightning Site-Directed Mutagenesis Kit (#210519, Agilent Technolgies), according to the manufacturer's instructions.

The luciferase plasmids WT or MUT were co-transfected with 100 pmol of miR-SCR, miR-186-3p or miR-186-5p mimics into MDA-MB-231 cells. After 48 hours, luciferase activity was measured using a Dual-Luciferase® Reporter Assay System (#E1910, Promega) according to the manufacturer's instructions. Data were normalized to Renilla luciferase activity.

20 miRNA extraction and transcript quantification

miRNA extraction was performed using the mirVana™ miRNA Isolation Kit (#AM1561, Invitrogen, Thermofisher Scientific), following the manufacturer's instructions. RNA quality was evaluated with spectrophotometer (Nanodrop, Thermo Fisher Scientific) - A260/A280 ratios between 1.8 and 2.0 were deemed appropriate for further miRNA usage. Reverse transcription was performed using the High Capacity cDNA synthesis kit (#4368814, Applied Biosystems) added with RNase inhibitor (#N8080119, Applied Biosystems). Specific stem-loop RT primers were used to retrotranscribe miR-186-3p, miR-186-5p and U6 snRNA as a control, as part of Taqman MicroRNA Assays (#4427975, Thermo Fisher Sceintific).

RT-qPCR analysis was performed using a standard TaqMan PCR protocol on a QuantStudio 3 Real-Time PCR Instrument (Applied Biosystems). The cDNA was then analyzed using the TaqMan gene expression assays from Thermo Fisher Scientific (#4427975) reported in Table 1. Relative quantification was performed on U6 snRNA expression levels.

21 Terminal Deoxynucleotidyl Transferase dUTP Nick End Labeling (TUNEL Assay)

For apoptosis detection, MDA-MB-231 cells were cultured in 12-well plates upon glass microscopy dishes and allowed to settle for 24 h at 37°C. pcDNA3-HAS2-AS1 L or S, or empty pcDNA3 vector were then transfected into MDA-MB-231 cells as previously described. Twenty-four hours after transfection, cells were fixed for 30 min in 4% paraformaldehyde and then permeabilized with 0.2% Triton X-100 for 5 min. TUNEL staining (DeadEnd™ Fluorometric TUNEL System, # G3250, Promega) was then performed according to the manufacturer's instructions. Finally, images were taken at 630x magnification using a confocal microscope. Similarly, MDA-MB-231 stable clones overexpressing exon 2 of HAS2-AS1 L isoform or pcDNA empty vector were seeded in a 12-well plate upon glass microscopy dishes and allowed to settle for 24 h at 37°C. Then, cells were fixed, permeabilized and stained as for transiently transfected MDA-MB-231 cells.

22 Caspase 3/7 activity assay

Caspase activity was detected by using Caspase-Glo 3/7 assay kit (#G8091, Promega). Briefly, MDA-MB-231 cells were seeded in 96-well white luminometer assay plates at a density of $11x10^6$ cells/well and allowed to settle for 24 h at 37°C. Cells were then transfected with either pcDNA3-HAS2-AS1 S, pcDNA3-HAS2-AS1 L or pcDNA3 empty vector. Twenty-four hours after transfection, 100 µl of caspase 3/7 reagents were added to each well and incubated for 3 hours at room temperature. The luminescence intensity was measured using a plate-reading luminometer.

23 Statistical analysis

All experiments were repeated at least three times in duplicates, if not differently indicated. Data are shown as the mean values ± SEM. The data were tested for significance employing the one-way Analysis of Variances (ANOVA) test followed by Tukey's post hoc test to identify differences between the means. Statistical comparison between two groups was made using an unpaired Student's t-test. The level of significance was set at $p<0.5$.

RESULTS

1. HAS2-AS1 expression is higher in ER-negative breast tumours and TNBC cell lines and correlates with better survival.

Even though it was already reported that invasive breast carcinomas express high levels of HAS2-AS1 [151], we wanted to better enucleate which type of correlation existed between HAS2-AS1 expression and breast tumours by stratifying them depending on their ER status. Taking advantage of data from the TCGA Breast Invasive Carcinoma Project [193], we analysed HAS2-AS1 expression levels in breast cancer tissues. As shown in figure 11A, we observed that HAS2-AS1 transcript levels were significantly higher in ER-negative compared to ER-positive breast cancer samples. Interestingly, this data was also supported by the RT-qPCR analysis we did on HAS2-AS1 expression levels in a panel of breast cancer cell lines, comprising three ER/PR/HER2-positive, four TNBC cell lines and HBL100, which was used as a non-cancerous control cell line. By the analysis, we found that HAS2-AS1 transcript levels were higher in TNBC cell lines compared to ER/PR/HER2-positive cell lines (Fig. 11B). Similarly, cBioPortal *in silico* analysis using data from the Cancer Cell Line Encyclopedia from the Broad Institute and Novartis, confirmed that ER-negative invasive breast cancer cell lines express higher levels of HAS2-AS1 with respect to ER-positive ones (Fig. 11C).

Survival analyses of the same TCGA dataset that we used for the previous analysis [193], highlighted that HAS2-AS1 expression was positively correlated with the overall survival of patients affected by ER-negative breast cancer (Fig. 11D). On the contrary, no significant correlation between HAS2-AS1 expression and survival was observed in ER-positive breast cancer patients (Fig. 11E).

Summing up, all these results suggest a differential HAS2-AS1 expression in invasive breast cancer cell lines, highlighting a higher expression in TNBC cell lines and ER-negative cancer patients' tissues. Notably, high HAS2-AS1 expression levels were correlated with longer survival.

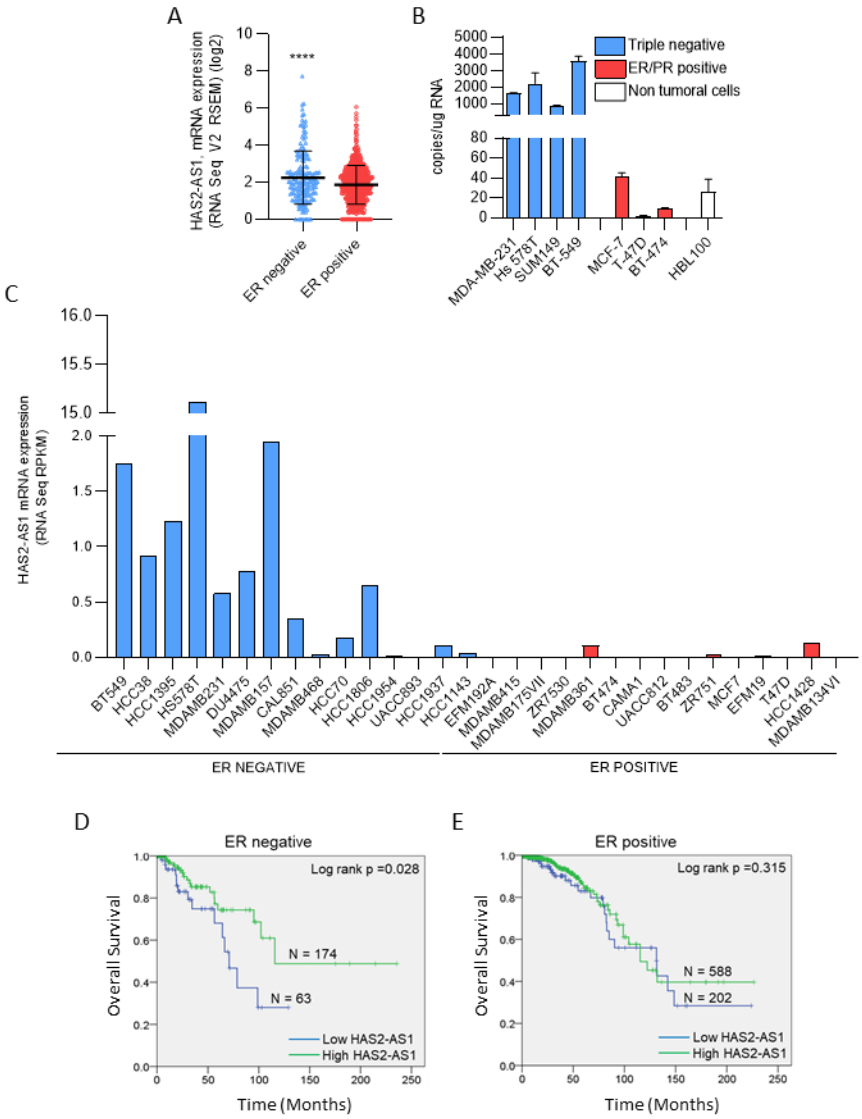

Figure 11. HAS2-AS1 expression is higher in TNBC cells and breast tumour samples and correlates with a good prognosis in ER-negative patients.

(A) *Unpaired analysis of HAS2-AS1 gene expression in patient samples derived from invasive breast carcinomas (TCGA-BRCA gene expression data, cBioPortal.org), stratified for ER expression. ****, p<0.0001. Data are expressed as mean ± SEM.* ***(B)*** *Absolute quantification of HAS2-AS1 copy numbers in triple-negative (blue) and ER/PR/HER2-positive (red) breast cancer cell lines. HBL100 (white) was used as non-tumoral control. Data are expressed as mean ± SEM of triplicates of three independent experiments.* ***(C)*** *HAS2-AS1 mRNA expression levels in invasive breast cancer cell lines, subdivided according to their ER status (ER-positive cell lines in red, ER-negative cell lines in blue). Values are from the Cancer Cell Line Encyclopedia from the Broad Institute and Novartis, updated 2019* [194]*. Data were downloaded via cBioportal and analysed with Prism software. Kaplan Meier survival analysis of either* ***(D)*** *ER-negative or* ***(E)*** *ER-positive TCGA-BRCA breast cancer tissues. A cut off of HAS2-AS1 expression at the 25th percentile was applied.*

2. HAS2-AS1 modulates cell viability, motility, and polarity of TNBC cell lines.

Experiments previously performed in our laboratory showed that HAS2-AS1 is involved in the regulation of cell motility, invasiveness, and vitality of the MDA-MB-231 TNBC cell line, but not of ER/PR/HER2-positive breast cancer cell line (MCF-7). In particular, transient silencing of HAS2-AS1 doubled cell viability with respect to control cells, whereas transient overexpression of the S or L isoforms of the exon 2 of HAS2-AS1, showed a statistically significant reduction of cell viability, of ~26% and ~38% respectively, compared to control cells (data not shown).

We decided to perform the same experiment on cell viability exploiting MTT assay on two other breast cancer cell lines that are routinely used as models for either aggressive TNBC (namely Hs 578T) or non-aggressive ER-positive cancers (namely T-47D). As shown in figure 12, T-47D cell viability was altered neither by HAS2-AS1 silencing (Fig. 12A) nor by HAS2-AS1 overexpression (Fig. 12B), similarly to what was previously observed in MCF-7 cells. Instead, when performing MTT assay on Hs 578T TNBC cell line, even though no significant alteration was observed when silencing HAS2-AS1 via interfering RNA (Fig. 12C), we observed a small but significant decrease of cell viability when overexpressing either S or L isoforms of exon 2 of HAS2-AS1, compared to control cells (Fig. 12D).

Taken together, these results suggest that the modulation, and in particular the overexpression of HAS2-AS1 expression levels affected the viability only of aggressive TNBC cell lines.

Similarly, to what was done with cell viability, also cell migration abilities were assayed in both MDA-MB-231 and MCF-7 cells (preliminary data not shown) and in Hs 578T and T-47D cell lines. Cell motility was evaluated exploiting a two-dimensional scratch assay, known also as wound healing assay, in the presence of 0.1% FBS to reduce cell proliferation. Particularly, the modulation of HAS2-AS1 expression in the non-aggressive ER-positive cell lines MCF-7 (data not shown) and T-47D (Fig. 12E, 12F) did not significantly alter the migratory properties of the cells. In both MCF-7 and T-47D cell lines, indeed, migratory abilities are physiologically lacking, as they are non-aggressive breast tumour cell lines. On the other hand, HAS2-AS1 silencing increased cell migration to a confluent monolayer compared to control cells in both MDA-MB-231 (data not shown) and Hs 578T cells (Fig. 12G). Ectopic overexpression of either L or S isoforms of HAS2-AS1 exon 2, instead, induced a significant decrease of cell migration in both MDA-MD-231 (data not shown) and Hs 578T (Fig. 12H) compared to control cell transfected with the empty pcDNA3 vector. Thus, for the further experiment, we decided to concentrate only on the MDA-MB-231

TNBC cell line, which showed to be the more responsive in terms of both cell viability and motility upon modulation of HAS2-AS1 expression.

As cell shape is an important factor related to cell motion, we performed morphometric analyses of MDA-MB-231 cells that were in the scratch area 24 hours after starting the wound healing assay. Cells were stained with DiI dye (Fig. 13A, 13B) and the ratio between the long and short axis of the cells was evaluated using NIH ImageJ software (Fig. 13C). As expected from the scratch assay experiments, HAS2-AS1 silenced cells, which showed increased motility, had a greater long:short axis ratio (Fig. 13D), whilst HAS2-AS1 L or S isoforms overexpressing cells showed a lower long:short axis ratio, which is explanatory of a more roundish shape typical of non-moving epithelial-like cells (Fig. 13E).

These results indicate that the modulation of HAS2-AS1 influenced the motility of TNBC cell lines, in which the overexpression of either one of the isoforms of HAS2-AS1 yielded a less aggressive phenotype of the cells.

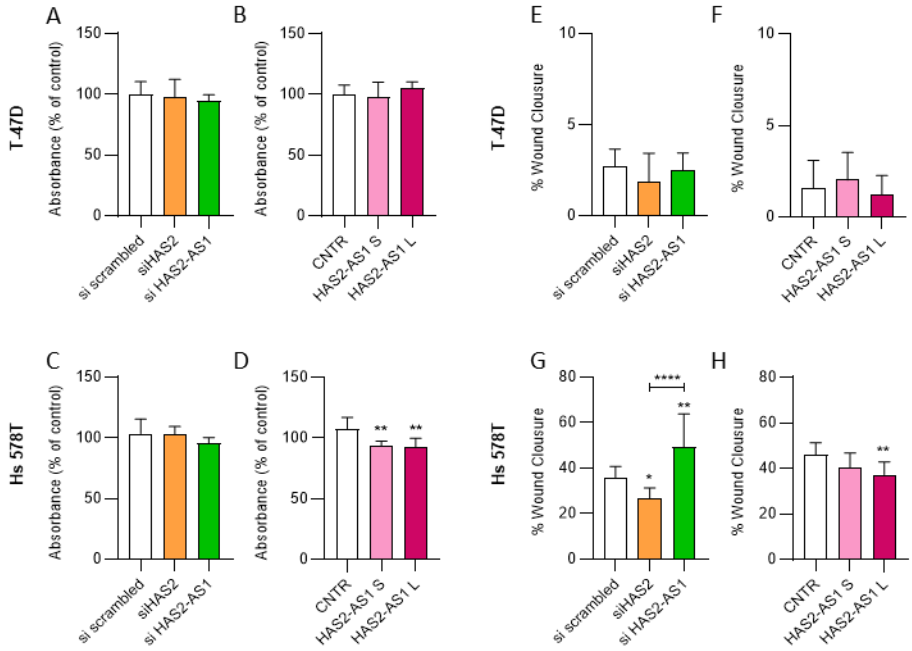

Figure 12. HAS2-AS1 selectively inhibits cell viability and motility in ER-negative breast cancer cells, thus reducing their aggressive phenotype.

(A) *MTT assay performed on T-47D cells after the transfection for 48 hours of HAS2, HAS2-AS1 or scrambled siRNA, or the transfection of* ***(B)*** *pcDNA3 vector overexpressing exon 2 of HAS2-AS1 S or L isoforms with relative control empty vector (CNTR).* ***(C)*** *Hs 578T viability tested through MTT assay upon the transfection of HAS2, HAS2-AS1 or scrambled siRNA or* ***(D)*** *the transfection of pcDNA3 plasmid overexpressing HAS2-AS1 S or L isoforms of exon 2 with relative empty control vector.* ***(E)*** *Scratch assay performed on T-47D cells after the transfection for 48hours of HAS2, HAS2-AS1 or scrambled siRNA or* ***(F)*** *the transfection of pcDNA3 vector overexpressing HAS2-AS1 exon 2 S or L isoforms, with relative empty control vectors.* ***(G)*** *Scratch assay performed on Hs 578T cells after the transfection for 48hours of HAS2, HAS2-AS1 or scrambled siRNA or* ***(H)*** *the transfection of pcDNA3 vector overexpressing HAS2-AS1 exon 2 S or L isoforms, with relative empty control vectors. Bars represent the % of wound closure after 24 hours of migration in absence of serum and are normalized on the initial wound area at time 0. Data were analysed using the free software TScratch. All the experiments were conducted four times in triplicates. Data are expressed as mean ± SEM. **, p<0.01.*

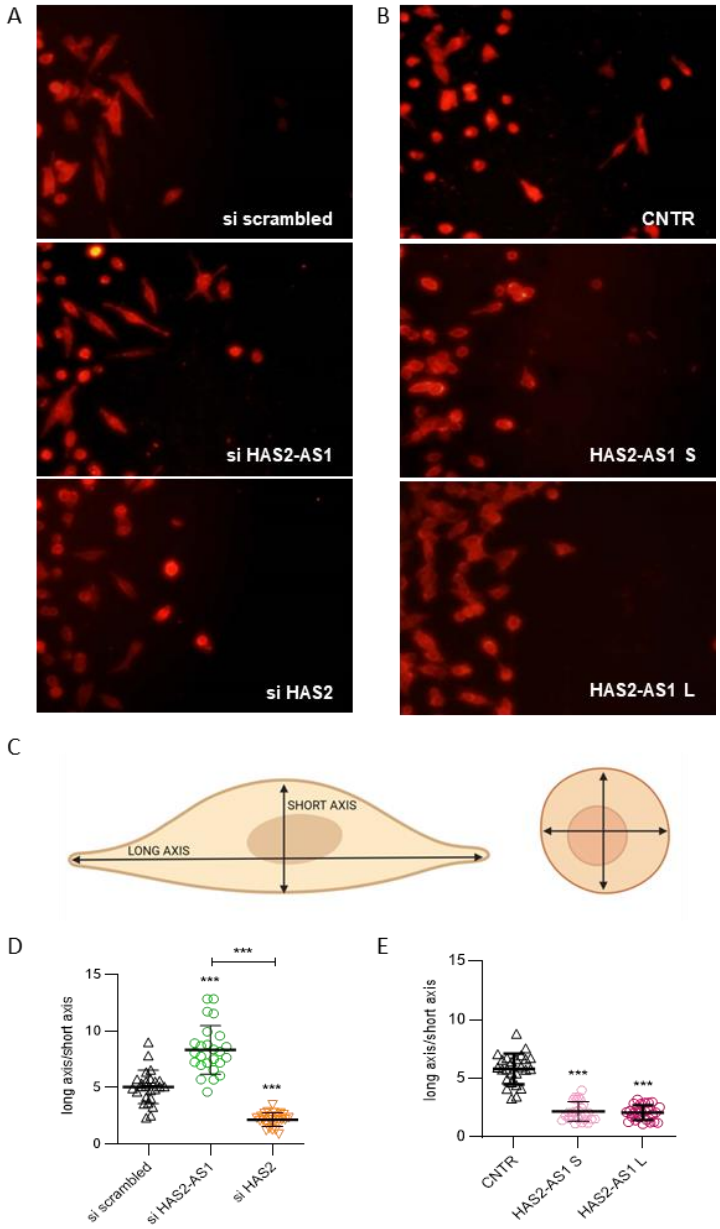

Figure 13: HAS2-AS1 reduces the tumorigenic phenotypes of ER-negative breast cancer cells.
(A) *MDA-MB-231 cell morphology 24 hours after scratch assay. Cells were transfected with 50 nM siRNA against HAS2-AS1 or HAS2 or a siRNA scrambled for 48 hours. siHAS2 was used as a negative control. Magnification 200X.* ***(B)*** *MDA-MB-231 cell morphology 24 hours after scratch assay. Cells were transfected for 48 hours with 2 µg of pcDNA3 vector overexpressing exon 2 of HAS2-AS1 S or L isoforms, or with pcDNA3 empty control vector. Magnification 200X.* ***(C)*** *Representative scheme explaining how cell morphology measures (i.e., short and long axis) were taken from images in panels A and B by using ImageJ software.* ***(D)*** *Quantification of cell morphology changes measuring long axis:short axis ratio in MDA-MB-231 cells in A panels.* ***(E)*** *Quantification of cell morphology changes measuring long axis:short axis ratio in MDA-MB-231 cells in B panels. All the experiments were conducted four times in triplicates. Data are expressed as mean ± SEM. **, p<0.01; ***, p<0.001.*

3. HAS2-AS1 does not alter HAS2 expression and HA levels in MDA-MB-231 cells.

It is well accepted that HAS2-AS1 regulates HA expression and, thus, HA deposition [53], eventually negatively influencing cancer progression [36,130]. In previous experiments, we already demonstrated that in MDA-MB-231 cells HAS2-AS1 modulation altered neither HA released in the culture medium (quantified by ELISA) nor pericellular HA (measured via particle exclusion assay) (data not shown). As a further confirmation, we stained pericellular HA with FITC-conjugated HABP and measured the fluorescence by flow cytometry of MDA-MB-231 cells overexpressing either HAS2-AS1 L or S isoforms of exon 2 or empty pcDNA3 vector, as a control. As shown in figures 14A and 14B, the mean fluorescence intensity did not change upon transient overexpression of the S or L isoform of exon 2 of HAS2-AS1.

As it was quite surprising finding that HAS2-AS1 seems to not be involved in the regulation of HA synthesis, we decided to measure by RT-qPCR the expression of HASes after HAS2-AS1 overexpression. In MDA-MB-231 untreated cells, HAS2 was found to be the more expressed HAS, about 35-fold more expressed than HAS3 (Fig. 14C). HAS1, instead, was non-detectable. Moreover, upon overexpression of the S or L isoforms of exon 2 of HAS2-AS1, both HAS2 (Fig. 14D) and HAS3 (Fig. 14E) transcripts remained at control levels.

These results suggest that in MDA-MB-231 cells, HAS2-AS1 is involved neither in the regulation of HASes expression nor in HA accumulation.

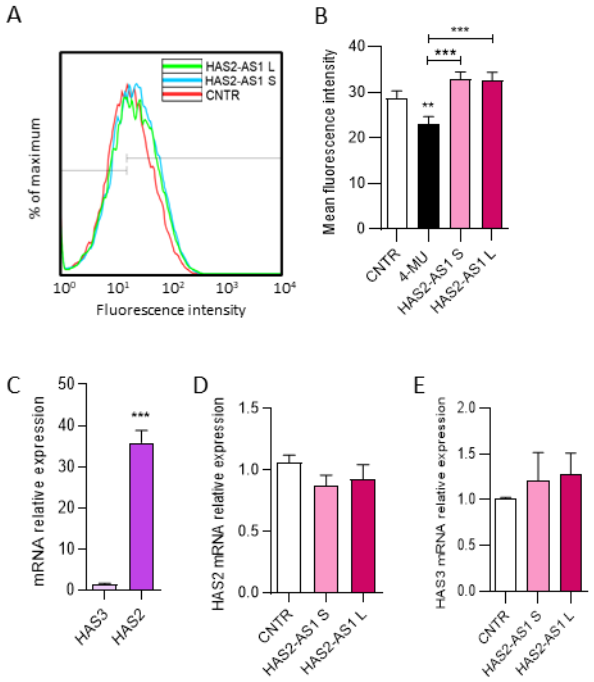

Figure 14. HAS2-AS1 overexpression does not alter HA synthesis in TNBC cell line MDA-MB-231.

(A) *Flow cytometric quantification of pericellular HA using FITC labelled HABP in MDA-MB-231 transfected with 2 µg of pCDNA3 plasmid coding for HAS2-AS1 S (light blue histogram), HAS2-AS1 L (green histogram) or empty control vector (red histogram).* ***(B)*** *Quantified mean fluorescence intensity of histogram A. As a control, 4-MU 0,5µM was used. Bars represent mean ± SEM of three independent experiments.* ***(C)*** *Relative HAS2 and HAS3 gene expression levels quantified via RT-qPCR.* ***(D)*** *RT-qPCR of HAS2 expression in MDA-MB-231 48 hours after transfection with pcDNA3 vector coding for HAS2-AS1 S or L isoforms of exon 2 or empty control vector.* ***(E)*** *RT-qPCR of HAS3 expression in MDA-MB-231 transfected for 48 hours with pcDNA3 vector coding for HAS2-AS1 S or L isoforms of exon 2 or empty control vector. Data are reported as mean ± SEM of four independent experiments. ***, p< 0.001.*

4. Establishment and characterization of a TNBC cellular model stably overexpressing ectopic L isoform of exon 2 of HAS2-AS1.

All the experiments described above have been obtained by transiently transfecting cells. The main problem related to this method derives from the possible arising of undesirable effects as cellular stress due to massive overexpression of the gene of interest, or even membrane damages due to lipofection. Hence, we decide to produce stable MDA-MB-231 clones overexpressing the L isoform of exon 2 of HAS2-AS1. In such a way, we were also able to perform experiments requiring lengthy cell cultivation. We concentrated on producing HAS2-AS1 L clones because the transient transfection of this 256 bp fragment (Fig. 15) was able to significantly reduce cell viability and motility in both MDA-MB-231 and Hs 578T cells, showing a length-dependent stronger effect compared to the S isoform in the MDA-MB-231 cell line (data not shown).
We managed to select two HAS2-AS1 L overexpressing clones (namely, cl. LONG 1 and cl. LONG 2) and two control clones overexpressing the empty pcDNA3 vector (namely, cl. CNTR 3 and cl. CNTR 4). As shown in figure 16A, both cl. LONG 1 and cl. LONG 2 expressed significantly higher levels of HAS2-AS1 exon 2 L isoform compared to cl. CNTRs. Interestingly, cl. LONG 2 expressed almost twice as much HAS2-AS1 L transcript levels as cl. LONG 1, providing us with the opportunity to investigate dose-dependent effects of HAS2-AS1 overexpression.

During the preliminary characterization of the clones, we confirmed that, as we observed with transient HAS2-AS1 L or S overexpression, HAS2-AS1 modulation has no implications in regulating HA deposition. Indeed, pericellular coating assay highlighted that the two cl. CNTRs had a significantly higher amount of pericellular HA compared to cl. LONG 1 and 2 (Fig. 16B), even though a slight increase in HAS2 mRNA expression levels was seen in cl. LONG 1 and 2 with respect to control clones (Fig. 16C). However, western blot analysis confirmed that, effectively, no significant increase in HAS2 protein level was detectable between LONG and CNTR clones (Fig. 16D, 16E).

At this point, we wanted to investigate deeper the ability of HAS2-AS1 in regulating MDA-MB-231 cell viability. As the stability of HAS2-AS1 exon 2 L isoform overexpression in the selected clones allowed us to perform growth experiments spanning from seven to twenty days, we firstly decided to evaluate the clonogenic abilities of LONG clones compared to CNTR clones, performing a 10-days two-dimensional colony formation assay. Interestingly, cl. LONG 2 generated significantly fewer and smaller colonies with respect to both cl. CNTRs (Fig. 16F, 16H). On the other hand, cl.

LONG 1, which expressed almost half as much HAS2-AS1 L exon 2 as cl. LONG 2, produced a number of colonies similar to cl. CNTRs.

In support of these data, we tested the anchorage-independent cell growth abilities in soft agar of the stable clones. Also in this case, cl. LONG 2 showed to be less prone to produce colonies, which were even significantly smaller than those of cl. CNTR 3 and 4 (Fig. 16G, 16I). Similarly, to the previous clonogenic experiment, cl. LONG 1 behaved more similarly to cl. CNTRs than cl. LONG 2.

As a final evaluation of the effect of HAS2-AS1 L overexpression on TNBC cell proliferation, cell numbers for each clone were counted each 24 hours, for a total of 7 days – live-cells numbers were eventually used to generate a cell growth curve. cl. LONG 2 appeared the less proliferative clone among all, even compared to cl. LONG 1 (Fig. 16L). Indeed, cl. LONG 2 had a mean population doubling of 3,12 compared to cl. LONG 1 with 4,85, cl. CNTR 3 with 4,68 and cl. CNTR 4 with 4,62.

We concluded the characterization of the HAS2-AS1 L overexpressing cellular model looking at their cellular shape and motility (Fig. 17A). Interestingly, both cl. LONG 1 and 2 confirmed that HAS2-AS1 L isoform overexpression induces a significant change in cellular shape, as they were more roundish and epithelial-like compared to the elongated mesenchymal-like cl. CNTR 3 and 4 (Fig. 17B). As a confirmation, upon scratch assay, both LONG clones showed even a significantly reduced motility compared to CNTR clones (Fig. 17C).

All these results on stable clones confirmed that high levels of HAS2-AS1 exon 2 reduced the tumorigenic phenotypes of MDA-MB231 cells, including migration, cell polarization, clonogenicity and growth. Interestingly, it appeared that the higher the overexpression levels of HAS2-AS1 L, the better the results in terms of tumour suppression, as cl. LONG 2 expressed almost twice as much HAS2-AS2 exon 2 L as cl. LONG 1.

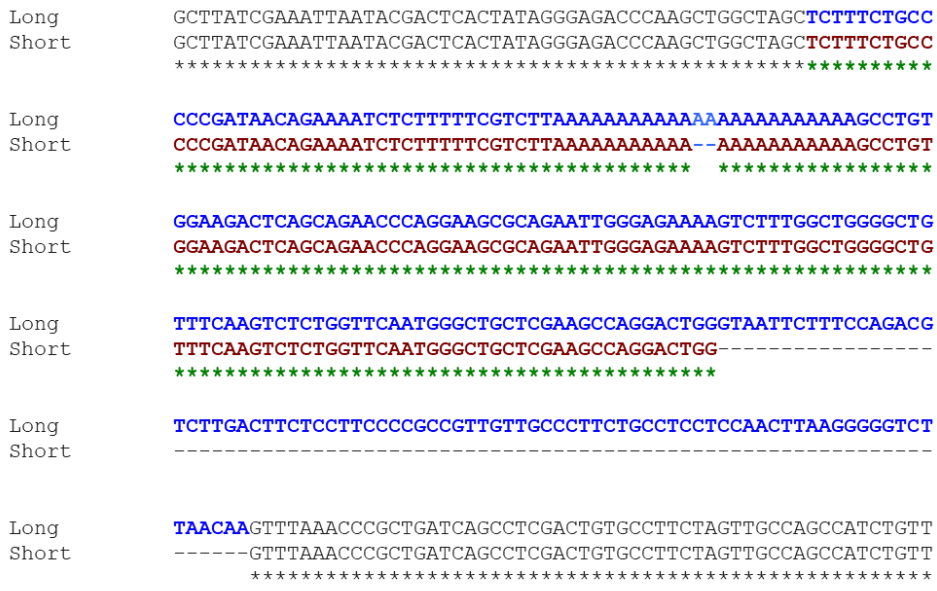

Figure 15. HAS2-AS1 S and L sequences.

Alignment of inserts of pcDNA3-HAS2-AS1 exon 2 long (L) and pcDNA3-HAS2-AS1 exon 2 short (S), a kind gift of Timothy Bowen (Cardiff University, UK). In black the vector sequence, in blue HAS2-AS1 exon 2 long, and in red HAS2-AS1 exon 2 short. The two AA missing in the short isoform are likely due to technical error due to the long poly-adenine string sequencing.

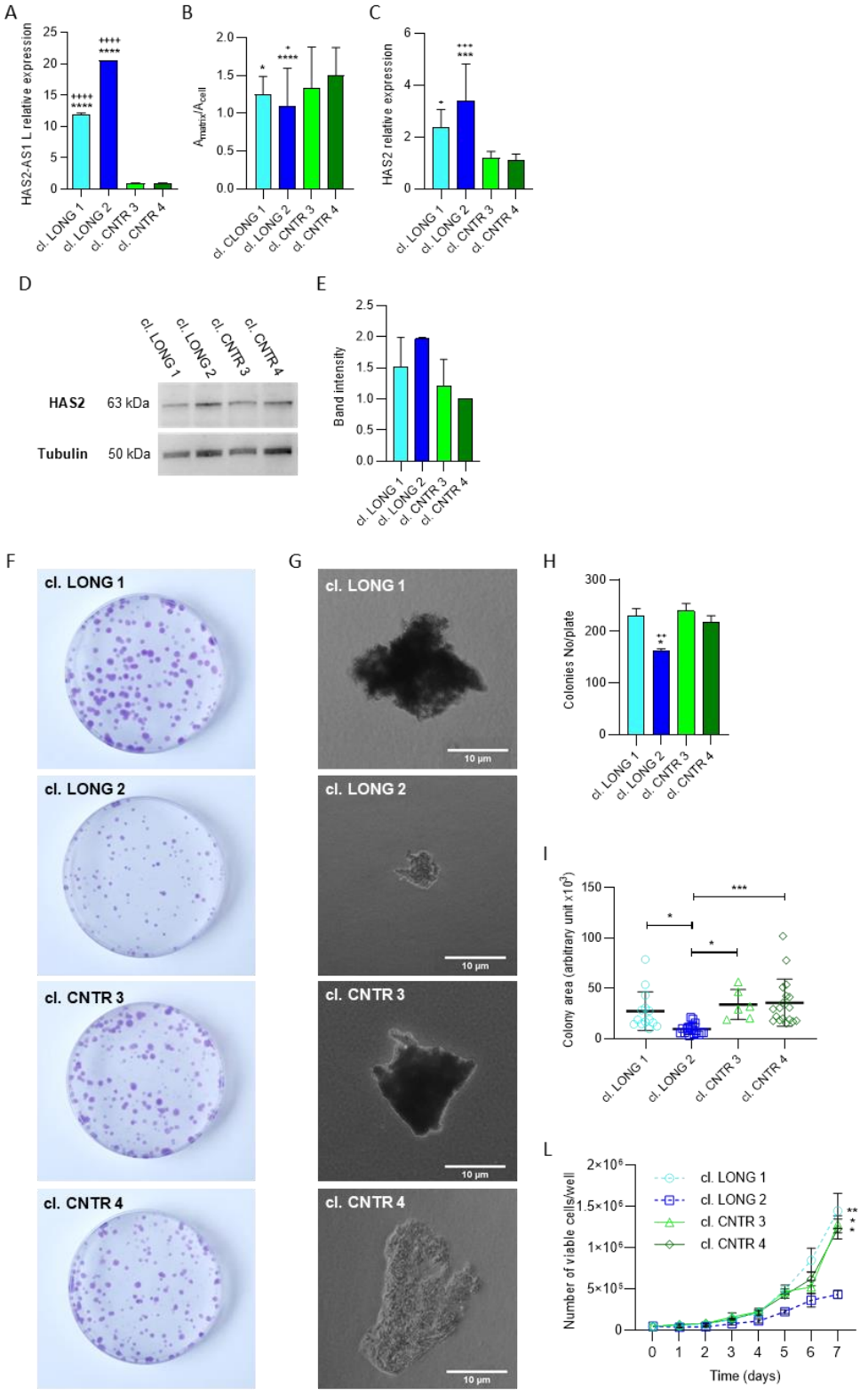
A
HAS2-AS1 L relative expression
cl. LONG 1
cl. LONG 2
cl. CNTR 3
cl. CNTR 4
B
A_{matrix}/A_{cell}
C
HAS2 relative expression
D
HAS2 63 kDa
Tubulin 50 kDa
E
Band intensity
F
cl. LONG 1
cl. LONG 2
cl. CNTR 3
cl. CNTR 4
G
10 µm
H
Colonies No/plate
I
Colony area (arbitrary unit x10^3)
L
Number of viable cells/well
Time (days)

Figure 16. Impact of HAS2-AS1 L stable clones on cell growth, clonogenicity, and migration.

(A) *RT-qPCR analyses measuring HAS2-AS1 exon 2 L expression levels in MDA-MB-231 cl. LONG 1 and cl. LONG 2 or cl. CNTR 3 and cl. CNTR 4. Data are reported as mean ± SEM of three independent triplicates.* ***(B)*** *Particle exclusion assay of cl. LONG 1, cl. LONG 2 or control clones cl. CNTR 3 and cl. CNTR 4. Cells were also treated with 2U/ml Hyaluronidase from Streptomyces hyalurolyticus, as a control for HA presence in the ECM. Results are expressed as the ratio between the area of ECM delimited by red blood cells and the area of the cell by using ImageJ. Data are shown as mean ± SEM of three independent experiments.* ***(C)*** *RT-qPCR analyses measuring HAS2 expression in cl. LONG 1 and cl. LONG 2 or control clones cl. CNTR 3 and cl. CNTR 4. Data are reported as mean ± SEM of three independent triplicates.* ***(D)*** *Representative blot of immunoreactive bands for HAS2 and tubulin from total protein extracts obtained from cl. LONG 1 and cl. LONG 2 or control clones cl. CNTR 3 and cl. CNTR 4. Numbers at the margins of the blots indicate relative molecular weights of the respective protein in kDa.* ***(E)*** *Relative band intensity of HAS2 immunoblotting. Values are expressed as mean±SEM of 2 experiments of the percentage variation of the normalized optical density (O.D.) obtained from each sample with respect to values obtained in cl. CNTR 4.* ***(F)*** *Representative images of clonogenic assay of MDA-MB-231 stable clones overexpressing HAS2-AS1 L or empty vector at 10 days after seeding.* ***(G)*** *Soft-agar colony formation assay of MDA-MB-231 stable clones overexpressing HAS2-AS1 L or empty vector at 20 days after seeding. Magnification 400X.* ***(H)*** *Numbers of colonies of MDA-MB-231 stable clones cl. LONG 1, cl. LONG 2 or control clones cl. CNTR 3 and cl. CNTR 4 at 10 days after seeding, from panel F. Data are shown as mean ± SEM of three independent experiments.* ***(I)*** *Quantification of soft-agar colony areas from panel G measured via ImageJ. Data are displayed as mean ± SEM of three independent duplicates.* ***(L)*** *Growth curve of MDA-MB-231 stable clones overexpressing HAS2-AS1 L or empty vector. Values are reported as the average of three triplicates ± SEM. *, p<0.5; **, p<0.01 ***, p<0.001; ****, p<0.0001. + represent significance with respect to cl. CNTR 3; * Represent significance with respect to cl. CNTR 4.*

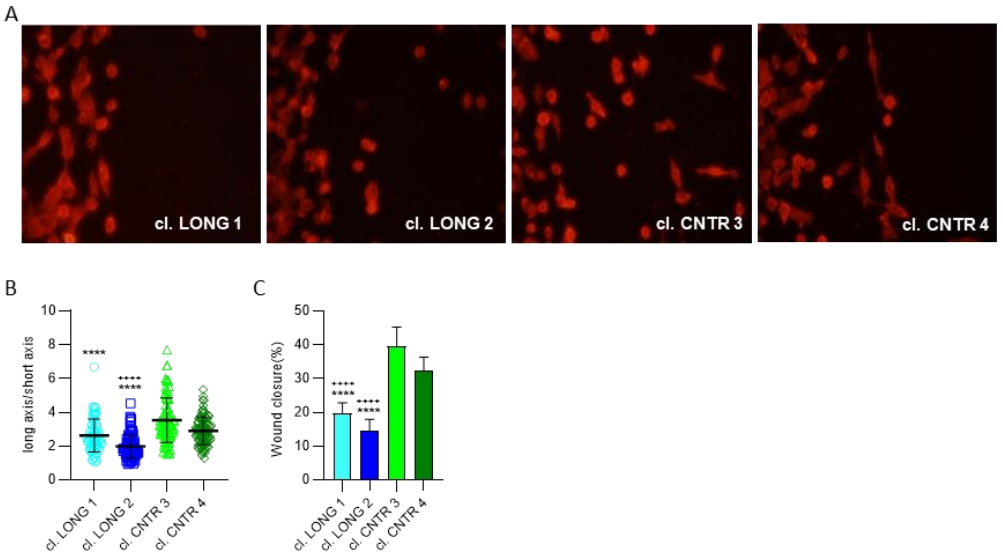

Figure 17. Impact of HAS2-AS1 L stable clones on cell polarity.

(A) *Representative images of cl. LONG 1 and cl. LONG 2 or control clones cl. CNTR 3 and cl. CNTR 4 24 hours after scratch assay, used to measure long axis:short axis ratio. Magnification 200X.* ***(B)*** *Quantification of cell morphology changes measuring long axis:short axis ratio in cl. LONG 1, cl. LONG 2 or control clones cl. CNTR 3 and cl. CNTR 4, from panel A. Data are expressed as mean ± SEM of three independent triplicates.* ***(C)*** *Scratch assay performed on cl. LONG 1, cl. LONG 2 or control clones cl. CNTR 3 and cl. CNTR 4. Bars represent the % of wound closure after 24 hours of migration in presence of 0,1% serum and are normalized on the initial wound area at time 0. Data were analysed using the free software TScratch and represented as mean ± SEM of four independent experiments. ****, p<0.0001. + represent significance with respect to cl. CNTR 3; * Represent significance with respect to cl. CNTR 4.*

5. HAS2-AS1 regulates mesenchymal-to-epithelial transition in TNBC cells.

Cells transitioning between epithelial and mesenchymal status because of EMT or MET, undergo conformational changes, which are related to the acquisition or loss of migratory capabilities [195]. As we observed a conformational switch of stable clones from the elongated shape of cl. CNTRs to the more roundish one of cl. LONGs (see Fig. 17), we decided to investigate deeper into the possibility of HAS2-AS1 regulating MET.

Immunofluorescence analysis of cl. CNTR 3 and 4, showing a mesenchymal-like morphology, displayed increased staining of Fibronectin and cytoplasmic ZO-1. On the contrary, cl. LONG 1 and 2 showed a decreased Fibronectin staining, but increased membrane-localised ZO-1, with cl. LONG 2 having a more marked difference compared to CNTR clones (Fig. 18A). As a validation, cl. LONG 1 and 2 showed a drop in transcript levels of mesenchymal markers Vimentin (Fig. 18B) and Fibronectin (Fig. 18C), but an increment in mRNA amounts of epithelial markers E-cadherin (Fig. 18D) and to some extent ZO-1 (Fig. 18E), compared to control clones.

HAS2-AS1 involvement in EMT regulation has already been demonstrated to function through the TGFβ pathway in mouse mammary cells [151]. In HAS2-AS1 overexpressing clones, and, in particular, in cl. LONG 2, receptor 3 for TGFβ (TGFBR3) expression was downregulated to cl. CNTR 3 and 4 (Fig. 18F). Similarly, the mRNA levels of the well-known EMT regulator and TGFβ-controlled Snai1 were significantly lower in cl. LONG 1 and 2 compared to cl. CNTR 3 and 4 (Fig. 18G).

Finally, we wanted to look at CD44s, whose expression is related to EMT and metastasis in breast cancer. As shown in figure 18H, cl. LONG 2 had a lower expression of CD44s with respect to cl. CNTRs and even cl. LONG 1.

All these data taken together suggest that HAS2-AS1 overexpression induces a switch of MDA-MB-231 cells from an aggressive mesenchymal phenotype (visible in cl. CNTR 3 and 4) to an epithelial one, thus prompting through a MET transition.

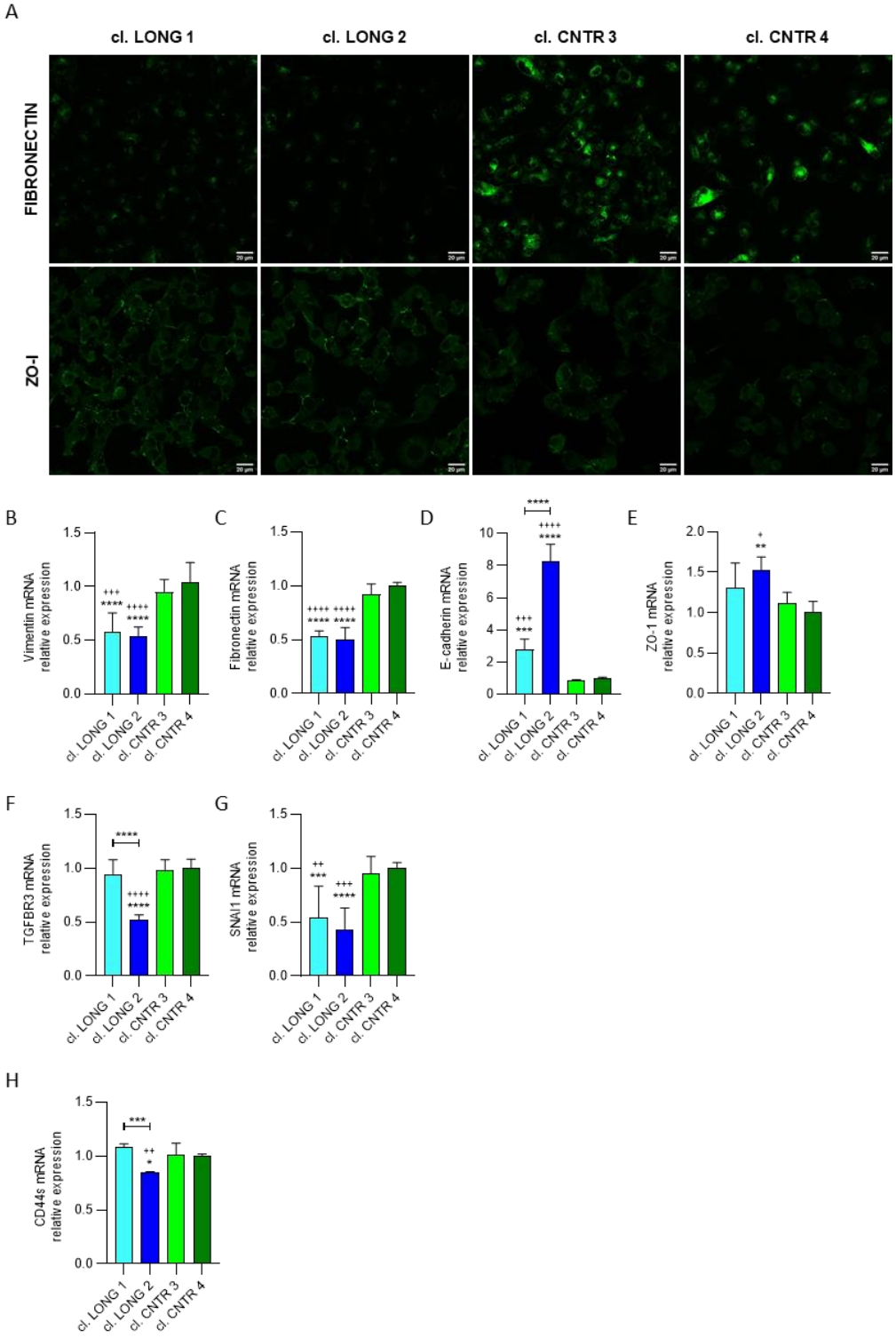
A
cl. LONG 1
cl. LONG 2
cl. CNTR 3
cl. CNTR 4
FIBRONECTIN
ZO-I
B
Vimentin mRNA relative expression
C
Fibronectin mRNA relative expression
D
E-cadherin mRNA relative expression
E
ZO-1 mRNA relative expression
F
TGFBR3 mRNA relative expression
G
SNAI1 mRNA relative expression
H
CD44s mRNA relative expression

Figure 18. Impact of HAS2-AS1 L overexpression on MET.

(A) Confocal microscopy images of Fibronectin deposition and the tight junction protein ZO-1 in HAS2-AS1 L overexpressing clones cl. LONG 1 and 2 or control clones cl. CNTR 3 and 4. Magnification 400X. RT-qPCR a*nalyses measuring **(B)** Vimentin, **(C)** Fibronectin, **(D)** E-cadherin, **(E)** ZO-1, **(F)** TGFBR3, **(G)** SNAI1 or **(H)** CD44s expression in MDA-MB-231 stable clones overexpressing HAS2-AS1 L exon 2 (cl. LONG 1, cl. LONG 2) or empty control vectors (cl. CNTR 3 and cl. CNTR 4). Values are reported as the average of three independent triplicates ± SEM. *, p<0.5; **, p<0.01 ***, p<0.001; ****, p<0.0001. + represent significance in respect to cl. CNTR 3; * Represent significance in respect to cl. CNTR 4.*

6. Affymetrix microarray analysis of stable clones overexpressing the L isoform of exon 2 of HAS2-AS1.

Due to our previously described discovery, that in MDA-MB-231 cells HAS2-AS1 does not regulate HA deposition (Fig. 14, 16B), we sought to investigate further into mechanistic pathways that may be effectively altered and regulated by this antisense transcript. cl. LONG 2 (the clone expressing higher levels of HAS2-AS1 exon 2 L isoform) and cl. CNTR 4 were subjected to transcriptome analysis using Affymetrix Clariom S microarrays. Genes that may be regulated by HAS2-AS1 were identified using the Transcriptome Analysis Control 4.0 software, applying the filtering criteria of the fold change of 4-fold or higher and FDR p-value of below 0.05. In total, 366 unique genes were found to satisfy these criteria, of which 146 were upregulated and 220 were downregulated (Fig. 19A). The list of 366 genes was then uploaded into Database for Annotation, Visualization, and Integrated Discovery (DAVID) v6.8 for categorization according to their GOTERM BP functions (Fig. 19B, 19C). The lists of upregulated and downregulated genes with their corresponding functional categories are provided in Supplemental tables 1 and 2.

We further analysed the list of differentially expressed genes using the Kyoto Encyclopedia of Genes and Genomes (KEGG) to identify possible pathways that may be regulated by overexpression of HAS2-AS1. The pathways that were identified amongst the downregulated genes include (Figure 19D): TGFβ and chemokine signalling pathways, focal adhesion, ECM-receptor interaction, pathways in cancer and PI3K/Akt signalling pathway. In contrast, Jak/Stat signalling (with five associated genes) was the only pathway of upregulated genes found by KEGG analysis of the upregulated genes (data not shown).

To validate data obtained from the microarray analysis, we measured via RT-qPCR the mRNA levels of some genes involved in regulating cell proliferation and, thus, cancer progression. Epiregulin (EREG) (Fig. 19E), CCND1 (Fig. 19F) and AKT1 (Fig. 19G) transcripts, coding for three master inducers of the cell cycle, showed to be significantly downregulated in HAS2-AS1 overexpressing cl. LONG 1 and 2 with respect to the control clones. Similarly, the transcript for

p21 (Fig. 19H) cell cycle inhibitor was upregulated in cl. LONG 1 and 2 compared to cl. CNTR 3 and 4. Notably, all the four analysed genes were found to be similarly deregulated by HAS2-AS1 exon 2 L isoform overexpression when microarray analysis was performed. Specifically, they all had a fold change > of 1.3, with a p-value<0.5.

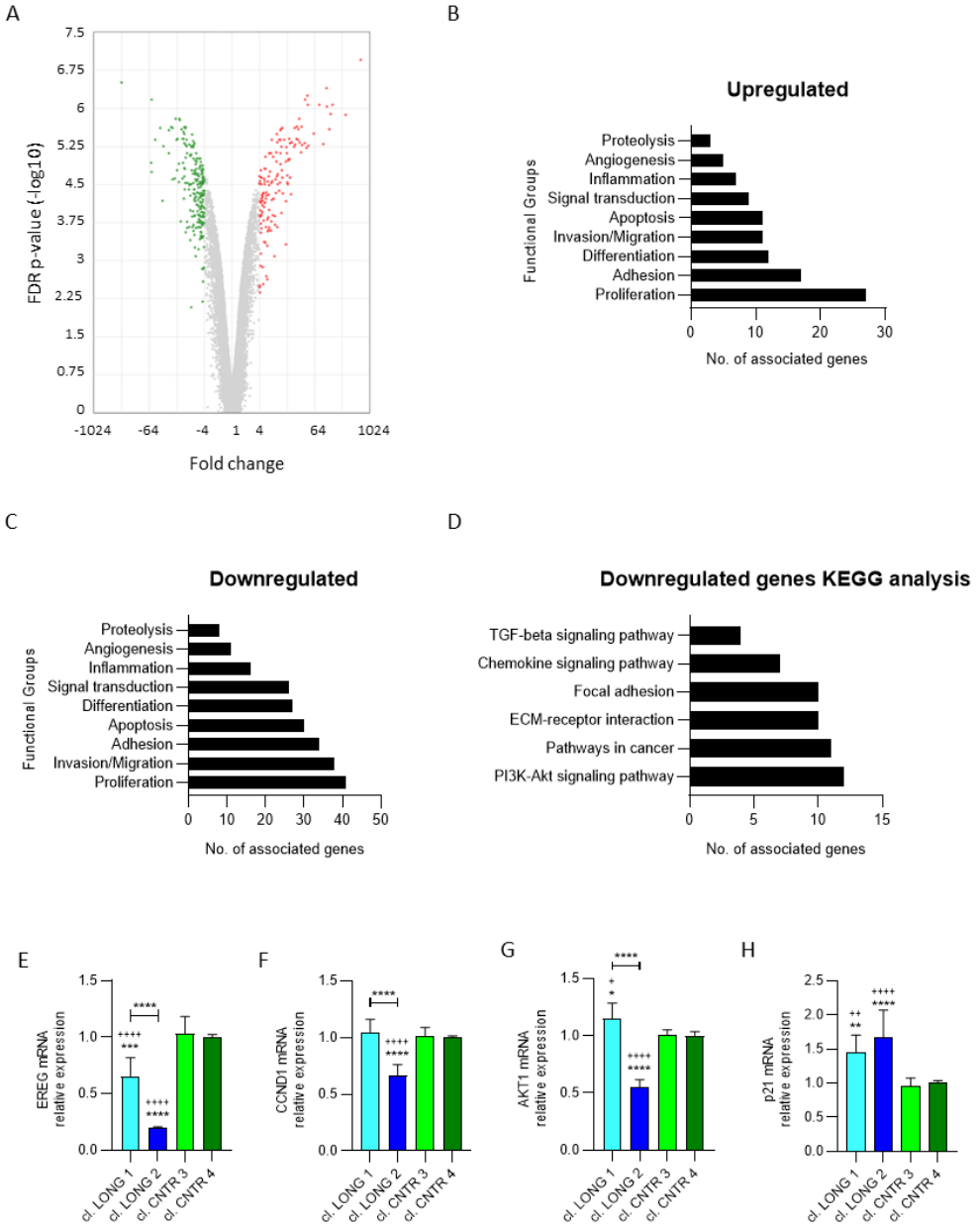

Figure 19: Analysis of differentially expressed genes in cl. LONG 2 or control cl. CNTR 4.
(A) *Volcano plot of transcriptome comparison. Genes that were significantly up- or downregulated by at least 4-fold are shown in red or green respectively. Statistical significance is defined as a false discovery rate (FDR) adjusted p-value of below 0.05.* ***(B)*** *Upregulated and* ***(C)*** *downregulated genes uploaded onto DAVID and functionally sorted.* ***(D)*** *Several pathways identified among the downregulated genes from KEGG analysis.* RT-qPCR *analyses measuring* ***(E)*** *EREG,* ***(F)*** *p21,* ***(G)*** *AKT1,* ***(H)*** *CCDND1 expression in MDA-MB-231 stable clones overexpressing HAS2-AS1 L exon 2 (cl. LONG 1, cl. LONG 2) or empty control vectors (cl. CNTR 3 and cl. CNTR 4). Values are reported as the average of three independent triplicates ± SEM. *, p<0.5; **, p<0.01 ***, p<0.001; ****, p<0.0001. + represent significance in respect to cl. CNTR 3; * Represent significance in respect to cl. CNTR 4.*

7. HAS2-AS1 acts as a ceRNA for miR-186-3p in MDA-MB-231 cells.

Given that the functions of lncRNAs are associated with their subcellular localization, we performed a nuclear/cytoplasmic fractioning to look at HAS2-AS1 relative abundance in the two cellular compartments. The analysis revealed that HAS2-AS1 is localized almost equally in both the nucleus and cytoplasm (Fig. 20A).

Therefore, as it seems that HAS2-AS1 is not involved in the regulation of HA deposition (Fig. 14D), we started investigating possible cytoplasmic functions of HAS2-AS1. In particular, we focused on the sponge effect, as a lot of studies have shown that lncRNAs can function as ceRNAs modulating miRNA expression [130,196–198].

The combined usage of different online tools (namely miRanda, DIANA-microT-CDS and RNAhybrid), allowed us to investigate possible miRNAs binding HAS2-AS1 sequence. We concentrated on exon 2 of HAS2-AS1, as all our previous experiments exploiting exon 2 L or S isoforms already demonstrated that it has significant effects in modulating cancer aggressiveness. According to the predicted results, HAS2-AS1 exon 2 showed to contain two putative binding sites for miR-186-3p, with a medium free energy (MFE) of -14.9 kcal/mol and -23.2 kcal/mol.

Thus, as a first confirmation, we measured miR-186-3p transcript levels in MDA-MB-231 cells via RT-qPCR, after HAS2-AS1 exon 2 S or L isoforms overexpression. In both cases, the overexpression of HAS2-AS1 exon 2 isoforms yielded a significant reduction of miR-186-3p levels (Fig. 20B), but not miR-186-5p (used as a control) (Fig. 20C), showing a stronger effect when overexpressing the L isoform. Moreover, a luciferase assay demonstrated that when overexpressing miR-186-3p in MDA-MB-231 cells, the luciferase expression of pmirGLO carrying HAS2-AS1 exon 2 S or L miRNA responsive element (MRE) was significantly decreased (Fig. 20D, 20E). Contrariwise, miR-186-5p overexpression did not affect luciferase expression (Fig. 20D, 20E). When mutating HAS2-AS1 exon 2 MRE (Fig. 20F) and overexpressing miR-186-3p, instead, luciferase expression was not affected, and its value was comparable to that of the control (Fig. 20G).

These data suggest that HAS2-AS1 can exert its functions as a regulator of gene expression both in the nucleus and in the cytoplasm, and that exon 2 can bind miR-186-3p, but not its companion miR-186-5p.

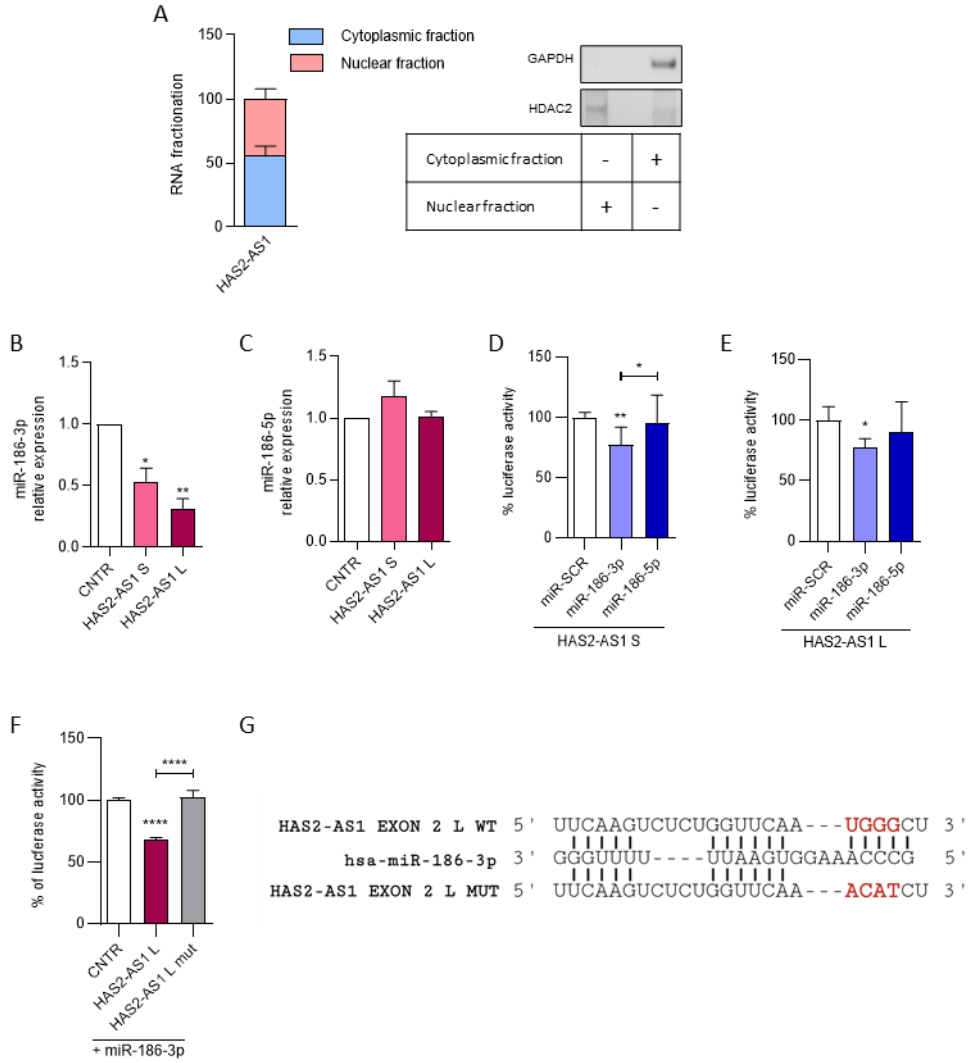

Figure 20. HAS2-AS1 can sponge miR-186-3p in TNBC cells.

(A) *Subcellular localization of HAS2-AS1. RNA fractionation was performed in MDA-MB-231 cells and the subcellular distribution of HAS2-AS1 transcripts is indicated. Corresponding immunoblotting against HDAC and GAPDH served as markers for nuclear and cytoplasmic, respectively. Values are reported as the average of three independent triplicates ± SEM. RT-qPCR analyses measuring* ***(B)*** *miR-186-3p and* ***(C)*** *miR-186-5p expression in MDA-MB-231 overexpressing HAS2-AS1 exon 2 L or S or empty pcDNA3 vector as a control. Values are reported as the average of three independent triplicates ± SEM. Dual-luciferase activity assay on MDA-MB-231 cells cotransfected with 2 µg of pMIR-GLO plasmid coding for HAS2-AS1* ***(D)*** *S,* ***(E)*** *L or* ***(F)*** *mutated L MRE and 100 pmol of miR-SCR, miR-186-3p or miR-186-5p mimics. Luciferase activity was normalised on Renilla. Data are reported as the average of six independent triplicates ± SEM. *, p<0.5; **, p<0.001; ****, p<0.0001.* ***(G)*** *Sequence alignment of the WT and MUT HAS2-AS1 exon 2 L isoform, indicating the potential binding sites for miR-183-3p.*

8. miR-186-3p sponging by HAS2-AS1 affects TNBC cell migration and viability

To confirm that miR-186-3p binding by HAS2-AS1 exon 2 was the explanation for the changes in cell behaviours we observed (see Fig. 12), we tested miR-186-3p ability to regulate cell migration and viability. Hence, we transfected MDA-MB-231 cells with either a mimetic or an antagonist of miR-186-3p, the latter to simulate the sponging of miR-186-3p by HAS2-AS1. As shown in figure 21A, miR-186-3p mimic induced a significant increase in two-dimensional cell migration, which was reverted when overexpressing the miR-186-3p antagonist, instead. Similarly, miR-186-3p overexpression induced a significant increase in MDA-MB-231 cell viability, which instead was significantly reduced compared to the control cells after miR-186-3p antagonist transfection (Fig. 21B).

In the same way, we also conducted scratch and MMT assays on MDA-MB-231 cells overexpressing either HAS2-AS1 exon 2 L in its wild-type (WT) or mutated (MUT) form. While HAS2-AS1 L overexpression caused a decrease in both cell motility and viability, the transfection of HAS2-AS1 L bearing mutations in the MRE for miR-186-3p, retrieved cell viability and motility almost at the control levels (Fig. 21C, 21D).

These results suggest that the manipulation of miR-186-3p expression, hypothetically via HAS2-AS1 overexpression, regulates both migration and viability of TNBC cells.

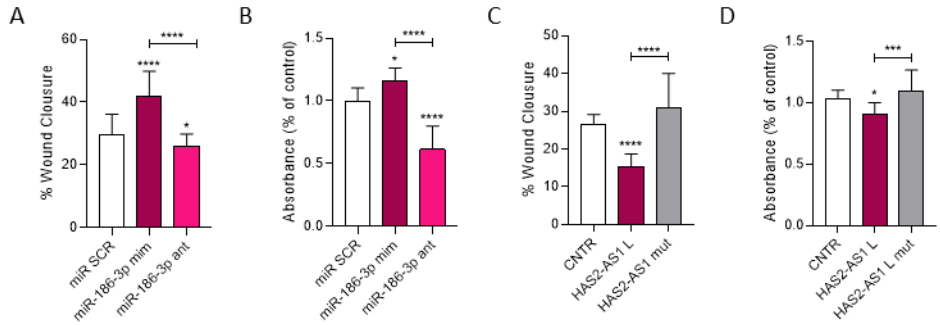

Figure 21. miR-186-3p involvement in regulating viability and migration of MDA-MB-231 TNBC cell line.
(A) *Scratch assay performed on MDA-MB-231 cells after the transfection for 24 hours of miR-186-3p mimic, antagonist or miR-SCR. Bars represent the % of wound closure after 24 hours of migration in absence of serum and are normalized on the initial wound area at time 0. Data were analysed using the free software Tscratch.* ***(B)*** *MTT assay performed on MDA-MB-231 cells after the transfection for 24 hours of miR-186-3p mimic, antagonist or miR-SCR.* ***(C)*** *Scratch assay performed on MDA-MB-231 cells after the transfection for 48 hours of HAS2-AS1 exon 2 L isoform WT or MUT, with relative pcDNA3 empty control vector. Bars represent the % of wound closure after 24 hours of migration in absence of serum and are normalized on the initial wound area at time 0. Data were analysed using the free software TScratch.* ***(D)*** *MTT assay performed on MDA-MB-231 cells upon the transfection for 48 hours of HAS2-AS1 exon 2 L isoform WT or MUT, with relative pcDNA3 empty control vector. All the experiments were conducted three times in triplicates. Data are expressed as mean± SEM. **, p<0.01; ***, p<0.001.*

9. HAS2-AS1 overexpression induces apoptosis in MDA-MB-231 cells.

Among the pathways found altered with the DAVID analysis performed on microarray results of MDA-MB-231 L overexpressing clone, there was apoptosis (Fig. 19B, 19C). As it is a pathway greatly altered in tumours and, since MDA-MB-231 HAS2-AS1 overexpressing stable clones showed reduced proliferation capabilities with respect to cl. CNTRs (see Fig. 16L), we felt it was necessary to investigate deeper into the regulation of apoptosis upon HAS2-AS1 modulation. Therefore, as a starting point, we performed a TUNEL assay, which allowed us to directly visualise apoptotic cells via confocal microscopy. Both transient and stable HAS2-AS1 overexpression gave promising results in terms of apoptosis induction. Indeed, when transiently overexpressing HAS2-AS1 either S or L isoforms, we observed an increase in the percentage of TUNEL-positive cells compared to control cells, with a stronger effect of L isoform (Fig. 22A, 22B). Moreover, overexpression of HAS2-AS1 exon 2 L bearing a mutation in miR-186-3p MRE, showed no induction of apoptosis with respect to the control, suggesting involvement of miR-186-3p in regulating apoptosis in TNBC cells. Similarly, both cl. LONG 1 and 2 showed a significantly higher number of TUNEL positive cells over the cl. CNTR 3 and 4, with cl. LONG 2 having a significantly stronger apoptotic-inducing effect compared to cl. LONG 1 (Fig. 22C, 22D).

RT-qPCR analysis of transcript levels of several apoptosis regulators confirmed the TUNEL assay data. mRNA levels of apoptosis inhibitors Bcl-2 (Fig. 23A) and XIAP (Fig. 23B) were not altered in any of the stable clones. PUMA (Fig, 23C), BAX (Fig. 23D) and NOXA (Fig. 23E) inducers, instead, were significantly upregulated in cl. LONG 2 and to some extent also in cl. LONG 1.

Interestingly, the pro-apoptotic gene P2RX7 was also significantly upregulated in cl. LONG 1 and 2 (Fig. 23F). This gene has been already described in the literature to be under the control of miR-186 [199].

Validating this data, caspase-3 and -7 activity was evaluated via a luminescence assay – HAS2-AS1 L or S overexpression provoked an increase in caspase activity compared to control cells (Fig. 24A). Via immunoblotting, we confirmed caspase-3 activation, as the amount of active cleaved caspase-3 is higher in cl. LONG 1 and 2 to cl. CNTR 3 and 4 (Fig. 24B, 24C).

To understand if apoptosis was promoted via the intrinsic or extrinsic pathways, we look at both caspase-8 and -9 activations. While no active cleaved caspase-8 was detected in none of MDA-MB-231 stable clones (i.e., neither cl. LONGs nor cl. CNTRs) (Fig. 24D), a significantly higher

amount of active cleaved caspase-9 was observed in Cl. LONG 2 (Fig. 24E, 24F), suggesting that the intrinsic pathway is the one upregulated via HAS2-AS1 modulation.

All these data suggest that HAS2-AS1 is involved in the regulation of apoptosis, inducing the intrinsic mitochondrial pathways. Moreover, at least the P2RX7 gene is involved, also providing proof that apoptosis in MDA-MB-231 could be regulated via miR-186-3p sponging by HAS2-AS1.

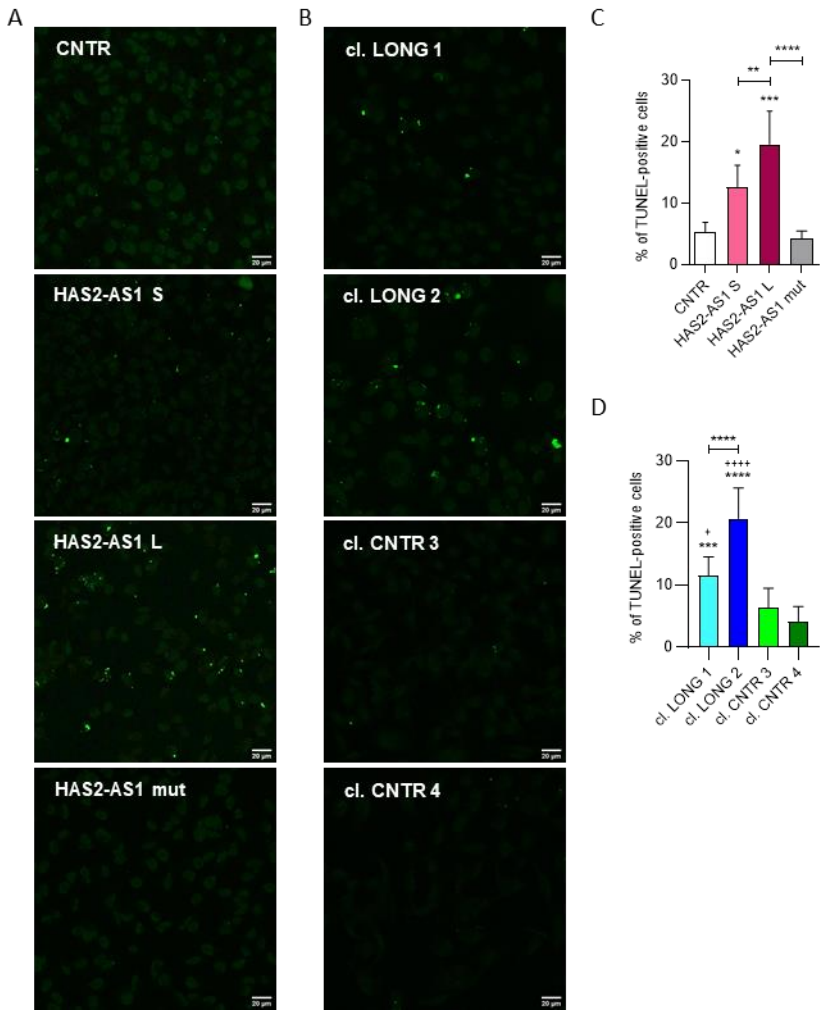

Figure 22. HAS2-AS1 overexpression induces apoptosis in MDA-MB-231 cells.
(A) *Apoptosis evaluation with TUNEL assay in MDA-MB-231 cells after the transfection for 48 hours of HAS2-AS1 exon 2 S or L WT isoforms or MUT L, with relative pcDNA3 empty control vector.* ***(B)*** *Quantification of the percentage of TUNEL-positive cells from panel A.* ***(C)*** *Apoptosis evaluation with TUNEL assay in MDA-MB-231 stable clones overexpressing HAS2-AS1 exon 2 L isoform (cl. LONG 1 and 2) or empty pcDNA3 vector (cl. CNTR 3 and 4).* ***(D)*** *Quantification of the percentage of TUNEL-positive cells from panel C. All the experiments were conducted three times in triplicates. Data are expressed as mean ± SEM. *, p<0.5; **, p<0.001; ***, p<0.001; ****, p<0.0001. + represent significance with respect to cl. CNTR 3; * Represent significance with respect to cl. CNTR 4.*

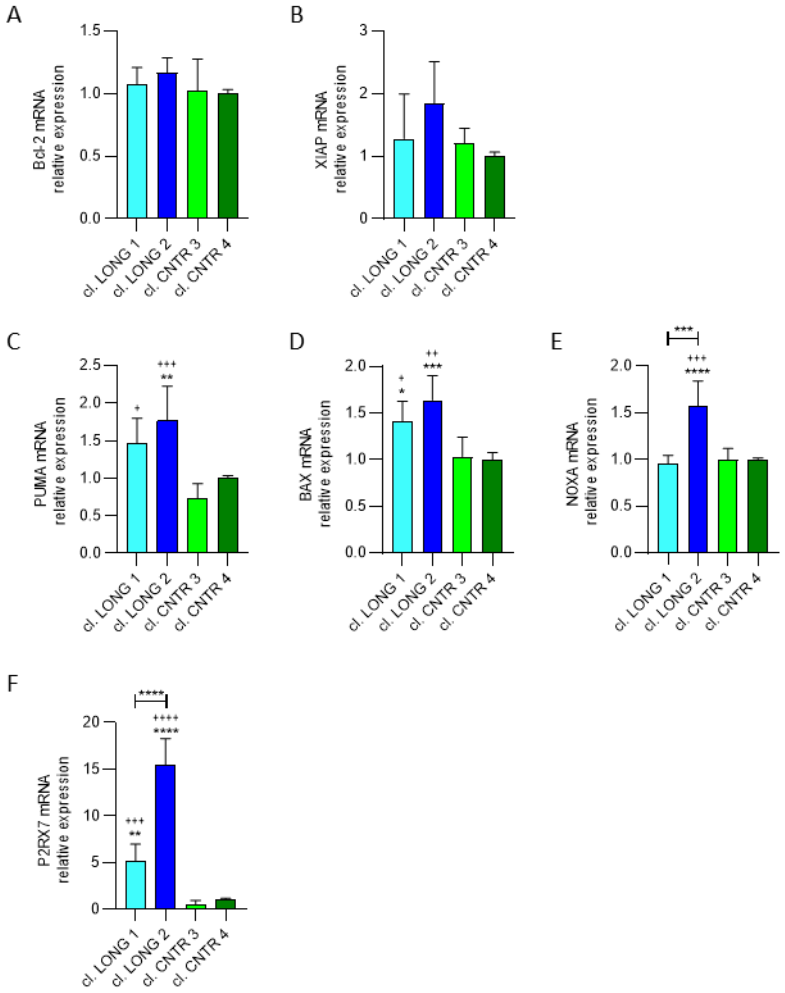

Figure 23. HAS2-AS1 regulates apoptosis in MDA-MB-231 cells via boosting the activity of apoptosis inducers. RT-qPCR a*nalyses measuring* ***(A)*** *Bcl.2,* ***(B)*** *XIAP,* ***(C)*** *PUMA,* ***(D)*** *BAX,* ***(E)*** *NOXA and* ***(F)*** *P2RX7 expression in MDA-MB-231 stable clones overexpressing HAS2-AS1 L exon 2 (cl. LONG 1, cl. LONG 2) or empty control vectors (cl. CNTR 3 and cl. CNTR 4). Values are reported as the average of three independent triplicates ± SEM. *, p<0.5; **, p<0.01 ***, p<0.001; ****, p<0.0001. + represent significance in respect to cl. CNTR 3; * Represent significance in respect to cl. CNTR 4.*

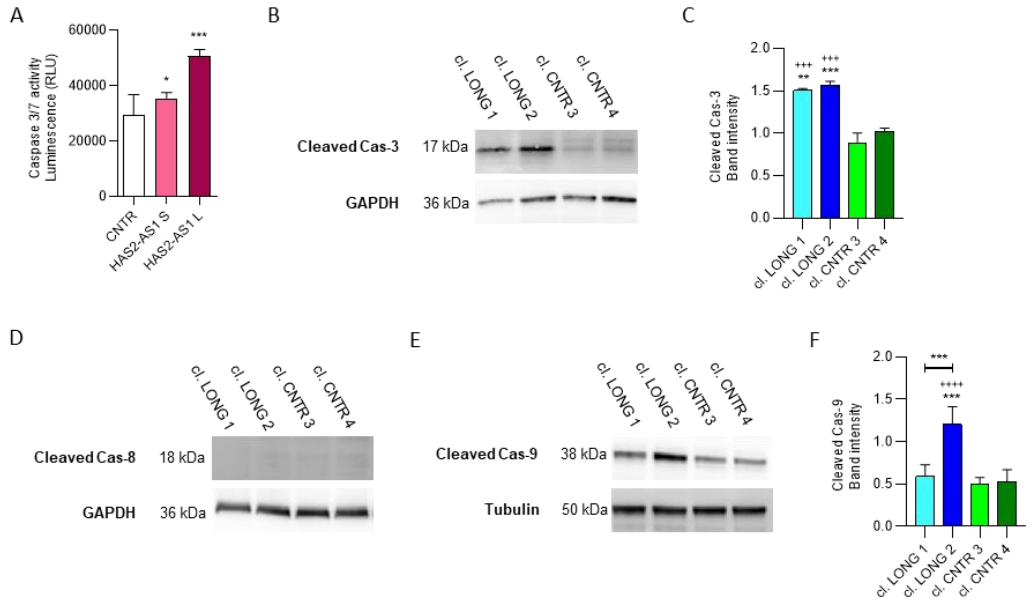

Figure 24. HAS2-AS1 induces apoptosis in TNBC cells via stimulating the intrinsic mitochondrial pathway. (A) *Caspase-Glo 3/7 assay analysis on MDA-MB-231 cells after the transfection for 48 hours of HAS2-AS1 exon 2 S or L WT isoforms or MUT L, with relative pcDNA3 empty control vector.* ***(B)*** *Representative blot of immunoreactive bands for Cleaved Caspase-3 and GAPDH from total protein extracts obtained from cl. LONG 2 or cl. CNTR 4. Numbers at the margins of the blots indicate relative molecular weights of the respective protein in kDa.* ***(C)*** *Relative band intensity of Cleaved Caspase-3 immunoblotting. Values are expressed as mean±SEM of 2 experiments of the percentage variation of the normalized O.D. obtained from each sample with respect to values obtained in cl. CNTR 4.* ***(D)*** *Representative blot of immunoreactive bands for Cleaved Caspase-8 and GAPDH from total protein extracts obtained from cl. LONG 1 and 2 or controls, cl. CNTR 3 and 4. Numbers at the margins of the blots indicate relative molecular weights of the respective protein in kDa.* ***(E)*** *Representative blot of immunoreactive bands for Cleaved Caspase-9 and GAPDH from total protein extracts obtained from cl. LONG 1 and 2 or controls, cl. CNTR 3 and 4. Numbers at the margins of the blots indicate relative molecular weights of the respective protein in kDa.* ***(F)*** *Relative band intensity of Cleaved Caspase-9 immunoblotting. Values are expressed as mean±SEM of 3 experiments of the percentage variation of the normalized O.D. obtained from each sample with respect to values obtained in cl. CNTR 4. **, p<0.01; ***, p<0.001; ****, p<0.0001. + represent significance in respect to cl. CNTR 3; * Represent significance in respect to cl. CNTR 4.*

DISCUSSION

Non-coding transcripts play a pivotal role in controlling gene expression at different levels, from transcription to post-translational modifications. Being a lncRNA, HAS2-AS1 is no exception – it finely tunes the expression of its cognate gene HAS2, eventually regulating ECM composition and affecting many pathophysiological mechanisms, such as inflammation and cancer. Indeed, HAS2-AS1 has already been described to be involved in cumulus cell migration [149,200] hypoxic pulmonary hypertension [201], cardiovascular diseases [60,202,203] as well as in several cancers as brain tumours [154,204], lung cancers [205], ovarian cancer [155], oral carcinoma [150] and osteosarcoma [43] in which, increasing HAS2 expression and favouring HA deposition, enhances cancer aggressiveness. Surprisingly, the role of HAS2-AS1 in breast cancers has not yet been deeply investigated, apart from its involvement in TGFβ-induced EMT in mouse mammary cells [151]. As HAS2-AS1 is highly expressed in invasive breast tumours, this work aimed to investigate the role of HAS-AS1 lncRNA in two breast cancer subtypes, namely ER-positive and ER-negative.

The TCGA-BRCA database showed that biopsies for patients with ER-positive cancers had a lower HAS2-AS1 expression with respect to ER-negative samples. This result was confirmed *in silico* on a panel of several breast cancer cell lines as well as in our experiments on well-known cellular models of ER-positive (namely, MCF-7, T-47D and BT-474) and ER-negative (namely, MDA-MB-231, Hs 578T, SUM149 and BT-549) breast cancer cells. These results could be explained by the fact that downregulation of HAS2-AS1 transcript in low aggressive ER-positive samples could be responsible for the low expression of HAS2 described in this type of breast cancer.
These preliminary data made us hypothesise that by downregulating HAS2-AS1 expression in TNBC cells, we would be able to lower cell aggressiveness of ER-negative cells, thus obtaining a phenotype more similar to that of ER-positive cell lines. However, our experiments on HAS2-AS1 silencing showed even a worsening of TNBC cell aggressiveness, thus proving our theory wrong. On the contrary, we observed that overexpression of the full-length sequence of HAS2-AS1 in MDA-MB-231 cells lowered their aggressive phenotype.

Therefore, we further correlated HAS2-AS1 expression with the survival rate of breast cancer patients, finding no correlation in ER-positive breast cancer samples. Surprisingly, in ER-negative tumours high HAS2-AS1 expression correlated with a higher survival probability. This latter result was unexpected, as literature highlights that HAS2-AS1 facilitates HAS2 expression thus correlating with poor survival in several cancers [48], but concordant with the preliminary results we obtained via HAS2-AS1 full-length overexpression in MDA-MB-231 cells. It must be considered that functional analyses of HAS2-AS1 were mainly based on studies made in tumour cell lines, while the dataset analysis contains expression data from whole tumours which comprise tumour

cells and stromal constituents (such as cancer-associated fibroblasts, tumour-infiltrating leukocytes, and blood vessels), which may have acted as a confounder. Furthermore, as discussed below, our transcriptomic analysis points out pathways different from HA synthesis that could be mechanistically linked to novel functions of HAS2-AS1.

Taking into consideration these preliminary results, we decided to investigate deeper how HAS2-AS1 is involved in invasive breast cancer progression, exploiting ER-negative versus ER-positive breast cancer cell lines. Previous experiments already conducted in our laboratory demonstrated that alterations in HAS2-AS1 expression in the MCF-7 cell line affected neither cell viability nor migration. Similar results were also obtained in T-47D cells, which we analysed as a confirmation of what we observed in MCF-7 cells. It can therefore be affirmed that HAS2-AS1 was not involved in the control of cell aggressiveness in ER-positive cell lines. Indeed, these data agree with ER-positive breast cancer patients survival rates, which were not affected by HAS2-AS1 expression levels.

On the other hand, when manipulating HAS2-AS1 expression levels in ER-negative breast cancer cell lines, alterations in both cell viability and migration were observed. Specifically, overexpression of HAS2-AS1, caused a significant drop in cell viability and migration, with a stronger effect visible in MDA-MB-231 cells. These results are in line with the observed positive impact of HAS2-AS1 on ER-negative patient prognosis. Thus, altogether these data indicate that HAS2-AS1 lncRNA could have a protective role on TNBC cells and that only these cells could stimulate its expression as a salvage mechanism.

As motility is distinctive of mesenchymal-like cells, which are characterized by a spindle-like aspect [206], we did a morphometric analysis of ER-negative breast cancer cells upon manipulation of HAS2-AS1 expression. We observed a switch from a more aggressive spindle-like phenotype of HAS2-AS1 silenced or untreated MDA-MB-231 cells, to a less aggressive roundish phenotype of HAS2-AS1 overexpressing cells. As spherical morphology is typical of epithelial cells that possess limited migratory capabilities [207], this change in cell morphology suggests a possible correlation between HAS2-AS1 and MET induction. Indeed, our transcriptome analysis of KEGG pathways identified downregulation of the TGFβ pathway – a well-known master regulator of EMT [208] – in cl. LONG2 vs control cells, which may have induced a shift towards a less invasive, epithelial phenotype, as reported for glioma and mouse mammary epithelial cells [151,209]. Interestingly, HAS2-AS1 has already been demonstrated to be a key regulator of HAS2 expression in TGFβ-induced EMT in mouse mammary epithelial cells [151]. However, we confirmed in our cell lines that HAS2-AS1 overexpression is correlated with a significantly decreased expression of both

TGFβR3 and SNAI1, a well-known TGFβ-controlled EMT inducer [210,211], suggesting that HAS2-AS1 is not involved in EMT induction in ER-negative breast tumours.

Further, the experiments on stably transfected cells overexpressing the L isoform of exon 2 of HAS2-AS1 still confirmed that such overexpressing led to a lower potential of MDA-MB-231 cells to form anchorage-independent clones compared to controls. As a consequence, these TNBC cells may be less prone to invade adjacent tissues and disseminate through the body to generate metastases. As a confirmation, we also observed both at transcriptional and protein levels, a reduction of mesenchymal markers but an upregulation of epithelial ones, with increased ZO-1-mediated tight-junction generation and less fibronectin deposition, validating our hypothesis.

Interestingly, HAS2-AS1 overexpression also downregulated the expression of the CD44s receptor. Several lines of evidence demonstrated the involvement of CD44 in breast carcinogenesis and metastasis, via activating a protein kinase cascade involving for example ERK, Akt, FAK, RAC and c-Src [63,89,212]. Indeed, CD44 has been described as a stimulator of cell proliferation and invasion [213] and, specifically, high expression of CD44s is essential for cells to undergo EMT [212] and metastasize to the liver when injected into immunodeficient mice [214]. Thus, is not surprising that cl. LONG 2, which was demonstrated to behave more similarly to epithelial than mesenchymal cells, expressed significantly lower levels of CD44s.

All these data together suggest that in TNBC cells HAS2-AS1 could induce a reversion from the mesenchymal to an epithelial phenotype, via inducing MET-related pathways, rather than being involved in EMT induction, as previously reported [151].

It is important to note that the exon 2 L isoform of HAS2-AS1 showed better results in terms of reduction of cell aggressiveness, compared to HAS2-AS1 S isoform. Therefore, we generated MDA-MB-231 L isoform overexpressing clones, as we demonstrated that it is a critical sequence involved in regulating ER-negative breast cancer cell aggressiveness. Moreover, being complementary to exon 1 of *HAS2* gene [149], we hypothesized having crucial functions to regulate *HAS2* transcription and HAS2 mRNA stability, as previously reported [53,149]. However, in the MDA-MB-231 cell line, HAS2-AS1 regulates neither HAS2 expression nor HA deposition. Indeed, all the methods we used to quantify both HA secreted in the culture medium and the pericellular coat of HA, indicated that HAS2-AS1 was not able to alter HA content in both stably transfected and transient overexpressing cells. Further, even if in HAS2-AS1 L stable clones a slight increase in HAS2 transcript was observed, no significant alterations were detected at the protein level. These results were surprising as it is well-known the strict relationship between HAS2-AS1

and its cognate gene product HAS2 that, in turn, regulates HA deposition [215]. Our research team was the first to characterize the role as chromatin organizer of HAS2-AS1 in the nucleus of human smooth muscle cells, describing its ability to modulate chromatin accessibility of *HAS2* promoter probably acting on histone post-translation modification as O-GlcNAcylation [53]. Although in different other tumour cell lines HAS2-AS1 sustains HAS2 expression [150,154,155,205], in MDA-MB-231 we found a different story suggesting the existence of different pathway(s) able to enhance HA synthesis in wild-type cells, probably controlling directly the HAS2 promoter or HAS2 protein, which is known to have fine transcriptional and post-translational regulations [68,216,217]. As an example, the HAS2-AS1-independent HAS2 expression could be driven by the constitutive activation of several tyrosine kinase receptors, thus leading to the triggering of different intracellular pathways as jak/stat, which, according to the microarray data, was found active in our HAS2-AS1 stable clones [218,219].

Moreover, it must be kept in mind that HAS2-AS1 is able to regulate HAS2 expression and activity differentially in distinct cell lines. Indeed, if our group demonstrated a positive correlation between HAS2-AS1 and HAS2 expression in AoSMCs [53], Chao and Spicer found that HAS2-AS1 overexpression in osteosarcoma cells induced a reduction of HAS2 expression and HA synthesis [43]. This different regulation of HAS2 could be explained by the strict tissue-specific action of lncRNAs. Indeed, their expression is much more cell-, tissue- and developmental specific than those of mRNAs. This accounts also for breast cancer, where lncRNAs expression is differential depending on breast cancer subtypes [220,221]. Thus, speculations regarding lncRNAs functions and target gens would not be meaningful if transferred from one cancer type to the other.

Since our results excluded that HAS2-AS1 could work via the canonical HAS2-HA axis, we decided to characterise the cellular pathways under the control of HAS2-AS1, via performing microarray analysis on HAS2-AS1 stably transfected MDA-MB-231 cells. We used the stable cl. LONG 2 that, having a higher exon 2 expression, showed to be more promising due to its reduced aggressiveness with respect to cl. LONG 1, whose behaviour, instead, was more similar to control clones. Among the identified genes, several belong to the pathways modulating cell migration and proliferation, which agrees with the altered aggressiveness we observed in cl. LONG 2. Additionally, genes involved in cell adhesion have been enriched, which could justify the altered epithelial-like morphology of such cells, thus corroborating our hypothesis of MET induction by HAS2-AS1 overexpression.

Interestingly, these analyses confirmed that no gene involved in HA synthesis (i.e., HASes) is regulated by HAS2-AS1 apart from the transcript coding for CEMIP that has been identified to be

significantly downregulated. As CEMIP is known to favour breast cancer cells growth and spreading [222], its reduced expression could contribute to the limited motility and viability of HAS2-AS1 overexpressing cells. Similarly, also the EREG messenger, the well-known Epidermal Growth Factor Receptor (EGFR) agonist involved in tumorigenesis and metabolic reprogramming [117,223], is downregulated in HAS2-AS1 overexpressing cells. Further, mRNAs coding for trefoil proteins (TFF1, 2 and 3) are among the most downregulated transcripts and these proteins are known to greatly induce breast cancer cell motility [224].

Additionally, numerous genes associated with tumour-suppressive functions were identified in the upregulated list. Teneurin transmembrane protein 1 (TENM1) is among the most upregulated transcripts in HAS2-AS1 cells. Although its role in breast cancer is still debated, TENM1 has been reported to correlate with a better survival outcome [225]. NCK associated protein 1 like (NCKAP1L) has been implicated in inhibiting breast cancer metastasis [225]. Although the role of Cadherin 18 (CDH18) has not been identified in breast cancer, it is known to suppress glioma cell invasiveness and correlate with the prognosis of glioma patients [226]. Hence, it may play a similar role in reducing breast cancer aggressiveness. Interleukin 24 (IL24), a well-studied tumour suppressor, is involved in diverse functions, including apoptosis, autophagy, and suppression of metastasis. Transcripts of IL24 were also found to be elevated in our analysis [227–229].

These data suggest for the first time that, at least in MDA-MB-231 TNBC cells, HAS2-AS1 can control several genes able to modulate different cellular pathways, which surprisingly are not related to HA.

Among all the altered genes, EREG attracted our attention as it was one of the most downregulated genes upon HAS2-AS1 L overexpression and due to its well described involvement in carcinogenesis and metastasis [230–232]. The RT-qPCR analysis confirmed that both stable clones overexpressing HAS2-AS1 L showed a significantly decreased EREG expression, with cl. LONG 2 expressing almost a fifth of EREG compared to control clones. EREG is known to stimulate the EGFR/ErbB receptors, activating downstream signalling pathways including MEK/ERK and PI3K/Akt pathways through an autocrine loop mechanism. As a final result, it is involved in regulating cell proliferation, invasion and also metastases [233]. Finding EREG downregulated by HAS2-AS1 L overexpression could explain at least part of the altered less-aggressive behaviours that we observed in HAS2-AS1-manipulated TNBC cell lines. Indeed, one of the main characteristics of cancer cells is their limitless replicative potential and their self-sufficiency in secreting growth signals [156]. EREG could act as an autocrine growth signal in TNBC cell, as already demonstrated in glioma [234]. Newsworthy, HAS2-AS1 overexpressing clones, and in

particular the cl. LONG 2, shown to be less proliferative and less prone to generating clones compared to control cells. Moreover, HAS2-AS1 has already been demonstrated to be involved in the regulation of cancer cell proliferation, via PI3K/Akt pathway [204], which is also shared by EREG [235]. Interestingly, also Akt1 transcript was found to be downregulated in cl. LONG 2 via both microarray analysis and RT-qPCR experiments, supporting the hypothesis that HAS2-AS1 could downregulate EREG transcription, blocking the downstream PI3K/Akt pathway and eventually slowing down cell growth.

Continuing looking at the cell cycle, we validated other two genes that were altered in the microarray analysis, after HAS2-AS1 overexpression: p21 and CCND1. Our RT-qPCR data agreed with the microarray results, validating that the cell cycle inhibitor p21 was upregulated when HAS2-AS1 was overexpressed, whereas CCND1 coding for cyclin D1, was downregulated in cl. LONG 2. Specifically, p21 is known to promote p53-dependent G1 cell cycle arrest or apoptosis [236]; on the other hand, its abrogation has been associated with cellular proliferation and tumorigenicity [237]. Thus, its upregulation could concur in the slowed cell growth of cl. LONG 2 compared to the control clones. Similarly, cyclin D1 is one of the major regulators of cell cycle progression in the G1 phase [238]. Interestingly, the literature reports that suppression of CCND1 expression in TNBC cells resulted in a rounded and epithelial-like phenotype and prevented TGFβ-induced EMT [239]. Thus, CCND1 downregulation resulting from HAS2-AS1 overexpression could explain not only the reduced proliferation of cl. LONG 2, but also the switch from a mesenchymal- to an epithelial-like phenotype of MDA-MB-231 cells.

During clonal selection, we encountered several problems regarding the number of viable and culturable clones overexpressing the exon 2 L isoform of HAS2-AS1. Indeed, even though a great number of clones overexpressing the lncRNA was initially selected, a lot of them started to die after about four weeks of cultivation. One of the reasons we started questioning was that maybe those clones stably expressed very high levels of HAS2-AS1, which would eventually lead them to death. And in fact, DAVID annotation revealed that the expression of several genes related to apoptosis was altered.

TUNEL assay confirmed that in both transiently and stably transfected MDA-MB-231 cells, HAS2-AS1 overexpression induced apoptosis of a greater number of cells compared to controls. Interestingly, the L isoform of exon 2 induced a stronger effect compared to the S isoform. Although we did not further investigate this point, we could speculate that a longer sequence of exon 2 of HAS2-AS1 could interact with more modulators compared to the S isoform. In fact, our data demonstrated that HAS2-AS1 could work as an endogenous competitor for miR-186-3p.

On the other hand, the TUNEL assay on stable clones highlighted that cl. LONG 2 presents a greater number of apoptotic cells, which is in line with all the previous experiments, describing cl. LONG 2 behaving quite differently from cl. LONG 1. This difference could be explained by the fact that HAS2-AS1 expression levels are almost twice as much as in cl. LONG 2 with respect to cl. LONG 1.

A deeper investigation into apoptosis induction by HAS2-AS1 overexpression in TNBC cell lines revealed that if mRNA levels of Bcl-2 and XIAP apoptosis inhibitors remained unchanged between the HAS2-AS1 overexpressing and control clones, several apoptosis inducers (namely, PUMA, BAX and NOXA), instead, were significantly upregulated in cl. LONG 1 and 2. These results suggest that HAS2-AS1 overexpression could be implied in apoptosis induction via stimulating the activity of apoptosis induced, instead of downregulating inhibitors of apoptosis. Conforming the effective activation of apoptosis pathway in MDA-MB-231 cells consequently to HAS2-AS1 L overexpression, we observed an induction of caspase-3, whose protein levels resulted significantly higher in cl. LONG 1 and 2 compared to control clones. As caspase-3 is the key downstream element being eventually activated either by the intrinsic or extrinsic pathways of apoptosis [240], we focused on the activation of upstream caspases (i.e., caspase-8 and -9). As shown in the results, HAS2-AS1 overexpression induced the activation of caspase-9, but not of caspase-8, suggesting that the designated pathway activating apoptosis in those TNBC cells is the intrinsic one, involving the mitochondria. Evasion of apoptosis is one of the major problems in dealing with breast cancer treatment. Preclinical studies showed that anti-apoptotic Bcl-2 family proteins promoted resistance to standard breast cancer therapies, including endocrine inhibitors [241], HER2 inhibitors [242] and chemotherapy [243].

lncRNAs can modulate gene expression through a variety of mechanisms, from transcription to post translational levels. Recently, an increasing number of studies are focusing on an intriguing regulatory mechanism identifying lncRNAs as modulators of mRNA translation into protein, via competing for the interaction with target shared miRNAs [244]. Interestingly, HAS2-AS1 has been found to work both as an epigenetic regulator in the nucleus [53,150] other and as an endogenous competitor for miRNAs, as already described for miR-466 [155] and miR-137 [153,245]. Kolliopoulos and collaborators found the murine ortholog of human HAS2-AS1 in the nucleus as well as in the cytosol [151]. Similarly, our RNA fractioning experiment confirmed that also in MDA-MB-231 cells, the full-length transcript for HAS2-AS1 could be fund in almost equivalent amounts in both nucleus and cytoplasm. This data allowed us to pursue our hypothesis that, since in our cellular models HAS2-AS1 seems to not be involved in regulating HAS2/HA pathway, it can work

into the cytoplasm, eventually sponging some miRNAs. Indeed, *in silico* analysis revealed that HAS2-AS1 exon 2 transcript contains several putative binding sites for different miRNAs. Among them miR-186-3p showed to have two binding sites on HAS2-AS1 exon 2 sequence with thermodynamic properties that convinced us to focus our attention on this miRNA.

We confirmed that effectively, HAS2-AS1 overexpression significantly reduced miR-186-3p levels in MDA-MB-231 cells, and not miR-186-5p, used as a control. Luciferase assay evaluating the effective binding of miR-186-3p on HAS2-AS1 MRE sequences (wild-type or mutated), confirmed that only miR-186-3p and not -5p could bind to HAS2-AS1 S and L isoforms. It is of considerable importance that among the two possible miRNAs arising from the miR-186 locus, is the -3p form that resulted to be effectively sponged by HAS2-AS1 lncRNA. Indeed, historically has been thought that the main functionalities of miRNAs resided in the -5p arm. However, at the time being the exact mechanism underling the miRNA arms fate remains still unclear. However, increasing evidence is reporting that miR-5p and -3p selection is strictly dependent on tissues, developmental stages, species, and pathologies, including cancer [246–248].

The role of miR-186 in cancer is still debated and controversial [249] – it inhibits tumour growth and metastasis in cervical and non-small cell lung cancers [250,251], while it stimulates tumorigenesis in breast cancer [252]. These variations could be explained by the differential expression of lncRNAs, whose interaction with miRNAs is tissue- and cell line-specific, eventually generating a plethora of possible lncRNA/miRNA interactions.

To corroborate that miR-186-3p interaction with HAS2-AS1 is the explanation for the changes in cell behaviours we observed upon manipulation of HAS2-AS1 overexpression, we transfected MDA-MB-231 cells with either a miR-186-3p mimetic, which induced its overexpression, or antagonist, which reduced miR-186-3p expression and mimicked HAS2-AS1 sponge effect. The results we obtained, that is a significant upregulation of cell viability and motility upon miR-186-3p overexpression, that were reverted when transfecting an antagonist for miR-186-3p, confirmed our starting hypothesis. Moreover, restoration of migration and vitality of MDA-MB-231 cells to control levels when overexpressing HAS2-AS1 bearing mutation in MRE sequence, finally validated that the miR-186-3p sponging via HAS2-AS1 is at least one of the causes leading to less tumorigenic and aggressive phenotype of MDA-MB-231 cells that we observed in this work.

A final connection that could be made between HAS2-AS1 and miR-186-3p expression, is the decreased P2RX7 transcript levels that we observed. Interestingly, the purinergic receptor P2X7

has already been demonstrated to regulate cell growth and apoptosis in breast cancer, through the interaction with miR-186 and miR150 [199].

TNBC cells, in general, can hardly be induced to die, as one of the major tracts of aggressive tumours is their ability to evade apoptosis. Therefore, finding a mechanism able to finally induce apoptosis in TNBC cells and tumours, could be a turning point in the treatment of such breast cancers. In the light of this premise, our data indicate that HAS2-AS1 could be considered as a novel tumour suppressor gene, as we demonstrated that its overexpression is implied at least in apoptosis and MET induction in MDA-MB-231 cells. In addition, our findings report for the first time that HAS2-AS1 could function as a sponge for miR-186-3p, thus modulating its effects in breast cancer cells.

As a conclusion, these findings could explain how increased HAS2-AS1 expression in ER-negative breast cancer patients correlated with better survival rate - the beneficial effect of HAS2-AS1 may not be the consequence of altered HA synthesis, but rather depend on independent mechanisms.

SUPPLEMENTAL TABLES

Supplemental table 1. *Functional classification of upregulated genes in MDA-MB-231 stable clone 2 overexpressing the exon 2 long isoform of HAS2-AS1.*

Functional classification	Gene	Fold change
Invasion / migration	Matrix metallopeptidase 1 (MMP1)	116.63
	NCK associated protein 1 like (NCKAP1L)	18
	Epithelial cell adhesion molecule (EPCAM)	12.43
	Semaphorin 3E (SEMA3E)	11.91
	Interleukin 24 (IL24)	9.53
	Wnt family member 5A (WNT5A)	9.45
	Matrilin 2 (MATN2)	6.95
	Protein tyrosine phosphatase, non-receptor type 22 (PTPN22)	5.33
	Doublecortin like kinase 1 (DCLK1)	5.29
	Ectonucleotide pyrophosphatase/phosphodiesterase 2 (ENPP2)	4.37
	Adhesion G protein-coupled receptor L3 (ADGRL3)	4.05
Adhesion	Teneurin transmembrane protein 1 (TENM1)	305.35
	Matrix metallopeptidase 1(MMP1)	116.63
	FAT atypical cadherin 3(FAT3)	39.77
	Thrombospondin 2(THBS2)	31.91
	Cadherin 18 (CDH18)	23.78
	Transmembrane protein 47 (TMEM47)	18.63
	NCK associated protein 1 like (NCKAP1L)	18
	Neurexin 1 (NRXN1)	12.97
	Epithelial cell adhesion molecule (EPCAM)	12.43
	Semaphorin 3E (SEMA3E)	11.91
	Dystrophin (DMD)	11.52
	Collagen type XVII alpha 1 chain (COL17A1)	11.49
	Wnt family member 5A (WNT5A)	9.45
	Membrane palmitoylated protein 7 (MPP7)	6.33
	CYLD lysine 63 deubiquitinase (CYLD)	4.34
	Collagen type XI alpha 1 chain (COL11A1)	4.16
	Adhesion G protein-coupled receptor L3 (ADGRL3)	4.05
Proliferation	Teneurin transmembrane protein 1 (TENM1)	305.35
	Cholinergic receptor muscarinic 3 (CHRM3)	46.95
	NCK associated protein 1 like (NCKAP1L)	18
	Cytidine deaminase (CDA)	15.82
	ADAM metallopeptidase with thrombospondin type 1 motif 1 (ADAMTS1)	15.29
	KiSS-1 metastasis-suppressor (KISS1)	15.05
	Epithelial cell adhesion molecule (EPCAM)	12.43
	Dynactin associated protein (DYNAP)	11.46
	Family with sequence similarity 83 member A (FAM83A)	9.94
	Interleukin 24 (IL24)	9.53
	Wnt family member 5A (WNT5A)	9.45
	Nik related kinase (NRK)	9.3
	Cyclin D2 (CCND2)	7.65
	ArfGAP with GTPase domain, ankyrin repeat and PH domain 2 (AGAP2)	6.79
	Dopachrome tautomerase (DCT)	6.46
	TSPY like 5 (TSPYL5)	6.41
	Serpin family B member 7 (SERPINB7)	6.28
	Retinoic acid receptor beta (RARB)	5.56
	Protein tyrosine phosphatase, non-receptor type 22 (PTPN22)	5.33
	Nuclear protein 1, transcriptional regulator (NUPR1)	5.17

	Ornithine decarboxylase 1 (ODC1)	5.12
	Inhibin beta A subunit (INHBA)	4.7
	Pellino E3 ubiquitin protein ligase 1 (PELI1)	4.36
	CYLD lysine 63 deubiquitinase (CYLD)	4.34
	Activating transcription factor 3 (ATF3)	4.33
	Ribosomal protein S6 kinase A1 (RPS6KA1)	4.12
	Interleukin 23 subunit alpha (IL23A)	4.03
Angiogenesis	Thrombospondin 2(THBS2)	31.91
	Neurexin 1(NRXN1	12.97
	Semaphorin 3E (SEMA3E)	11.91
	Wnt family member 5A (WNT5A)	9.45
	Ectonucleotide pyrophosphatase/phosphodiesterase 2 (ENPP2)	4.37
Signal transduction	Teneurin transmembrane protein 1 (TENM1)	305.35
	Cholinergic receptor muscarinic 3 (CHRM3)	46.95
	Phosphodiesterase 1C (PDE1C)	38.83
	Transmembrane phosphatase with tensin homology (TPTE)	17.69
	Neurexin 1 (NRXN1)	12.97
	Dedicator of cytokinesis 3 (DOCK3)	8.6
	RAS guanyl releasing protein 3 (RASGRP3)	7.3
	ArfGAP with GTPase domain, ankyrin repeat and PH domain 2 (AGAP2)	6.79
	Rho GTPase activating protein 28 (ARHGAP28)	4.76
Apoptosis	Epithelial cell adhesion molecule (EPCAM)	12.43
	Dynactin associated protein (DYNAP)	11.46
	MAGE family member A3 (MAGEA3)	9.96
	Interleukin 24 (IL24)	9.53
	Cyclin D2 (CCND2)	7.65
	Serpin family B member 2 (SERPINB2)	7.45
	ArfGAP with GTPase domain, ankyrin repeat and PH domain 2(AGAP2)	6.79
	Retinoic acid receptor beta (RARB)	5.56
	Nuclear protein 1, transcriptional regulator (NUPR1)	5.17
	CYLD lysine 63 deubiquitinase (CYLD)	4.34
	Ribosomal protein S6 kinase A1 (RPS6KA1)	4.12
Inflammation	Proteolipid protein 1 (PLP1)	10.76
	Interleukin 24 (IL24)	9.53
	Wnt family member 5A (WNT5A)	9.45
	Sphingomyelin phosphodiesterase acid like 3B (SMPDL3B)	6.11
	Nuclear protein 1, transcriptional regulator (NUPR1)	5.17
	Lipoic acid synthetase (LIAS)	4.05
	Interleukin 23 subunit alpha (IL23A)	4.03
Differentiation	Thymocyte expressed, positive selection associated 1 (TESPA1)	23.58
	NCK associated protein 1 like (NCKAP1L)	18
	ADAM metallopeptidase with thrombospondin type 1 motif 9 (ADAMTS9)	13.89
	Neurexin 1 (NRXN1)	12.97
	Dystrophin (DMD)	11.52
	Fli-1 proto-oncogene, ETS transcription factor (FLI1)	9.79
	Wnt family member 5A (WNT5A)	9.45
	Retinoic acid receptor beta (RARB)	5.56
	Protein tyrosine phosphatase, non-receptor type 22 (PTPN22)	5.33
	Nuclear protein 1, transcriptional regulator (NUPR1)	5.17
	Inhibin beta A subunit (INHBA	4.7
	Activating transcription factor 3 (ATF3)	4.33
Proteolysis	ADAM metallopeptidase with thrombospondin type 1 motif 1 (ADAMTS1)	15.29
	ADAM metallopeptidase with thrombospondin type 1 motif 9 (ADAMTS9)	13.89
	Carboxypeptidase A3 (CPA3)	7.81

Supplemental table 2. *Functional classification of downregulated genes in MDA-MB-231 stable clone 2 overexpressing the exon 2 long isoform of HAS2-AS1.*

Functional classification	Gene	Fold change
Invasion / migration	Trefoil factor 1 (TFF1)	-258.07
	Trefoil factor 3 (TFF3)	-57.74
	Trefoil factor 2 (TFF2)	-47.11
	Shroom family member 2 (SHROOM2)	-20
	C-C motif chemokine ligand 20 (CCL20)	-17.92
	C-C motif chemokine ligand 28(CCL28)	-14.34
	Delta/notch like EGF repeat containing (DNER)	-13.12
	C-X-C motif chemokine ligand 1 (CXCL1)	-11.99
	Cell migration inducing hyaluronan binding protein (CEMIP)	-10.65
	Secretogranin II (SCG2)	-10.44
	Enah/Vasp-like (EVL)	-10.17
	S100 calcium binding protein A2 (S100A2)	-7.79
	Dedicator of cytokinesis 2 (DOCK2)	-7.78
	Collagen type V alpha 1 chain (COL5A1)	-7.69
	Interleukin 6 (IL6)	-6.75
	Myb like, SWIRM and MPN domains 1 (MYSM1)	-6.66
	Phospholipid phosphatase 3 (PLPP3)	-6.61
	Guanylate binding protein 1 (GBP1)	-6.36
	Brain abundant membrane attached signal protein 1 (BASP1)	-5.99
	Collagen type IV alpha 1 chain (COL4A1)	-5.89
	C-X-C motif chemokine ligand 8 (CXCL8)	-5.85
	Integrin subunit beta 3(ITGB3)	-5.5
	Fuzzy planar cell polarity protein (FUZ)	-5.47
	Epiregulin (EREG)	-5.42
	Spectrin repeat containing nuclear envelope protein 2 (SYNE2)	-5
	Integrin subunit alpha 1 (ITGA1)	-5.05
	Angiotensinogen (AGT)	-4.86
	C-X-C motif chemokine ligand 11(CXCL11)	-4.47
	Calcium/calmodulin dependent protein kinase ID (CAMK1D)	-4.44
	Fibronectin 1 (FN1)	-4.41
	Laminin subunit alpha 3 (LAMA3)	-4.34
	Selectin P ligand (SELPLG)	-4.34
	Podocalyxin like (PODXL)	-4.26
	Semaphorin 4B (SEMA4B)	-4.26
	Semaphorin 6B (SEMA6B)	-4.26
	Serum amyloid A1 (SAA1)	-4.11
	Laminin subunit alpha 4 (LAMA4)	-4.08
	CD74 molecule (CD74)	-4.01
Adhesion	Protocadherin gamma subfamily B, 7 (PCDHGB7)	-31.37
	Transforming growth factor beta induced (TGFBI)	-24.13
	Collectin subfamily member 12 (COLEC12)	-23.76
	C-C motif chemokine ligand 28 (CCL28)	-14.34
	SMAD family member 6 (SMAD6)	-9.61
	Collagen type V alpha 1 chain (COL5A1)	-7.69
	Cathepsin S (CTSS)	-7.43
	Transglutaminase 2(TGM2)	-6.94
	Tubulointerstitial nephritis antigen like 1 (TINAGL1)	-6.94
	Inhibitor of DNA binding 1, HLH protein (ID1)	-6.89
	Phospholipid phosphatase 3 (PLPP3)	-6.61
	Guanylate binding protein 1 (GBP1)	-6.36
	Pleiotrophin (PTN)	-6.09
	Protocadherin 7 (PCDH7)	-5.86
	C-X-C motif chemokine ligand 8 (CXCL8)	-5.85
	Protocadherin beta 14 (PCDHB14)	-5.6

	Integrin subunit alpha 1 (ITGA1)	-5.05
	Integrin subunit beta 3 (ITGB3)	-5.5
	Contactin associated protein-like 3 (CNTNAP3)	-4.54
	Protocadherin beta 13 (PCDHB13)	-4.75
	Collagen type VI alpha 1 chain (COL6A1)	-4.59
	Adhesion molecule with Ig like domain 2 (AMIGO2)	-4.45
	Protocadherin beta 10 (PCDHB10)	-4.42
	Fibronectin 1 (FN1)	-4.41
	Protocadherin beta 9 (PCDHB9)	-4.4
	Collagen type IV alpha 2 chain (COL4A2)	-4.36
	Laminin subunit alpha 3 (LAMA3)	-4.34
	Selectin P ligand (SELPLG)	-4.3
	Protocadherin 1 (PCDH1)	-4.3
	Podocalyxin like (PODXL)	-4.26
	Serum amyloid A1 (SAA1)	-4.11
	Laminin subunit alpha 4 (LAMA4)	-4.08
Proliferation	Trefoil factor 1 (TFF1)	-258.07
	Transforming growth factor beta induced (TGFBI)	-24.13
	Lipase G, endothelial type (LIPG)	-21.1
	NADPH oxidase 5 (NOX5)	-19.76
	Scinderin (SCIN)	-15.43
	MX dynamin like GTPase 2 (MX2)	-14.07
	Retinoic acid receptor responder 3 (RARRES3)	-13.89
	Egl-9 family hypoxia inducible factor 3 (EGLN3)	-12.56
	C-X-C motif chemokine ligand 1 (CXCL1)	-11.99
	Interferon regulatory factor 1 (IRF1)	-11.56
	Vasoactive intestinal peptide receptor 1 (VIPR1)	-11.39
	Echinoderm microtubule associated protein like 1(EML1)	-11.14
	PBX homeobox 1 (PBX1)	-10.79
	Secretogranin II (SCG2)	-10.44
	Prostaglandin E synthase (PTGES)	-9.73
	SMAD family member 6 (SMAD6)	-9.61
	Sushi, nidogen and EGF like domains 1 (SNED1)	-8.56
	Collagen type VI alpha 2 chain (COL6A2)	-8.5
	Indoleamine 2,3-dioxygenase 1 (IDO1)	-8.22
	Transglutaminase 2(TGM2)	-6.94
	Inhibitor of DNA binding 1, HLH protein (ID1)	-6.89
	Interleukin 6 (IL6)	-6.75
	Tumor necrosis factor superfamily member 13b (TNFSF13B)	-6.27
	Transcription factor AP-2 gamma (TFAP2C)	-6.1
	Pleiotrophin (PTN)	-6.09
	Transforming growth factor alpha (TGFA)	-5.86
	C-X-C motif chemokine ligand 8 (CXCL8)	-5.85
	Integrin subunit alpha 1 (ITGA1)	-5.05
	Integrin subunit beta 3 (ITGB3)	-5.5
	Fuzzy planar cell polarity protein (FUZ)	-5.47
	Epiregulin (EREG)	-5.42
	Oncostatin M receptor (OSMR)	-5.26
	Cyclin A1 (CCNA1)	-5.04
	Angiotensinogen (AGT)	-4.86
	Coiled-coil domain containing 8 (CCDC8)	-4.7
	Leucine rich repeat containing G protein-coupled receptor 4 (LGR4)	-4.66
	Aldo-keto reductase family 1 member C3 (AKR1C3)	-4.56
	C-X-C motif chemokine ligand 11 (CXCL11)	-4.47
	Adrenomedullin (ADM)	-4.47
	Fibronectin 1 (FN1)	-4.41
	Actin filament associated protein 1 like 2 (AFAP1L2)	-4.11
	CD74 molecule (CD74)	-4.01
Angiogenesis	Complement C3(C3)	-56.6

	Transforming growth factor beta induced (TGFBI)	-24.13
	Inhibitor of DNA binding 1, HLH protein (ID1)	-6.89
	TNF alpha induced protein 2(TNFAIP2)	-6.47
	Pleiotrophin (PTN)	-6.09
	Transforming growth factor alpha (TGFA)	-5.86
	Integrin subunit beta 3 (ITGB3)	-5.5
	Epiregulin (EREG)	-5.42
	Angiotensinogen (AGT)	-4.86
	Fibronectin 1 (FN1)	-4.41
	Collagen type IV alpha 2 chain (COL4A2)	-4.36
Signal Transduction	ATP binding cassette subfamily C member 3 (ABCC3)	-32.8
	C-C motif chemokine ligand 20 (CCL20)	-17.92
	Phosphodiesterase 7B (PDE7B)	-16.28
	C-X-C motif chemokine ligand 1 (CXCL1)	-11.99
	PBX homeobox 1 (PBX1)	-10.79
	Secretogranin II (SCG2)	-10.44
	Prostaglandin E synthase (PTGES)	-9.73
	Connector enhancer of kinase suppressor of Ras 2 (CNKSR2)	-9.6
	Chloride intracellular channel 3 (CLIC3)	-7.76
	Iinhibin beta B subunit (INHBB)	-7.53
	Tumor necrosis factor superfamily member 13b (TNFSF13B)	-6.27
	C-X-C motif chemokine ligand 8 (CXCL8)	-5.85
	Ras related dexamethasone induced 1 (RASD1)	-5.73
	Killer cell lectin like receptor C2 (KLRC2)	-5.31
	Guanylate cyclase 1 soluble subunit beta (GUCY1B3)	-5.26
	FYN binding protein (FYB)	-5.23
	Bone morphogenetic protein 1 (BMP1)	-4.99
	Phospholipid phosphatase 4 (PLPP4)	-4.86
	Phosphodiesterase 8A (PDE8A)	-4.8
	Killer cell lectin like receptor C3 (KLRC3)	-4.74
	C-X-C motif chemokine ligand 11 (CXCL11)	-4.47
	Adrenomedullin (ADM)	-4.47
	MX dynamin like GTPase 1 (MX1)	-4.46
	ADAM metallopeptidase domain 32 (ADAM32)	-4.29
	CD74 molecule (CD74)	-4.01
	Basic leucine zipper ATF-like transcription factor (BATF)	-4.01
Apoptosis	Complement C3 (C3)	-56.6
	C-C motif chemokine ligand 20 (CCL20)	-17.92
	Egl-9 family hypoxia inducible factor 3 (EGLN3)	-12.56
	Interferon regulatory factor 1 (IRF1)	-11.56
	Secretogranin II (SCG2)	-10.44
	Prostaglandin E synthase (PTGES)	-9.73
	SMAD family member 6 (SMAD6)	-9.61
	Indoleamine 2,3-dioxygenase 1 (IDO1)	-8.22
	Iinhibin beta B subunit (INHBB)	-7.53
	Transglutaminase 2(TGM2)	-6.94
	Interleukin 6 (IL6)	-6.75
	Pleiotrophin (PTN)	-6.09
	Transforming growth factor alpha (TGFA)	-5.86
	C-X-C motif chemokine ligand 8 (CXCL8)	-5.85
	Integrin subunit alpha 1 (ITGA1)	-5.05
	Zinc finger matrin-type 4 (ZMAT4)	-5.39
	NAD(P)H quinone dehydrogenase 1 (NQO1)	-5.27
	SAM pointed domain containing ETS transcription factor (SPDEF)	-5.05
	Bone morphogenetic protein 1 (BMP1)	-4.99
	Toll like receptor 3 (TLR3)	-4.9
	Interferon induced protein with tetratricopeptide repeats 2 (IFIT2)	-4.62
	Aldo-keto reductase family 1 member C3 (AKR1C3)	-4.56
	Caspase recruitment domain family member 6 (CARD6)	-4.48

	Adrenomedullin (ADM)	-4.47
	CREB binding protein (CREBBP)	-4.45
	Adhesion molecule with Ig like domain 2 (AMIGO2)	-4.45
	Calcium/calmodulin dependent protein kinase ID (CAMK1D)	-4.44
	Ubiquitin D (UBD)	-4.21
	DnaJ heat shock protein family (Hsp40) member C3 (DNAJC3)	-4.14
	CD74 molecule (CD74)	-4.01
Inflammation	Complement C3 (C3)	-56.6
	C-C motif chemokine ligand 20 (CCL20)	-17.92
	Delta/notch like EGF repeat containing (DNER)	-13.12
	Serpin family A member 3 (SERPINA3)	-11.94
	C-type lectin domain family 2 member B (CLEC2B)	-10.95
	Arachidonate 5-lipoxygenase activating protein (ALOX5AP)	-10.54
	Indoleamine 2,3-dioxygenase 1 (IDO1)	-8.22
	Transient receptor potential cation channel subfamily V member 4 (TRPV4)	-7.4
	Transglutaminase 2 (TGM2)	-6.94
	Interleukin 6 (IL6)	-6.75
	Oncostatin M receptor(OSMR)	-5.26
	G protein-coupled receptor class C group 5 member B (GPRC5B)	-4.93
	Toll like receptor 3 (TLR3)	-4.9
	Calcium/calmodulin dependent protein kinase ID (CAMK1D)	-4.44
	Actin filament associated protein 1 like 2 (AFAP1L2)	-4.11
Differentiation	Trefoil factor 1 (TFF1)	-258.07
	ATP binding cassette subfamily G member 1 (ABCG1)	-36.91
	solute carrier organic anion transporter family member 4C1 (SLCO4C1)	-15.79
	Scinderin (SCIN)	-15.43
	C-X-C motif chemokine ligand 1 (CXCL1)	-11.99
	Echinoderm microtubule associated protein like 1(EML1)	-11.14
	Collagen type V alpha 1 chain (COL5A1)	-7.69
	Inhibin beta B subunit (INHBB)	-7.53
	transient receptor potential cation channel subfamily V member 4(TRPV4)	-7.4
	Inhibitor of DNA binding 1, HLH protein (ID1)	-6.89
	Interleukin 6 (IL6)	-6.75
	Phospholipid phosphatase 3 (PLPP3)	-6.61
	TNF alpha induced protein 2 (TNFAIP2)	-6.47
	Pirin (PIR)	-6.4
	Pleiotrophin (PTN)	-6.09
	Brain abundant membrane attached signal protein 1 (BASP1)	-5.99
	Collagen type IV alpha 1 chain (COL4A1)	-5.89
	Integrin subunit beta 3 (ITGB3)	-5.5
	Epiregulin (EREG)	-5.42
	Leucine rich repeat containing G protein-coupled receptor 4(LGR4)	-4.66
	Collagen type VI alpha 1 chain (COL6A1)	-4.59
	Fibronectin 1 (FN1)	-4.41
	Tribbles pseudokinase 2 (TRIB2)	-4.4
	Collagen type IV alpha 2 chain (COL4A2)	-4.36
	Laminin subunit alpha 3 (LAMA3)	-4.34
	Ubiquitin D (UBD)	-4.21
	Basic leucine zipper ATF-like transcription factor (BATF)	-4.01
Proteolysis	Complement C3 (C3)	-56.6
	Complement C1s (C1S)	-8.18
	ADAM metallopeptidase domain 28 (ADAM28)	-8.07
	Complement C1r (C1R)	-7.19
	Protease, serine 23 (PRSS23)	-6.8
	Bone morphogenetic protein 1 (BMP1)	-4.99
	ADAM metallopeptidase domain 32 (ADAM32)	-4.29
	Complement factor B (CFB)	-4.01

BIBLIOGRAPHY

[1] H. Sung, J. Ferlay, R.L. Siegel, M. Laversanne, I. Soerjomataram, A. Jemal, F. Bray, Global cancer statistics 2020: GLOBOCAN estimates of incidence and mortality worldwide for 36 cancers in 185 countries, CA: A Cancer Journal for Clinicians. 71 (2021). https://doi.org/10.3322/caac.21660.

[2] N. Breen, J.F. Gentleman, J.S. Schiller, Update on Mammography Trends: Comparisons of Rates in 2000, 2005, and 2008, Cancer. 117 (2011) 2209. https://doi.org/10.1002/CNCR.25679.

[3] J.E. Rossouw, G.L. Anderson, R.L. Prentice, A.Z. LaCroix, C. Kooperberg, M.L. Stefanick, R.D. Jackson, S.A. Beresford, B. v Howard, K.C. Johnson, J.M. Kotchen, J. Ockene, W.G. for the W.H.I. Investigators, Risks and benefits of estrogen plus progestin in healthy postmenopausal women: Principal results from the women's health initiative randomized controlled trial, JAMA. 288 (2002) 321–333. https://doi.org/10.1001/JAMA.288.3.321.

[4] L.A. Torre, F. Islami, R.L. Siegel, E.M. Ward, A. Jemal, Global Cancer in Women: Burden and Trends, Cancer Epidemiology and Prevention Biomarkers. 26 (2017) 444–457. https://doi.org/10.1158/1055-9965.EPI-16-0858.

[5] K. Polyak, Heterogeneity in breast cancer, The Journal of Clinical Investigation. 121 (2011) 3786–3788. https://doi.org/10.1172/JCI60534.

[6] G. Viale, The current state of breast cancer classification, Annals of Oncology. 23 (2012) x207–x210. https://doi.org/10.1093/ANNONC/MDS326.

[7] J.Y.S. Tsang, G.M. Tse, Molecular Classification of Breast Cancer, (2019). www.anatomicpathology.com (accessed October 31, 2021).

[8] C.M. Perou, T. Sørile, M.B. Eisen, M. van de Rijn, S.S. Jeffrey, C.A. Ress, J.R. Pollack, D.T. Ross, H. Johnsen, L.A. Akslen, Ø. Fluge, A. Pergammenschlkov, C. Williams, S.X. Zhu, P.E. Lønning, A.L. Børresen-Dale, P.O. Brown, D. Botstein, Molecular portraits of human breast tumours, Nature. 406 (2000) 747–752. https://doi.org/10.1038/35021093.

[9] N.A. Bhowmick, H.L. Moses, Tumour stroma interactions, Current Opinion in Genetics & Development. 15 (2005) 97. https://doi.org/10.1016/J.GDE.2004.12.003.

[10] M.M. Mueller, N.E. Fusenig, Friends or foes — bipolar effects of the tumour stroma in cancer, Nature Reviews Cancer 2004 4:11. 4 (2004) 839–849. https://doi.org/10.1038/nrc1477.

[11] N.K. Karamanos, A.D. Theocharis, T. Neill, R. v. Iozzo, Matrix modeling and remodeling: A biological interplay regulating tissue homeostasis and diseases, Matrix Biology. 75–76 (2019) 1–11. https://doi.org/10.1016/j.matbio.2018.08.007.

[12] M. Mongiat, S. Buraschi, E. Andreuzzi, T. Neill, R. v. Iozzo, Extracellular matrix: the gatekeeper of tumor angiogenesis, Biochemical Society Transactions. 47 (2019) 1543–1555. https://doi.org/10.1042/BST20190653.

[13] A. Xiong, S. Kundu, K. Forsberg-Nilsson, Heparan sulfate in the regulation of neural differentiation and glioma development, The FEBS Journal. 281 (2014) 4993–5008. https://doi.org/10.1111/FEBS.13097.

[14] Z. Piperigkou, M. Götte, A.D. Theocharis, N.K. Karamanos, Insights into the key roles of epigenetics in matrix macromolecules-associated wound healing, Advanced Drug Delivery Reviews. 129 (2018) 16–36. https://doi.org/10.1016/J.ADDR.2017.10.008.

[15] A.D. Theocharis, D. Manou, N.K. Karamanos, The extracellular matrix as a multitasking player in disease, The FEBS Journal. 286 (2019) 2830–2869. https://doi.org/10.1111/FEBS.14818.

[16] F.C.O.B. Teixeira, M. Götte, Involvement of Syndecan-1 and Heparanase in Cancer and Inflammation, Advances in Experimental Medicine and Biology. 1221 (2020) 97–135. https://doi.org/10.1007/978-3-030-34521-1_4.

[17] D. Manou, I. Caon, P. Bouris, I.E. Triantaphyllidou, C. Giaroni, A. Passi, N.K. Karamanos, D. Vigetti, A.D. Theocharis, The complex interplay between extracellular matrix and cells in tissues, Methods in Molecular Biology. 1952 (2019) 1–20. https://doi.org/10.1007/978-1-4939-9133-4_1.

[18] N.K. Karamanos, A.D. Theocharis, Z. Piperigkou, D. Manou, A. Passi, S.S. Skandalis, D.H. Vynios, V. Orian-Rousseau, S. Ricard-Blum, C.E.H. Schmelzer, L. Duca, M. Durbee, N.A. Afratis, L. Troeberg, M. Franchi, V. Masola, M. Onisto, A guide to the composition and functions of the extracellular matrix, FEBS Journal. (2021). https://doi.org/10.1111/FEBS.15776.

[19] P. Lu, V.M. Weaver, Z. Werb, The extracellular matrix: A dynamic niche in cancer progression, The Journal of Cell Biology. 196 (2012) 395. https://doi.org/10.1083/JCB.201102147.

[20] M. Marozzi, A. Parnigoni, A. Negri, M. Viola, D. Vigetti, A. Passi, E. Karousou, F. Rizzi, Inflammation, Extracellular Matrix Remodeling, and Proteostasis in Tumor Microenvironment, International Journal of Molecular Sciences. 22 (2021). https://doi.org/10.3390/IJMS22158102.

[21] N.A. Bhowmick, E.G. Neilson, H.L. Moses, Stromal fibroblasts in cancer initiation and progression, Nature 2004 432:7015. 432 (2004) 332–337. https://doi.org/10.1038/nature03096.

[22] M. Viola, D. Vigetti, E. Karousou, M.L. D'Angelo, I. Caon, P. Moretto, G. de Luca, A. Passi, Biology and biotechnology of hyaluronan, Glycoconjugate Journal. 32 (2015) 93–103. https://doi.org/10.1007/s10719-015-9586-6.

[23] M.K. Cowman, H.-G. Lee, K.L. Schwertfeger, J.B. McCarthy, E.A. Turley, The Content and Size of Hyaluronan in Biological Fluids and Tissues, Frontiers in Immunology. 6 (2015). https://doi.org/10.3389/FIMMU.2015.00261.

[24] A.G. Tavianatou, I. Caon, M. Franchi, Z. Piperigkou, D. Galesso, N.K. Karamanos, Hyaluronan: molecular size-dependent signaling and biological functions in inflammation and cancer, (n.d.). https://doi.org/10.1111/febs.14777.

[25] P. Heldin, K. Basu, B. Olofsson, H. Porsch, I. Kozlova, K. Kahata, Deregulation of hyaluronan synthesis, degradation and binding promotes breast cancer, Journal of Biochemistry. 154 (2013) 395–408. https://doi.org/10.1093/jb/mvt085.

[26] A.D. Theocharis, M.E. Tsara, N. Papageorgacopoulou, D.D. Karavias, D.A. Theocharis, Pancreatic carcinoma is characterized by elevated content of hyaluronan and chondroitin sulfate with altered disaccharide composition, Biochimica et Biophysica Acta (BBA) - Molecular Basis of Disease. 1502 (2000) 201–206. https://doi.org/10.1016/S0925-4439(00)00051-X.

[27] X.-B. Cheng, N. Sato, S. Kohi, K. Yamaguchi, Prognostic Impact of Hyaluronan and Its Regulators in Pancreatic Ductal Adenocarcinoma, PLOS ONE. 8 (2013) e80765. https://doi.org/10.1371/JOURNAL.PONE.0080765.

[28] P. Auvinen, R. Tammi, J. Parkkinen, M. Tammi, U. Ågren, R. Johansson, P. Hirvikoski, M. Eskelinen, V.M. Kosma, Hyaluronan in peritumoral stroma and malignant cells associates with breast cancer spreading and predicts survival, American Journal of Pathology. 156 (2000) 529–536. https://doi.org/10.1016/S0002-9440(10)64757-8.

[29] M. Tammi, J. Parkkinen, M. Eskelinen, Tumor cell-associated hyaluronan as an unfavorable prognostic factor in colorectal cancer Metal-on-Metal side-effects View project, (1998). https://www.researchgate.net/publication/13788018 (accessed November 4, 2021).

[30] A. Josefsson, H. Adamo, P. Hammarsten, T. Granfors, P. Stattin, L. Egevad, A.E. Laurent, P. Wikström, A. Bergh, Prostate Cancer Increases Hyaluronan in Surrounding Nonmalignant Stroma, and This Response Is Associated with Tumor Growth and an Unfavorable Outcome, The American Journal of Pathology. 179 (2011) 1961. https://doi.org/10.1016/J.AJPATH.2011.06.005.

[31] L. Jadin, S. Pastorino, R. Symons, N. Nomura, P. Jiang, T. Juarez, M. Makale, S. Kesari, Hyaluronan expression in primary and secondary brain tumors, Annals of Translational Medicine. 3 (2015) 80. https://doi.org/10.3978/J.ISSN.2305-5839.2015.04.07.

[32] J.M. Karjalainen, R.H. Tammi, M.I. Tammi, M.J. Eskelinen, U.M. Ågren, J.J. Parkkinen, E.M. Alhava, V.-M. Kosma, Reduced Level of CD44 and Hyaluronan Associated with Unfavorable Prognosis in

Clinical Stage I Cutaneous Melanoma, The American Journal of Pathology. 157 (2000) 957. https://doi.org/10.1016/S0002-9440(10)64608-1.

[33] A. Kosunen, K. Ropponen, J. Kellokoski, M. Pukkila, J. Virtaniemi, H. Valtonen, E. Kumpulainen, R. Johansson, R. Tammi, M. Tammi, J. Nuutinen, V.M. Kosma, Reduced expression of hyaluronan is a strong indicator of poor survival in oral squamous cell carcinoma, Oral Oncology. 40 (2004) 257–263. https://doi.org/10.1016/J.ORALONCOLOGY.2003.08.004.

[34] D. Vigetti, M. Viola, E. Karousou, G. de Luca, A. Passi, Metabolic control of hyaluronan synthases, Matrix Biology. 35 (2014) 8–13. https://doi.org/10.1016/j.matbio.2013.10.002.

[35] N. Itano, K. Kimata, Mammalian Hyaluronan Synthases, IUBMB Life. 54 (2002) 195–199. https://doi.org/10.1080/15216540214929.

[36] A. Passi, D. Vigetti, S. Buraschi, R. v. Iozzo, Dissecting the role of hyaluronan synthases in the tumor microenvironment, FEBS Journal. 286 (2019) 2937–2949. https://doi.org/10.1111/febs.14847.

[37] S.S. Skandalis, T. Karalis, P. Heldin, Intracellular hyaluronan: Importance for cellular functions, Seminars in Cancer Biology. 62 (2020) 20–30. https://doi.org/10.1016/J.SEMCANCER.2019.07.002.

[38] N. Itano, T. Sawai, M. Yoshida, P. Lenas, Y. Yamada, M. Imagawa, T. Shinomura, M. Hamaguchi, Y. Yoshida, Y. Ohnuki, S. Miyauchi, A.P. Spicer, J.A. McDonald, K. Kimata, Three isoforms of mammalian hyaluronan synthases have distinct enzymatic properties, Journal of Biological Chemistry. 274 (1999) 25085–25092. https://doi.org/10.1074/jbc.274.35.25085.

[39] N. Kobayashi, S. Miyoshi, T. Mikami, H. Koyama, M. Kitazawa, M. Takeoka, K. Sano, J. Amano, Z. Isogai, S. Niida, K. Oguri, M. Okayama, J.A. McDonald, K. Kimata, ichiro Taniguchi, N. Itano, Hyaluronan Deficiency in Tumor Stroma Impairs Macrophage Trafficking and Tumor Neovascularization, (2010). https://doi.org/10.1158/0008-5472.CAN-09-4687.

[40] H. Koyama, T. Hibi, Z. Isogai, M. Yoneda, M. Fujimori, J. Amano, M. Kawakubo, R. Kannagi, K. Kimata, S. Taniguchi, N. Itano, Hyperproduction of Hyaluronan in Neu-Induced Mammary Tumor Accelerates Angiogenesis through Stromal Cell Recruitment : Possible Involvement of Versican/PG-M, The American Journal of Pathology. 170 (2007) 1086. https://doi.org/10.2353/AJPATH.2007.060793.

[41] P. Heldin, K. Basu, B. Olofsson, H. Porsch, I. Kozlova, K. Kahata, Deregulation of hyaluronan synthesis, degradation and binding promotes breast cancer, The Journal of Biochemistry. 154 (2013) 395–408. https://doi.org/10.1093/JB/MVT085.

[42] H. Urakawa, Y. Nishida, J. Wasa, E. Arai, L. Zhuo, K. Kimata, E. Kozawa, N. Futamura, N. Ishiguro, Inhibition of hyaluronan synthesis in breast cancer cells by 4-methylumbelliferone suppresses tumorigenicity in vitro and metastatic lesions of bone in vivo, International Journal of Cancer. 130 (2012) 454–466. https://doi.org/10.1002/ijc.26014.

[43] H. Chao, A.P. Spicer, Natural antisense mRNAs to hyaluronan synthase 2 inhibit hyaluronan biosynthesis and cell proliferation, Journal of Biological Chemistry. 280 (2005) 27513–27522. https://doi.org/10.1074/jbc.M411544200.

[44] Y. Li, L. Li, T.J. Brown, P. Heldin, Silencing of hyaluronan synthase 2 suppresses the malignant phenotype of invasive breast cancer cells, International Journal of Cancer. 120 (2007) 2557–2567. https://doi.org/10.1002/ijc.22550.

[45] T.T. Karalis, P. Heldin, D.H. Vynios, T. Neill, S. Buraschi, R. v. Iozzo, N.K. Karamanos, S.S. Skandalis, Tumor-suppressive functions of 4-MU on breast cancer cells of different ER status: Regulation of hyaluronan/HAS2/CD44 and specific matrix effectors, Matrix Biology. 78–79 (2019) 118–138. https://doi.org/10.1016/j.matbio.2018.04.007.

[46] I. Kakizaki, K. Kojima, K. Takagaki, M. Endo, R. Kannagi, M. Ito, Y. Maruo, H. Sato, T. Yasuda, S. Mita, K. Kimata, N. Itano, A Novel Mechanism for the Inhibition of Hyaluronan Biosynthesis by 4-Methylumbelliferone *, Journal of Biological Chemistry. 279 (2004) 33281–33289. https://doi.org/10.1074/JBC.M405918200.

[47] D. Vigetti, M. Rizzi, M. Viola, E. Karousou, A. Genasetti, M. Clerici, B. Bartolini, V.C. Hascall, G. de Luca, A. Passi, The effects of 4-methylumbelliferone on hyaluronan synthesis, MMP2 activity, proliferation, and motility of human aortic smooth muscle cells, Glycobiology. 19 (2009) 537–546. https://doi.org/10.1093/glycob/cwp022.

[48] I. Caon, B. Bartolini, A. Parnigoni, E. Caravà, P. Moretto, M. Viola, E. Karousou, D. Vigetti, A. Passi, Revisiting the hallmarks of cancer: The role of hyaluronan, Seminars in Cancer Biology. 62 (2020) 9–19. https://doi.org/10.1016/j.semcancer.2019.07.007.

[49] P. Heldin, C.Y. Lin, C. Kolliopoulos, Y.H. Chen, S.S. Skandalis, Regulation of hyaluronan biosynthesis and clinical impact of excessive hyaluronan production, Matrix Biology. 78–79 (2019) 100–117. https://doi.org/10.1016/j.matbio.2018.01.017.

[50] D. Vigetti, E. Karousou, M. Viola, S. Deleonibus, G. de Luca, A. Passi, Hyaluronan: Biosynthesis and signaling, Biochimica et Biophysica Acta - General Subjects. 1840 (2014) 2452–2459. https://doi.org/10.1016/j.bbagen.2014.02.001.

[51] S. Twarock, C. Reichert, U. Peters, D.J. Gorski, K. Röck, J.W. Fischer, Hyperglycaemia and aberrated insulin signalling stimulate tumour progression via induction of the extracellular matrix component hyaluronan, International Journal of Cancer. 141 (2017) 791–804. https://doi.org/10.1002/IJC.30776.

[52] D. Vigetti, S. Deleonibus, P. Moretto, E. Karousou, M. Viola, B. Bartolini, V.C. Hascall, M. Tammi, G. de Luca, A. Passi, Role of UDP-N-Acetylglucosamine (GlcNAc) and O-GlcNAcylation of Hyaluronan Synthase 2 in the Control of Chondroitin Sulfate and Hyaluronan Synthesis, The Journal of Biological Chemistry. 287 (2012) 35544. https://doi.org/10.1074/JBC.M112.402347.

[53] D. Vigetti, S. Deleonibus, P. Moretto, T. Bowen, J.W. Fischer, M. Grandoch, A. Oberhuber, D.C. Love, J.A. Hanover, R. Cinquetti, E. Karousou, M. Viola, M.L. D'Angelo, V.C. Hascall, G. de Luca, A. Passi, Natural antisense transcript for hyaluronan synthase 2 (HAS2-AS1) induces transcription of HAS2 via protein O-GlcNAcylation, Journal of Biological Chemistry. 289 (2014) 28816–28826. https://doi.org/10.1074/jbc.M114.597401.

[54] D. Vigetti, M. Clerici, S. Deleonibus, E. Karousou, M. Viola, P. Moretto, P. Heldin, V.C. Hascall, G. de Luca, A. Passi, Hyaluronan Synthesis Is Inhibited by Adenosine Monophosphate-activated Protein Kinase through the Regulation of HAS2 Activity in Human Aortic Smooth Muscle Cells, The Journal of Biological Chemistry. 286 (2011) 7917. https://doi.org/10.1074/JBC.M110.193656.

[55] D.R. Alessi, K. Sakamoto, J.R. Bayascas, LKB1-dependent signaling pathways, Annual Review of Biochemistry. 75 (2006) 137–163. https://doi.org/10.1146/ANNUREV.BIOCHEM.75.103004.142702.

[56] D. Vigetti, M. Rizzi, P. Moretto, S. Deleonibus, J.M. Dreyfuss, E. Karousou, M. Viola, M. Clerici, V.C. Hascall, M.F. Ramoni, G. de Luca, A. Passi, Glycosaminoglycans and Glucose Prevent Apoptosis in 4-Methylumbelliferone-treated Human Aortic Smooth Muscle Cells, The Journal of Biological Chemistry. 286 (2011) 34497. https://doi.org/10.1074/JBC.M111.266312.

[57] M. Suzuki, T. Asplund, H. Yamashita, C.H. Heldin, P. Heldin, Stimulation of hyaluronan biosynthesis by platelet-derived growth factor-BB and transforming growth factor-β1 involves activation of protein kinase C, Biochemical Journal. 307 (1995) 817–821. https://doi.org/10.1042/BJ3070817.

[58] E. Karousou, M. Kamiryo, S.S. Skandalis, A. Ruusala, T. Asteriou, A. Passi, H. Yamashita, U. Hellman, C.H. Heldin, P. Heldin, The activity of hyaluronan synthase 2 is regulated by dimerization and ubiquitination, Journal of Biological Chemistry. 285 (2010) 23647–23654. https://doi.org/10.1074/jbc.M110.127050.

[59] M. Viola, B. Bartolini, D. Vigetti, E. Karousou, P. Moretto, S. Deleonibus, T. Sawamura, T.N. Wight, V.C. Hascall, G. de Luca, A. Passi, Oxidized low density lipoprotein (LDL) affects hyaluronan synthesis in human aortic smooth muscle cells, Journal of Biological Chemistry. 288 (2013) 29595–29603. https://doi.org/10.1074/jbc.M113.508341.

[60] I. Caon, B. Bartolini, P. Moretto, A. Parnigoni, E. Caravà, D.L. Vitale, L. Alaniz, M. Viola, E. Karousou, G. de Luca, V.C. Hascall, A. Passi, D. Vigetti, Sirtuin 1 reduces hyaluronan synthase 2 expression by

inhibiting nuclear translocation of NF-κB and expression of the long-noncoding RNA HAS2–AS1, Journal of Biological Chemistry. 295 (2020) 3485–3496. https://doi.org/10.1074/jbc.RA119.011982.

[61] C.J. Narvaez, D. Grebenc, S. Balinth, J.E. Welsh, Vitamin D regulation of HAS2, hyaluronan synthesis and metabolism in triple negative breast cancer cells, Journal of Steroid Biochemistry and Molecular Biology. 201 (2020). https://doi.org/10.1016/j.jsbmb.2020.105688.

[62] T.T. Karalis, A. Chatzopoulos, A. Kondyli, A.J. Aletras, N.K. Karamanos, P. Heldin, S.S. Skandalis, Salicylate suppresses the oncogenic hyaluronan network in metastatic breast cancer cells, Matrix Biology Plus. 6–7 (2020). https://doi.org/10.1016/j.mbplus.2020.100031.

[63] P. Heldin, K. Basu, I. Kozlova, H. Porsch, HAS2 and CD44 in Breast Tumorigenesis, Advances in Cancer Research. 123 (2014) 211–229. https://doi.org/10.1016/B978-0-12-800092-2.00008-3.

[64] C.G. Chen, M.A. Gubbiotti, A. Kapoor, X. Han, Y. Yu, R.J. Linhardt, R. v. Iozzo, Autophagic degradation of HAS2 in endothelial cells: A novel mechanism to regulate angiogenesis, Matrix Biology. 90 (2020) 1–19. https://doi.org/10.1016/j.matbio.2020.02.001.

[65] P.W. NOBLE, J. LIANG, D. JIANG, Hyaluronan as an Immune Regulator in Human Diseases, Physiological Reviews. 91 (2011) 221. https://doi.org/10.1152/PHYSREV.00052.2009.

[66] L. Bohaumilitzky, A.-K. Huber, E.M. Stork, S. Wengert, F. Woelfl, H. Boehm, A Trickster in Disguise: Hyaluronan's Ambivalent Roles in the Matrix, Frontiers in Oncology. 7 (2017) 1. https://doi.org/10.3389/FONC.2017.00242.

[67] A.B. Csoka, G.I. Frost, R. Stern, The six hyaluronidase-like genes in the human and mouse genomes, Matrix Biology. 20 (2001) 499–508. https://doi.org/10.1016/S0945-053X(01)00172-X.

[68] I. Caon, A. Parnigoni, M. Viola, E. Karousou, A. Passi, D. Vigetti, Cell Energy Metabolism and Hyaluronan Synthesis, Journal of Histochemistry and Cytochemistry. (2020). https://doi.org/10.1369/0022155420929772.

[69] H. Yamamoto, Y. Tobisawa, T. Inubushi, F. Irie, C. Ohyama, Y. Yamaguchi, A mammalian homolog of the zebrafish transmembrane protein 2 (TMEM2) is the long-sought-after cell-surface hyaluronidase, The Journal of Biological Chemistry. 292 (2017) 7304. https://doi.org/10.1074/JBC.M116.770149.

[70] H. Yoshida, A. Nagaoka, A. Kusaka-Kikushima, M. Tobiishi, K. Kawabata, T. Sayo, S. Sakai, Y. Sugiyama, H. Enomoto, Y. Okada, S. Inoue, KIAA1199, a deafness gene of unknown function, is a new hyaluronan binding protein involved in hyaluronan depolymerization, Proceedings of the National Academy of Sciences of the United States of America. 110 (2013) 5612. https://doi.org/10.1073/PNAS.1215432110.

[71] R. Stern, M.J. Jedrzejas, The Hyaluronidases: Their Genomics, Structures, and Mechanisms of Action, Chemical Reviews. 106 (2006) 818. https://doi.org/10.1021/CR050247K.

[72] C. Tolg, H. Yuan, S.M. Flynn, K. Basu, J. Ma, K.C.K. Tse, B. Kowalska, D. Vulkanesku, M.K. Cowman, J.B. McCarthy, E.A. Turley, Hyaluronan modulates growth factor induced mammary gland branching in a size dependent manner, Matrix Biology. 63 (2017) 117–132. https://doi.org/10.1016/J.MATBIO.2017.02.003.

[73] A. Motolese, F. Vignati, R. Brambilla, M. Cerati, A. Passi, Interaction between a Regenerative Matrix and Wound Bed in Nonhealing Ulcers: Results with 16 Cases, BioMed Research International. 2013 (2013). https://doi.org/10.1155/2013/849321.

[74] X. Tian, J. Azpurua, C. Hine, A. Vaidya, M. Myakishev-Rempel, J. Ablaeva, Z. Mao, E. Nevo, V. Gorbunova, A. Seluanov, High molecular weight hyaluronan mediates the cancer resistance of the naked mole-rat, Nature. 499 (2013) 346. https://doi.org/10.1038/NATURE12234.

[75] D. del Marmol, S. Holtze, N. Kichler, A. Sahm, B. Bihin, V. Bourguignon, S. Dogné, K. Szafranski, T.B. Hildebrandt, B. Flamion, Abundance and size of hyaluronan in naked mole-rat tissues and plasma, Scientific Reports. 11 (2021). https://doi.org/10.1038/S41598-021-86967-9.

[76] L.K. Boroughs, R.J. Deberardinis, Metabolic pathways promoting cancer cell survival and growth, Nature Cell Biology. 17 (2015) 351. https://doi.org/10.1038/NCB3124.

[77] J.X. Tan, X.Y. Wang, H.Y. Li, X.L. Su, L. Wang, L. Ran, K. Zheng, G.S. Ren, HYAL1 overexpression is correlated with the malignant behavior of human breast cancer, International Journal of Cancer. 128 (2011) 1303–1315. https://doi.org/10.1002/IJC.25460.

[78] L. Udabage, G.R. Brownlee, S.K. Nilsson, T.J. Brown, The over-expression of HAS2, Hyal-2 and CD44 is implicated in the invasiveness of breast cancer, Experimental Cell Research. 310 (2005) 205–217. https://doi.org/10.1016/J.YEXCR.2005.07.026.

[79] S. Hanna, P. Mari, T.K. Kristiina, S. Reijo, P.S. Sanna, Inverse expression of hyaluronidase 2 and hyaluronan synthases 1-3 is associated with reduced hyaluronan content in malignant cutaneous melanoma, BMC Cancer. 13 (2013) 1–12. https://doi.org/10.1186/1471-2407-13-181/FIGURES/5.

[80] D. Jiang, J. Liang, P.W. Noble, Hyaluronan as an immune regulator in human diseases, Physiological Reviews. 91 (2011) 221–264. https://doi.org/10.1152/PHYSREV.00052.2009/ASSET/IMAGES/LARGE/Z9J0041025640014.JPEG.

[81] B.P. Toole, Hyaluronan: from extracellular glue to pericellular cue, Nature Reviews Cancer 2004 4:7. 4 (2004) 528–539. https://doi.org/10.1038/nrc1391.

[82] I. Morath, T.N. Hartmann, V. Orian-Rousseau, CD44: More than a mere stem cell marker, The International Journal of Biochemistry & Cell Biology. 81 (2016) 166–173. https://doi.org/10.1016/J.BIOCEL.2016.09.009.

[83] S. Misra, V.C. Hascall, R.R. Markwald, S. Ghatak, Interactions between Hyaluronan and Its Receptors (CD44, RHAMM) Regulate the Activities of Inflammation and Cancer, Frontiers in Immunology. 6 (2015). https://doi.org/10.3389/FIMMU.2015.00201.

[84] Z. Luo, R.R. Wu, L. Lv, P. Li, L.Y. Zhang, Q.L. Hao, W. Li, Prognostic value of CD44 expression in non-small cell lung cancer: a systematic review, International Journal of Clinical and Experimental Pathology. 7 (2014) 3632. /pmc/articles/PMC4128975/ (accessed November 8, 2021).

[85] M. Todaro, M. Gaggianesi, V. Catalano, A. Benfante, F. Iovino, M. Biffoni, T. Apuzzo, I. Sperduti, S. Volpe, G. Cocorullo, G. Gulotta, F. Dieli, R. de Maria, G. Stassi, CD44v6 Is a Marker of Constitutive and Reprogrammed Cancer Stem Cells Driving Colon Cancer Metastasis, Cell Stem Cell. 14 (2014) 342–356. https://doi.org/10.1016/J.STEM.2014.01.009.

[86] S. di Franco, A. Turdo, A. Benfante, M.L. Colorito, M. Gaggianesi, T. Apuzzo, R. Kandimalla, A. Chinnici, D. Barcaroli, L.R. Mangiapane, G. Pistone, S. Vieni, E. Gulotta, F. Dieli, J.P. Medema, G. Stassi, V. de Laurenzi, M. Todaro, S. di Franco, A. Turdo, A. Benfante, M.L. Colorito, M. Gaggianesi, T. Apuzzo, R. Kandimalla, A. Chinnici, D. Barcaroli, L.R. Mangiapane, G. Pistone, S. Vieni, E. Gulotta, F. Dieli, J.P. Medema, G. Stassi, V. de Laurenzi, M. Todaro, ΔNp63 drives metastasis in breast cancer cells via PI3K/CD44v6 axis, Oncotarget. 7 (2016) 54157–54173. https://doi.org/10.18632/ONCOTARGET.11022.

[87] J. Wang, L. Xiao, C.H. Luo, H. Zhou, L. Zeng, J. Zhong, Y. Tang, X.H. Zhao, M. Zhao, Y. Zhang, CD44v6 promotes β-catenin and TGF-β expression, inducing aggression in ovarian cancer cells, Molecular Medicine Reports. 11 (2015) 3505–3510. https://doi.org/10.3892/MMR.2015.3145/HTML.

[88] C. Chen, S. Zhao, A. Karnad, J.W. Freeman, The biology and role of CD44 in cancer progression: therapeutic implications, Journal of Hematology & Oncology. 11 (2018). https://doi.org/10.1186/S13045-018-0605-5.

[89] E. Olsson, G. Honeth, P.O. Bendahl, L.H. Saal, S. Gruvberger-Saal, M. Ringnér, J. Vallon-Christersson, G. Jönsson, K. Holm, K. Lövgren, M. Fernö, D. Grabau, Å. Borg, C. Hegardt, CD44 isoforms are heterogeneously expressed in breast cancer and correlate with tumor subtypes and cancer stem cell markers, BMC Cancer. 11 (2011) 418. https://doi.org/10.1186/1471-2407-11-418.

[90] S.A. Ibrahim, R. Gadalla, E.A. El-Ghonaimy, O. Samir, H.T. Mohamed, H. Hassan, B. Greve, M. El-Shinawi, M.M. Mohamed, M. Götte, Syndecan-1 is a novel molecular marker for triple negative inflammatory breast cancer and modulates the cancer stem cell phenotype via the IL-6/STAT3,

Notch and EGFR signaling pathways, Molecular Cancer 2017 16:1. 16 (2017) 1–19. https://doi.org/10.1186/S12943-017-0621-Z.

[91] Z. Wang, K. Zhao, T. Hackert, M. Zöller, CD44/CD44v6 a reliable companion in cancer-initiating cell maintenance and tumor progression, Frontiers in Cell and Developmental Biology. 6 (2018) 97. https://doi.org/10.3389/FCELL.2018.00097/BIBTEX.

[92] Q. Yu, I. Stamenkovic, Cell surface-localized matrix metalloproteinase-9 proteolytically activates TGF-β and promotes tumor invasion and angiogenesis, Genes & Development. 14 (2000) 163. https://doi.org/10.1101/gad.14.2.163.

[93] R. Gao, D. Li, J. Xun, W. Zhou, J. Li, J. Wang, C. Liu, X. Li, W. Shen, H. Qiao, D.G. Stupack, N. Luo, CD44ICD promotes breast cancer stemness via PFKFB4-mediated glucose metabolism, Theranostics. 8 (2018) 6248–6262. https://doi.org/10.7150/THNO.28721.

[94] M. Kajita, Y. Itoh, T. Chiba, H. Mori, A. Okada, H. Kinoh, M. Seiki, Membrane-type 1 matrix metalloproteinase cleaves CD44 and promotes cell migration, Journal of Cell Biology. 153 (2001) 893–904. https://doi.org/10.1083/JCB.153.5.893.

[95] Y. Cho, H.-W. Lee, H.-G. Kang, H.-Y. Kim, S.-J. Kim, K.-H. Chun, Y. Cho, H.-W. Lee, H.-G. Kang, H.-Y. Kim, S.-J. Kim, K.-H. Chun, Cleaved CD44 intracellular domain supports activation of stemness factors and promotes tumorigenesis of breast cancer, Oncotarget. 6 (2015) 8709–8721. https://doi.org/10.18632/ONCOTARGET.3325.

[96] F. Korkes, M.G. de Castro, S. de Cassio Zequi, L. Nardi, A. del Giglio, A.C. de Lima Pompeo, Hyaluronan-mediated motility receptor (RHAMM) immunohistochemical expression and androgen deprivation in normal peritumoral, hyperplasic and neoplastic prostate tissue, BJU International. 113 (2014) 822–829. https://doi.org/10.1111/BJU.12339.

[97] D.T. Rein, K. Roehrig, T. Schöndorf, A. Lazar, M. Fleisch, D. Niederacher, H.G. Bender, P. Dall, Expression of the hyaluronan receptor RHAMM in endometrial carcinomas suggests a role in tumour progression and metastasis, Journal of Cancer Research and Clinical Oncology. 129 (2003) 161–164. https://doi.org/10.1007/S00432-003-0415-0/TABLES/2.

[98] H. Zhang, L. Ren, Y. Ding, F. Li, { Xiangfu Chen, Y. Ouyang, Y. Zhang, D. Zhang, H.- Zhang, L. Ren, Y. Li, F. Chen, X. Ouyang, Y. Zhang, D. Hyaluronan, Hyaluronan-mediated motility receptor confers resistance to chemotherapy via TGFβ/Smad2-induced epithelial-mesenchymal transition in gastric cancer, The FASEB Journal. 33 (2019) 6365–6377. https://doi.org/10.1096/FJ.201802186R.

[99] V. Mele, L. Sokol, V.H. Kölzer, D. Pfaff, M.G. Muraro, I. Keller, Z. Stefan, I. Centeno, L.M. Terracciano, H. Dawson, I. Zlobec, G. Iezzi, A. Lugli, The hyaluronan-mediated motility receptor RHAMM promotes growth, invasiveness and dissemination of colorectal cancer, Oncotarget. 8 (2017) 70617. https://doi.org/10.18632/ONCOTARGET.19904.

[100] K. Kouvidi, A. Berdiaki, D. Nikitovic, P. Katonis, N. Afratis, V.C. Hascall, N.K. Karamanos, G.N. Tzanakakis, Role of Receptor for Hyaluronic Acid-mediated Motility (RHAMM) in Low Molecular Weight Hyaluronan (LMWHA)-mediated Fibrosarcoma Cell Adhesion, Journal of Biological Chemistry. 286 (2011) 38509–38520. https://doi.org/10.1074/JBC.M111.275875.

[101] D. Nikitovic, K. Kouvidi, N.K. Karamanos, G.N. Tzanakakis, The roles of hyaluronan/RHAMM/CD44 and their respective interactions along the insidious pathways of fibrosarcoma progression, BioMed Research International. 2013 (2013). https://doi.org/10.1155/2013/929531.

[102] K. Hally, S. Fauteux-Daniel, H. Hamzeh-Cognasse, P. Larsen, F. Cognasse, Revisiting Platelets and Toll-Like Receptors (TLRs): At the Interface of Vascular Immunity and Thrombosis, International Journal of Molecular Sciences 2020, Vol. 21, Page 6150. 21 (2020) 6150. https://doi.org/10.3390/IJMS21176150.

[103] A. di Lorenzo, E. Bolli, L. Tarone, F. Cavallo, L. Conti, Toll-Like Receptor 2 at the Crossroad between Cancer Cells, the Immune System, and the Microbiota, International Journal of Molecular Sciences 2020, Vol. 21, Page 9418. 21 (2020) 9418. https://doi.org/10.3390/IJMS21249418.

[104] W. Zheng, Q. Xu, Y. Zhang, E. Xiaofei, W. Gao, M. Zhang, W. Zhai, R.S. Rajkumar, Z. Liu, Toll-like receptor-mediated innate immunity against herpesviridae infection: a current perspective on viral infection signaling pathways, Virology Journal. 17 (2020) 1–15. https://doi.org/10.1186/S12985-020-01463-2/FIGURES/2.

[105] S. Makkar, T.E. Riehl, B. Chen, Y. Yan, D.M. Alvarado, M.A. Ciorba, W.F. Stenson, Hyaluronic Acid Binding to TLR4 Promotes Proliferation and Blocks Apoptosis in Colon Cancer, Molecular Cancer Therapeutics. 18 (2019) 2446–2456. https://doi.org/10.1158/1535-7163.MCT-18-1225.

[106] E. Ferrandez, O. Gutierrez, D.S. Segundo, J.L. Fernandez-Luna, NFκB activation in differentiating glioblastoma stem-like cells is promoted by hyaluronic acid signaling through TLR4, Scientific Reports 2018 8:1. 8 (2018) 1–10. https://doi.org/10.1038/s41598-018-24444-6.

[107] M.S. Rugg, A.C. Willis, D. Mukhopadhyay, V.C. Hascall, E. Fries, C. Fülöp, C.M. Milner, A.J. Day, Characterization of complexes formed between TSG-6 and inter-α- inhibitor that act as intermediates in the covalent transfer of heavy chains onto hyaluronan, Journal of Biological Chemistry. 280 (2005) 25674–25686. https://doi.org/10.1074/JBC.M501332200/ATTACHMENT/D1AAF1B2-EDA1-43C0-9FE9-8655B0983A2A/MMC1.PDF.

[108] D.L. Vitale, F.M. Spinelli, L. Alaniz, Determination of Cell-Surface Hyaluronan Through Flow Cytometry, Methods in Molecular Biology. 1952 (2019) 111–116. https://doi.org/10.1007/978-1-4939-9133-4_10.

[109] G. Zhang, Y. He, Y. Liu, Y. Du, C. Yang, F. Gao, Reduced hyaluronan cross-linking induces breast cancer malignancy in a CAF-dependent manner, Cell Death & Disease 2021 12:6. 12 (2021) 1–14. https://doi.org/10.1038/s41419-021-03875-6.

[110] S. Djebali, C.A. Davis, A. Merkel, A. Dobin, T. Lassmann, A. Mortazavi, A. Tanzer, J. Lagarde, W. Lin, F. Schlesinger, C. Xue, G.K. Marinov, J. Khatun, B.A. Williams, C. Zaleski, J. Rozowsky, M. Röder, F. Kokocinski, R.F. Abdelhamid, T. Alioto, I. Antoshechkin, M.T. Baer, N.S. Bar, P. Batut, K. Bell, I. Bell, S. Chakrabortty, X. Chen, J. Chrast, J. Curado, T. Derrien, J. Drenkow, E. Dumais, J. Dumais, R. Duttagupta, E. Falconnet, M. Fastuca, K. Fejes-Toth, P. Ferreira, S. Foissac, M.J. Fullwood, H. Gao, D. Gonzalez, A. Gordon, H. Gunawardena, C. Howald, S. Jha, R. Johnson, P. Kapranov, B. King, C. Kingswood, O.J. Luo, E. Park, K. Persaud, J.B. Preall, P. Ribeca, B. Risk, D. Robyr, M. Sammeth, L. Schaffer, L.H. See, A. Shahab, J. Skancke, A.M. Suzuki, H. Takahashi, H. Tilgner, D. Trout, N. Walters, H. Wang, J. Wrobel, Y. Yu, X. Ruan, Y. Hayashizaki, J. Harrow, M. Gerstein, T. Hubbard, A. Reymond, S.E. Antonarakis, G. Hannon, M.C. Giddings, Y. Ruan, B. Wold, P. Carninci, R. Guig, T.R. Gingeras, Landscape of transcription in human cells, Nature. 489 (2012) 101–108. https://doi.org/10.1038/nature11233.

[111] K. Zhang, Z.M. Shi, Y.N. Chang, Z.M. Hu, H.X. Qi, W. Hong, The ways of action of long non-coding RNAs in cytoplasm and nucleus, Gene. 547 (2014) 1–9. https://doi.org/10.1016/j.gene.2014.06.043.

[112] S. Hombach, M. Kretz, Non-coding RNAs: Classification, biology and functioning, Advances in Experimental Medicine and Biology. 937 (2016) 3–17. https://doi.org/10.1007/978-3-319-42059-2_1.

[113] E. Giovannetti, A. Erozenci, J. Smit, R. Danesi, G.J. Peters, Molecular mechanisms underlying the role of microRNAs (miRNAs) in anticancer drug resistance and implications for clinical practice, Critical Reviews in Oncology/Hematology. 81 (2012) 103–122. https://doi.org/10.1016/J.CRITREVONC.2011.03.010.

[114] L. Guo, Z. Lu, The Fate of miRNA* Strand through Evolutionary Analysis: Implication for Degradation As Merely Carrier Strand or Potential Regulatory Molecule?, PLOS ONE. 5 (2010) e11387. https://doi.org/10.1371/JOURNAL.PONE.0011387.

[115] J. Chen, C. Ding, X. Yang, J. Zhao, BMSCs-Derived Exosomal MiR-126-3p Inhibits the Viability of NSCLC Cells by Targeting PTPN9, Journal of B.U.ON. : Official Journal of the Balkan Union of Oncology. 26 (2021) 1832–1841. https://pubmed.ncbi.nlm.nih.gov/34761590/ (accessed November 12, 2021).

[116] Y. Jin, J. Cao, X. Hu, H. Cheng, Long noncoding RNA TUG1 upregulates VEGFA to enhance malignant behaviors in stomach adenocarcinoma by sponging miR-29c-3p, Journal of Clinical Laboratory Analysis. (2021). https://doi.org/10.1002/JCLA.24106.

[117] M. He, Q. Jin, C. Chen, Y. Liu, X. Ye, Y. Jiang, F. Ji, H. Qian, D. Gan, S. Yue, W. Zhu, T. Chen, The miR-186-3p/EREG axis orchestrates tamoxifen resistance and aerobic glycolysis in breast cancer cells, Oncogene 2019 38:28. 38 (2019) 5551–5565. https://doi.org/10.1038/s41388-019-0817-3.

[118] Y. Peng, C.M. Croce, The role of MicroRNAs in human cancer, Signal Transduction and Targeted Therapy 2016 1:1. 1 (2016) 1–9. https://doi.org/10.1038/sigtrans.2015.4.

[119] W. Si, J. Shen, H. Zheng, W. Fan, The role and mechanisms of action of microRNAs in cancer drug resistance, Clinical Epigenetics 2019 11:1. 11 (2019) 1–24. https://doi.org/10.1186/S13148-018-0587-8.

[120] P. Paul, A. Chakraborty, D. Sarkar, M. Langthasa, M. Rahman, M. Bari, R.K.S. Singha, A.K. Malakar, S. Chakraborty, Interplay between miRNAs and human diseases, Journal of Cellular Physiology. 233 (2018) 2007–2018. https://doi.org/10.1002/JCP.25854.

[121] A. Adam-Artigues, I. Garrido-Cano, S. Simón, B. Ortega, S. Moragón, A. Lameirinhas, V. Constâncio, S. Salta, O. Burgués, B. Bermejo, R. Henrique, A. Lluch, C. Jerónimo, P. Eroles, J.M. Cejalvo, Circulating miR-30b-5p levels in plasma as a novel potential biomarker for early detection of breast cancer, ESMO Open. 6 (2021). https://doi.org/10.1016/J.ESMOOP.2020.100039/ATTACHMENT/08B45CE3-1F13-4C5A-BEFE-DB83317DEE7E/MMC1.DOCX.

[122] P. D'Antona, M. Cattoni, L. Dominioni, A. Poli, F. Moretti, R. Cinquetti, E. Gini, E. Daffre, D.M. Noonan, A. Imperatori, N. Rotolo, P. Campomenosi, Serum miR-223: A Validated Biomarker for Detection of Early-Stage Non–Small Cell Lung Cancer, Cancer Epidemiology and Prevention Biomarkers. 28 (2019) 1926–1933. https://doi.org/10.1158/1055-9965.EPI-19-0626.

[123] G.A. Calin, C.D. Dumitru, M. Shimizu, R. Bichi, S. Zupo, E. Noch, H. Aldler, S. Rattan, M. Keating, K. Rai, L. Rassenti, T. Kipps, M. Negrini, F. Bullrich, C.M. Croce, Frequent deletions and down-regulation of micro- RNA genes miR15 and miR16 at 13q14 in chronic lymphocytic leukemia, Proceedings of the National Academy of Sciences of the United States of America. 99 (2002) 15524. https://doi.org/10.1073/PNAS.242606799.

[124] G.A. Calin, A. Cimmino, M. Fabbri, M. Ferracin, S.E. Wojcik, M. Shimizu, C. Taccioli, N. Zanesi, R. Garzon, R.I. Aqeilan, H. Alder, S. Volinia, L. Rassenti, X. Liu, C.G. Liu, T.J. Kipps, M. Negrini, C.M. Croce, MiR-15a and miR-16-1 cluster functions in human leukemia, Proceedings of the National Academy of Sciences of the United States of America. 105 (2008) 5166. https://doi.org/10.1073/PNAS.0800121105.

[125] A. Cimmino, G.A. Calin, M. Fabbri, M. v. Iorio, M. Ferracin, M. Shimizu, S.E. Wojcik, R.I. Aqeilan, S. Zupo, M. Dono, L. Rassenti, H. Alder, S. Volinia, C.G. Liu, T.J. Kipps, M. Negrini, C.M. Croce, miR-15 and miR-16 induce apoptosis by targeting BCL2, Proceedings of the National Academy of Sciences of the United States of America. 102 (2005) 13944. https://doi.org/10.1073/PNAS.0506654102.

[126] L.Y.W. Bourguignon, C.C. Spevak, G. Wong, W. Xia, E. Gilad, Hyaluronan-CD44 Interaction with Protein Kinase Cε Promotes Oncogenic Signaling by the Stem Cell Marker Nanog and the Production of MicroRNA-21, Leading to Down-regulation of the Tumor Suppressor Protein PDCD4, Anti-apoptosis, and Chemotherapy Resistance in Breast Tumor Cells *, Journal of Biological Chemistry. 284 (2009) 26533–26546. https://doi.org/10.1074/JBC.M109.027466.

[127] L.Y.W. Bourguignon, Matrix Hyaluronan-CD44 Interaction Activates MicroRNA and LncRNA Signaling Associated With Chemoresistance, Invasion, and Tumor Progression, Frontiers in Oncology. 0 (2019) 492. https://doi.org/10.3389/FONC.2019.00492.

[128] K.K. Wentz-Hunter, J.A. Potashkin, The Role of miRNAs as Key Regulators in the Neoplastic Microenvironment, Molecular Biology International. 2011 (2011) 1–8. https://doi.org/10.4061/2011/839872.

[129] M. Guttman, I. Amit, M. Garber, C. French, M.F. Lin, D. Feldser, M. Huarte, O. Zuk, B.W. Carey, J.P. Cassady, M.N. Cabili, R. Jaenisch, T.S. Mikkelsen, T. Jacks, N. Hacohen, B.E. Bernstein, M. Kellis, A. Regev, J.L. Rinn, E.S. Lander, Chromatin signature reveals over a thousand highly conserved large non-coding RNAs in mammals, Nature. 458 (2009) 223–227. https://doi.org/10.1038/nature07672.

[130] A. Parnigoni, I. Caon, P. Moretto, M. Viola, E. Karousou, A. Passi, D. Vigetti, P.P. A, C. I, M. P, V. M, K. E, P.P. A, V. D, The role of the multifaceted long non-coding RNAs: A nuclear-cytosolic interplay to regulate hyaluronan metabolism, 11 (2021) 100060. https://pubmed.ncbi.nlm.nih.gov/34435179/ (accessed May 14, 2021).

[131] M. Cabili, C. Trapnell, L. Goff, M. Koziol, B. Tazon-Vega, A. Regev, J.L. Rinn, Integrative annotation of human large intergenic noncoding RNAs reveals global properties and specific subclasses, Genes and Development. 25 (2011) 1915–1927. https://doi.org/10.1101/gad.17446611.

[132] J. Xing, H. Liu, W. Jiang, L. Wang, LncRNA-Encoded Peptide: Functions and Predicting Methods, Frontiers in Oncology. 10 (2021) 3071. https://doi.org/10.3389/fonc.2020.622294.

[133] M.P. Dragomir, G.C. Manyam, L.F. Ott, L. Berland, E. Knutsen, C. Ivan, L. Lipovich, B.M. Broom, G.A. Calin, Funcpep: A database of functional peptides encoded by non-coding rnas, Non-Coding RNA. 6 (2020) 1–18. https://doi.org/10.3390/ncrna6040041.

[134] P. Wu, Y. Mo, M. Peng, T. Tang, Y. Zhong, X. Deng, F. Xiong, C. Guo, X. Wu, Y. Li, X. Li, G. Li, Z. Zeng, W. Xiong, Emerging role of tumor-related functional peptides encoded by lncRNA and circRNA, Molecular Cancer. 19 (2020) 1–14. https://doi.org/10.1186/s12943-020-1147-3.

[135] R.A. Chodroff, L. Goodstadt, T.M. Sirey, P.L. Oliver, K.E. Davies, E.D. Green, Z. Molnár, C.P. Ponting, Long noncoding RNA genes: conservation of sequence and brain expression among diverse amniotes, Genome Biology. 11 (2010) R72. https://doi.org/10.1186/gb-2010-11-7-r72.

[136] T. Derrien, R. Johnson, G. Bussotti, A. Tanzer, S. Djebali, H. Tilgner, G. Guernec, D. Martin, A. Merkel, D.G. Knowles, J. Lagarde, L. Veeravalli, X. Ruan, Y. Ruan, T. Lassmann, P. Carninci, J.B. Brown, L. Lipovich, J.M. Gonzalez, M. Thomas, C.A. Davis, R. Shiekhattar, T.R. Gingeras, T.J. Hubbard, C. Notredame, J. Harrow, R. Guigó, The GENCODE v7 catalog of human long noncoding RNAs: Analysis of their gene structure, evolution, and expression, (n.d.). https://doi.org/10.1101/gr.132159.111.

[137] J. Ponjavic, C.P. Ponting, G. Lunter, Functionality or transcriptional noise? Evidence for selection within long noncoding RNAs, Genome Research. 17 (2007) 556–565. https://doi.org/10.1101/gr.6036807.

[138] J. Carlevaro-Fita, R. Johnson, Global Positioning System: Understanding Long Noncoding RNAs through Subcellular Localization, Molecular Cell. 73 (2019) 869–883. https://doi.org/10.1016/j.molcel.2019.02.008.

[139] Y. Zhuang, X. Wang, H.T. Nguyen, Y. Zhuo, X. Cui, C. Fewell, E.K. Flemington, B. Shan, Induction of long intergenic non-coding RNA HOTAIR in lung cancer cells by type i collagen, Journal of Hematology and Oncology. 6 (2013) 35. https://doi.org/10.1186/1756-8722-6-35.

[140] M. Li, X. Li, Y. Zhuang, E.K. Flemington, Z. Lin, B. Shan, Induction of a novel isoform of the lnc <scp>RNA HOTAIR</scp> in Claudin-low breast cancer cells attached to extracellular matrix, Molecular Oncology. 11 (2017) 1698–1710. https://doi.org/10.1002/1878-0261.12133.

[141] M. Piipponen, J. Heino, V.M. Kähäri, L. Nissinen, Long non-coding RNA PICSAR decreases adhesion and promotes migration of squamous carcinoma cells by downregulating α2β1 and α5β1 integrin expression, Biology Open. 7 (2018). https://doi.org/10.1242/bio.037044.

[142] Y. Zheng, B. Zheng, X. Meng, Y. Yan, J. He, Y. Liu, LncRNA DANCR promotes the proliferation, migration, and invasion of tongue squamous cell carcinoma cells through miR-135a-5p/KLF8 axis, Cancer Cell International. 19 (2019) 1–14. https://doi.org/10.1186/s12935-019-1016-6.

[143] X. Zhang, W. Wang, W. Zhu, J. Dong, Y. Cheng, Z. Yin, F. Shen, Mechanisms and functions of long non-coding RNAs at multiple regulatory levels, International Journal of Molecular Sciences. 20 (2019). https://doi.org/10.3390/ijms20225573.

[144] M. Morlando, M. Ballarino, A. Fatica, Long non-coding RNAs: New players in hematopoiesis and leukemia, Frontiers in Medicine. 2 (2015). https://doi.org/10.3389/fmed.2015.00023.

[145] A.M. Schmitt, H.Y. Chang, Long Noncoding RNAs in Cancer Pathways, Cancer Cell. 29 (2016) 452–463. https://doi.org/10.1016/j.ccell.2016.03.010.

[146] O. van Grembergen, M. Bizet, E.J. de Bony, E. Calonne, P. Putmans, S. Brohée, C. Olsen, M. Guo, G. Bontempi, C. Sotiriou, M. Defrance, F. Fuks, Portraying breast cancers with long noncoding RNAs, Science Advances. 2 (2016) 1600220. https://doi.org/10.1126/SCIADV.1600220.

[147] M. Lv, P. Xu, Y. Wu, L. Huang, W. Li, S. Lv, X. Wu, X. Zeng, R. Shen, X. Jia, Y. Yin, Y. Gu, H. Yuan, H. Xie, Z. Fu, LncRNAs as new biomarkers to differentiate triple negative breast cancer from non-triple negative breast cancer, Oncotarget. 7 (2016) 13047–13059. https://doi.org/10.18632/ONCOTARGET.7509.

[148] S. Cerk, D. Schwarzenbacher, J.B. Adiprasito, M. Stotz, G.C. Hutterer, A. Gerger, H. Ling, G.A. Calin, M. Pichler, Current Status of Long Non-Coding RNAs in Human Breast Cancer, International Journal of Molecular Sciences. 17 (2016). https://doi.org/10.3390/IJMS17091485.

[149] D.R. Michael, A.O. Phillips, A. Krupa, J. Martin, J.E. Redman, A. Altaher, R.D. Neville, J. Webber, M.Y. Kim, T. Bowen, The human hyaluronan synthase 2 (HAS2) gene and its natural antisense RNA exhibit coordinated expression in the renal proximal tubular epithelial cell, Journal of Biological Chemistry. 286 (2011) 19523–19532. https://doi.org/10.1074/jbc.M111.233916.

[150] G. Zhu, S. Wang, J. Chen, Z. Wang, X. Liang, X. Wang, J. Jiang, J. Lang, L. Li, Long noncoding RNA HAS2-AS1 mediates hypoxia-induced invasiveness of oral squamous cell carcinoma, Molecular Carcinogenesis. 56 (2017) 2210–2222. https://doi.org/10.1002/mc.22674.

[151] C. Kolliopoulos, C.Y. Lin, C.H. Heldin, A. Moustakas, P. Heldin, Has2 natural antisense RNA and Hmga2 promote Has2 expression during TGFβ-induced EMT in breast cancer, Matrix Biology. 80 (2019) 29–45. https://doi.org/10.1016/j.matbio.2018.09.002.

[152] G.Q. Zhu, Y.L. Tang, L. Li, M. Zheng, J. Jiang, X.Y. Li, S.X. Chen, X.H. Liang, Hypoxia inducible factor 1α and hypoxia inducible factor 2α play distinct and functionally overlapping roles in oral squamous cell carcinoma, Clinical Cancer Research. 16 (2010) 4732–4741. https://doi.org/10.1158/1078-0432.CCR-10-1408.

[153] J. Wang, Y. Zhang, A. You, J. Li, J. Gu, G. Rao, X. Ge, K. Zhang, H. Fu, X. Liu, J. Li, Q. Wang, X. Wu, L. Cheng, M. Zhu, D. Wang, HAS2-AS1 Acts as a Molecular Sponge for miR-137 and Promotes the Invasion and Migration of Glioma Cells by Targeting EZH2, Cell Cycle. (2020). https://doi.org/10.1080/15384101.2020.1826237.

[154] L. Zhang, H. Wang, M. Xu, F. Chen, W. Li, H. Hu, Q. Yuan, Y. Su, X. Liu, J. Wuri, T. Yan, Long noncoding RNA HAS2-AS1 promotes tumor progression in glioblastoma via functioning as a competing endogenous RNA, Journal of Cellular Biochemistry. 121 (2020) 661–671. https://doi.org/10.1002/jcb.29313.

[155] L. Tong, Y. Wang, Y. Ao, X. Sun, CREB1 induced lncRNA HAS2-AS1 promotes epithelial ovarian cancer proliferation and invasion via the miR-466/RUNX2 axis, Biomedicine and Pharmacotherapy. 115 (2019) 108891. https://doi.org/10.1016/j.biopha.2019.108891.

[156] D. Hanahan, R.A. Weinberg, Hallmarks of Cancer: The Next Generation, Cell. 144 (2011) 646–674. https://doi.org/10.1016/J.CELL.2011.02.013.

[157] B.D. Manning, A. Toker, AKT/PKB Signaling: Navigating the Network, Cell. 169 (2017) 381–405. https://doi.org/10.1016/J.CELL.2017.04.001.

[158] C.C. Dibble, L.C. Cantley, Regulation of mTORC1 by PI3K signaling, Trends in Cell Biology. 25 (2015) 545–555. https://doi.org/10.1016/J.TCB.2015.06.002.

[159] S. Liu, C. Cheng, Akt Signaling Is Sustained by a CD44 Splice Isoform–Mediated Positive Feedback Loop, Cancer Research. 77 (2017) 3791–3801. https://doi.org/10.1158/0008-5472.CAN-16-2545.

[160] V. Mele, L. Sokol, V.H. Kölzer, D. Pfaff, M.G. Muraro, I. Keller, Z. Stefan, I. Centeno, L.M. Terracciano, H. Dawson, I. Zlobec, G. Iezzi, A. Lugli, V. Mele, L. Sokol, V. Hendrik Kölzer, D. Pfaff, M. Giuseppe Muraro, I. Keller, Z. Stefan, I. Centeno, L. Maria Terracciano, H. Dawson, I. Zlobec, G. Iezzi, A. Lugli, The hyaluronan-mediated motility receptor RHAMM promotes growth, invasiveness and dissemination of colorectal cancer, Oncotarget. 8 (2017) 70617–70629. https://doi.org/10.18632/ONCOTARGET.19904.

[161] Y.-T. Chen, Z. Chen, Y.-C.N. Du, Y.-T. Chen, Z. Chen, Y.-C. Nancy Du, Immunohistochemical analysis of RHAMM expression in normal and neoplastic human tissues: a cell cycle protein with distinctive expression in mitotic cells and testicular germ cells, Oncotarget. 9 (2018) 20941–20952. https://doi.org/10.18632/ONCOTARGET.24939.

[162] S. Ghafouri-Fard, H. Shoorei, F.T. Anamag, M. Taheri, The Role of Non-Coding RNAs in Controlling Cell Cycle Related Proteins in Cancer Cells, Frontiers in Oncology. 10 (2020) 2616. https://doi.org/10.3389/FONC.2020.608975/BIBTEX.

[163] L. Chang, R. Guo, Z. Yuan, H. Shi, D. Zhang, LncRNA HOTAIR Regulates CCND1 and CCND2 Expression by Sponging miR-206 in Ovarian Cancer, Cellular Physiology and Biochemistry. 49 (2018) 1289–1303. https://doi.org/10.1159/000493408.

[164] V. Tripathi, Z. Shen, A. Chakraborty, S. Giri, S.M. Freier, X. Wu, Y. Zhang, M. Gorospe, S.G. Prasanth, A. Lal, K. v. Prasanth, Long Noncoding RNA MALAT1 Controls Cell Cycle Progression by Regulating the Expression of Oncogenic Transcription Factor B-MYB, PLoS Genetics. 9 (2013). https://doi.org/10.1371/JOURNAL.PGEN.1003368.

[165] E. Karousou, S. Misra, S. Ghatak, K. Dobra, M. Götte, D. Vigetti, A. Passi, N.K. Karamanos, S.S. Skandalis, Roles and targeting of the HAS/hyaluronan/CD44 molecular system in cancer, Matrix Biology. 59 (2017) 3–22. https://doi.org/10.1016/J.MATBIO.2016.10.001.

[166] T.A. Werfel, D.L. Elion, B. Rahman, D.J. Hicks, V. Sanchez, P.I. Gonzales-Ericsson, M.J. Nixon, J.L. James, J.M. Balko, P.A. Scherle, H.K. Koblish, R.S. Cook, Treatment-Induced Tumor Cell Apoptosis and Secondary Necrosis Drive Tumor Progression in the Residual Tumor Microenvironment through MerTK and IDO1, Cancer Research. 79 (2019) 171–182. https://doi.org/10.1158/0008-5472.CAN-18-1106.

[167] B. Weigelt, J.L. Peterse, L.J. Van't Veer, Breast cancer metastasis: markers and models, Nature Reviews Cancer 2005 5:8. 5 (2005) 591–602. https://doi.org/10.1038/nrc1670.

[168] D.S. Micalizzi, S.M. Farabaugh, H.L. Ford, Epithelial-Mesenchymal Transition in Cancer: Parallels Between Normal Development and Tumor Progression, Journal of Mammary Gland Biology and Neoplasia. 15 (2010) 117. https://doi.org/10.1007/S10911-010-9178-9.

[169] B.-T. Preca, K. Bajdak, K. Mock, W. Lehmann, V. Sundararajan, P. Bronsert, A. Matzge-Ogi, V. Orian-Rousseau, S. Brabletz, T. Brabletz, J. Maurer, M.P. Stemmler, B.-T. Preca, K. Bajdak, K. Mock, W. Lehmann, V. Sundararajan, P. Bronsert, A. Matzge-Ogi, V. Orian-Rousseau, S. Brabletz, T. Brabletz, J. Maurer, M.P. Stemmler, A novel ZEB1/HAS2 positive feedback loop promotes EMT in breast cancer, Oncotarget. 8 (2017) 11530–11543. https://doi.org/10.18632/ONCOTARGET.14563.

[170] H. Porsch, B. Bernert, M. Mehić, A.D. Theocharis, C.H. Heldin, P. Heldin, Efficient TGFβ-induced epithelial-mesenchymal transition depends on hyaluronan synthase HAS2, Oncogene. 32 (2013) 4355–4365. https://doi.org/10.1038/onc.2012.475.

[171] R.L. Brown, L.M. Reinke, M.S. Damerow, D. Perez, L.A. Chodosh, J. Yang, C. Cheng, CD44 splice isoform switching in human and mouse epithelium is essential for epithelial-mesenchymal transition and breast cancer progression, Journal of Clinical Investigation. 121 (2011) 1064–1074. https://doi.org/10.1172/JCI44540.

[172] K. Mima, H. Okabe, T. Ishimoto, H. Hayashi, S. Nakagawa, H. Kuroki, M. Watanabe, T. Beppu, M. Tamada, O. Nagano, H. Saya, H. Baba, CD44s Regulates the TGF-β–Mediated Mesenchymal Phenotype and Is Associated with Poor Prognosis in Patients with Hepatocellular Carcinoma, Cancer Research. 72 (2012) 3414–3423. https://doi.org/10.1158/0008-5472.CAN-12-0299.

[173] S. Zaman, R. Wang, V. Gandhi, Targeting the Apoptosis Pathway in Hematologic Malignancies, Leukemia & Lymphoma. 55 (2014) 1980. https://doi.org/10.3109/10428194.2013.855307.

[174] C.M. Pfeffer, A.T.K. Singh, Apoptosis: A Target for Anticancer Therapy, International Journal of Molecular Sciences. 19 (2018). https://doi.org/10.3390/IJMS19020448.

[175] L. Chen, L.Y.W. Bourguignon, Hyaluronan-CD44 interaction promotes c-Jun signaling and miRNA21 expression leading to Bcl-2 expression and chemoresistance in breast cancer cells, Molecular Cancer. 13 (2014) 1–13. https://doi.org/10.1186/1476-4598-13-52/FIGURES/6.

[176] J.M. Song, K. Molla, A. Anandharaj, I. Cornax, M. Gerard O'Sullivan, A.R. Kirtane, J. Panyam, F. Kassie, Triptolide suppresses the in vitro and in vivo growth of lung cancer cells by targeting hyaluronan-CD44/RHAMM signaling, Oncotarget. 8 (2017) 26927–26940. https://doi.org/10.18632/ONCOTARGET.15879.

[177] Y.J. Lee, S.A. Kim, S.H. Lee, Hyaluronan suppresses lidocaine-induced apoptosis of human chondrocytes in vitro by inhibiting the p53-dependent mitochondrial apoptotic pathway, Acta Pharmacologica Sinica 2016 37:5. 37 (2016) 664–673. https://doi.org/10.1038/aps.2015.151.

[178] S. Kumar, J.R. Inigo, R. Kumar, A.K. Chaudhary, J. O'Malley, S. Balachandar, J. Wang, K. Attwood, N. Yadav, S. Hochwald, X. Wang, D. Chandra, Nimbolide reduces CD44 positive cell population and induces mitochondrial apoptosis in pancreatic cancer cells, Cancer Letters. 413 (2018) 82–93. https://doi.org/10.1016/J.CANLET.2017.10.029.

[179] D. Vigetti, M. Rizzi, P. Moretto, S. Deleonibus, J.M. Dreyfuss, E. Karousou, M. Viola, M. Clerici, V.C. Hascall, M.F. Ramoni, G. de Luca, A. Passi, Glycosaminoglycans and Glucose Prevent Apoptosis in 4-Methylumbelliferone-treated Human Aortic Smooth Muscle Cells, The Journal of Biological Chemistry. 286 (2011) 34497. https://doi.org/10.1074/JBC.M111.266312.

[180] K. Ikuta, T. Ota, L. Zhuo, H. Urakawa, E. Kozawa, S. Hamada, K. Kimata, N. Ishiguro, Y. Nishida, Antitumor effects of 4-methylumbelliferone, a hyaluronan synthesis inhibitor, on malignant peripheral nerve sheath tumor, International Journal of Cancer. 140 (2017) 469–479. https://doi.org/10.1002/IJC.30460.

[181] H. Nagase, D. Kudo, A. Suto, E. Yoshida, S. Suto, M. Negishi, I. Kakizaki, K. Hakamada, 4-methylumbelliferone suppresses hyaluronan synthesis and tumor progression in SCID mice intra-abdominally inoculated with pancreatic cancer cells, Pancreas. 46 (2017) 190–197. https://doi.org/10.1097/MPA.0000000000000741.

[182] D.S. Morera, M.S. Hennig, A. Talukder, S.D. Lokeshwar, J. Wang, M. Garcia-Roig, N. Ortiz, T.J. Yates, L.E. Lopez, G. Kallifatidis, M.W. Kramer, A.R. Jordan, A.S. Merseburger, M. Manoharan, M.S. Soloway, M.K. Terris, V.B. Lokeshwar, Hyaluronic acid family in bladder cancer: potential prognostic biomarkers and therapeutic targets, British Journal of Cancer 2017 117:10. 117 (2017) 1507–1517. https://doi.org/10.1038/bjc.2017.318.

[183] W.E.I. Cao, L.E. Fang, S. Teng, H. Chen, T. Liu, Microrna-466 inhibits osteosarcoma cell proliferation and induces apoptosis by targeting ccnd1, Experimental and Therapeutic Medicine. 16 (2018) 5117–5122. https://doi.org/10.3892/ETM.2018.6888/HTML.

[184] Y. Jin, Z. Cui, X. Li, X. Jin, J. Peng, Y. Jin, Z. Cui, X. Li, X. Jin, J. Peng, Upregulation of long non-coding RNA PlncRNA-1 promotes proliferation and induces epithelial-mesenchymal transition in prostate cancer, Oncotarget. 8 (2017) 26090–26099. https://doi.org/10.18632/ONCOTARGET.15318.

[185] J. Li, M. Zhang, G. An, Q. Ma, LncRNA TUG1 acts as a tumor suppressor in human glioma by promoting cell apoptosis, Experimental Biology and Medicine. 241 (2016) 644. https://doi.org/10.1177/1535370215622708.

[186] J. Liu, F. Tu, W. Yao, X. Li, Z. Xie, H. Liu, Q. Li, Z. Pan, Conserved miR-26b enhances ovarian granulosa cell apoptosis through HAS2-HA-CD44-Caspase-3 pathway by targeting HAS2, Scientific Reports 2016 6:1. 6 (2016) 1–11. https://doi.org/10.1038/srep21197.

[187] T. Gebäck, M.M.P. Schulz, P. Koumoutsakos, M. Detmar, TScratch: a novel and simple software tool for automated analysis of monolayer wound healing assays, Https://Doi.Org/10.2144/000113083. 46 (2018) 265–274. https://doi.org/10.2144/000113083.

[188] C.A. Schneider, W.S. Rasband, K.W. Eliceiri, NIH Image to ImageJ: 25 years of image analysis, Nature Methods 2012 9:7. 9 (2012) 671–675. https://doi.org/10.1038/nmeth.2089.

[189] M. Rehmsmeier, P. Steffen, M. Höchsmann, R. Giegerich, Fast and effective prediction of microRNA/target duplexes, RNA (New York, N.Y.). 10 (2004) 1507–1517. https://doi.org/10.1261/RNA.5248604.

[190] D. Betel, A. Koppal, P. Agius, C. Sander, C. Leslie, Comprehensive modeling of microRNA targets predicts functional non-conserved and non-canonical sites, Genome Biology. 11 (2010) 1–14. https://doi.org/10.1186/GB-2010-11-8-R90/FIGURES/6.

[191] D. Betel, M. Wilson, A. Gabow, D.S. Marks, C. Sander, The microRNA.org resource: targets and expression, Nucleic Acids Research. 36 (2008). https://doi.org/10.1093/NAR/GKM995.

[192] M.D. Paraskevopoulou, G. Georgakilas, N. Kostoulas, I.S. Vlachos, T. Vergoulis, M. Reczko, C. Filippidis, T. Dalamagas, A.G. Hatzigeorgiou, DIANA-microT web server v5.0: service integration into miRNA functional analysis workflows, Nucleic Acids Research. 41 (2013). https://doi.org/10.1093/NAR/GKT393.

[193] M. Ghandi, F.W. Huang, J. Jané-Valbuena, G. v. Kryukov, C.C. Lo, E.R. McDonald, III, J. Barretina, E.T. Gelfand, C.M. Bielski, H. Li, K. Hu, A.Y. Andreev-Drakhlin, J. Kim, J.M. Hess, B.J. Haas, F. Aguet, B.A. Weir, M. v. Rothberg, B.R. Paolella, M.S. Lawrence, R. Akbani, Y. Lu, H.L. Tiv, P.C. Gokhale, A. de Weck, A.A. Mansour, C. Oh, J. Shih, K. Hadi, Y. Rosen, J. Bistline, K. Venkatesan, A. Reddy, D. Sonkin, M. Liu, J. Lehar, J.M. Korn, D.A. Porter, M.D. Jones, J. Golji, G. Caponigro, J.E. Taylor, C.M. Dunning, A.L. Creech, A.C. Warren, J.M. McFarland, M. Zamanighomi, A. Kauffmann, N. Stransky, M. Imielinski, Y.E. Maruvka, A.D. Cherniack, A. Tsherniak, F. Vazquez, J.D. Jaffe, A.A. Lane, D.M. Weinstock, C.M. Johannessen, M.P. Morrissey, F. Stegmeier, R. Schlegel, W.C. Hahn, G. Getz, G.B. Mills, J.S. Boehm, T.R. Golub, L.A. Garraway, W.R. Sellers, Next-generation characterization of the Cancer Cell Line Encyclopedia, Nature. 569 (2019) 503. https://doi.org/10.1038/S41586-019-1186-3.

[194] M. Ghandi, F.W. Huang, J. Jané-Valbuena, G. v. Kryukov, C.C. Lo, E.R. McDonald, J. Barretina, E.T. Gelfand, C.M. Bielski, H. Li, K. Hu, A.Y. Andreev-Drakhlin, J. Kim, J.M. Hess, B.J. Haas, F. Aguet, B.A. Weir, M. v. Rothberg, B.R. Paolella, M.S. Lawrence, R. Akbani, Y. Lu, H.L. Tiv, P.C. Gokhale, A. de Weck, A.A. Mansour, C. Oh, J. Shih, K. Hadi, Y. Rosen, J. Bistline, K. Venkatesan, A. Reddy, D. Sonkin, M. Liu, J. Lehar, J.M. Korn, D.A. Porter, M.D. Jones, J. Golji, G. Caponigro, J.E. Taylor, C.M. Dunning, A.L. Creech, A.C. Warren, J.M. McFarland, M. Zamanighomi, A. Kauffmann, N. Stransky, M. Imielinski, Y.E. Maruvka, A.D. Cherniack, A. Tsherniak, F. Vazquez, J.D. Jaffe, A.A. Lane, D.M. Weinstock, C.M. Johannessen, M.P. Morrissey, F. Stegmeier, R. Schlegel, W.C. Hahn, G. Getz, G.B. Mills, J.S. Boehm, T.R. Golub, L.A. Garraway, W.R. Sellers, Next-generation characterization of the Cancer Cell Line Encyclopedia, Nature 2019 569:7757. 569 (2019) 503–508. https://doi.org/10.1038/s41586-019-1186-3.

[195] D. Ribatti, R. Tamma, T. Annese, Epithelial-Mesenchymal Transition in Cancer: A Historical Overview, Translational Oncology. 13 (2020) 100773. https://doi.org/10.1016/J.TRANON.2020.100773.

[196] D. D'Angelo, P. Mussnich, R. Sepe, M. Raia, L. del Vecchio, P. Cappabianca, S. Pellecchia, S. Petrosino, S. Saggio, D. Solari, F. Fraggetta, A. Fusco, RPSAP52 lncRNA is overexpressed in pituitary tumors and promotes cell proliferation by acting as miRNA sponge for HMGA proteins, Journal of Molecular Medicine. 97 (2019) 1019–1032. https://doi.org/10.1007/S00109-019-01789-7/FIGURES/7.

[197] S. Chen, M. Wang, H. Yang, L. Mao, Q. He, H. Jin, Z. ming Ye, X. ying Luo, Y. peng Xia, B. Hu, LncRNA TUG1 sponges microRNA-9 to promote neurons apoptosis by up-regulated Bcl2l11 under ischemia, Biochemical and Biophysical Research Communications. 485 (2017) 167–173. https://doi.org/10.1016/J.BBRC.2017.02.043.

[198] F. Xu, J. Zhang, Long non-coding RNA HOTAIR functions as miRNA sponge to promote the epithelial to mesenchymal transition in esophageal cancer, Biomedicine & Pharmacotherapy. 90 (2017) 888–896. https://doi.org/10.1016/J.BIOPHA.2017.03.103.

[199] L. Zhou, X. Qi, J.A. Potashkin, F.W. Abdul-Karim, G.I. Gorodeski, MicroRNAs miR-186 and miR-150 down-regulate expression of the pro-apoptotic purinergic P2X7 receptor by activation of instability sites at the 3′-untranslated region of the gene that decrease steady-state levels of the transcript, Journal of Biological Chemistry. 283 (2008) 28274–28286. https://doi.org/10.1074/jbc.M802663200.

[200] Y. Yung, L. Ophir, G.M. Yerushalmi, M. Baum, A. Hourvitz, E. Maman, HAS2-AS1 is a novel LH/hCG target gene regulating HAS2 expression and enhancing cumulus cells migration, Journal of Ovarian Research. 12 (2019) 21. https://doi.org/10.1186/s13048-019-0495-3.

[201] X. Yang, F. Qi, S. Wei, L. Lin, X. Liu, The Transcription Factor C/EBPβ Promotes HFL-1 Cell Migration, Proliferation, and Inflammation by Activating lncRNA HAS2-AS1 in Hypoxia, Frontiers in Cell and Developmental Biology. 9 (2021) 651913. https://doi.org/10.3389/FCELL.2021.651913.

[202] J.B. Pierce, M.W. Feinberg, Long Noncoding RNAs in Atherosclerosis and Vascular Injury, Arteriosclerosis, Thrombosis, and Vascular Biology. 40 (2020) 2002–2017. https://doi.org/10.1161/ATVBAHA.120.314222.

[203] M.D. Ballantyne, K. Pinel, R. Dakin, A.T. Vesey, L. Diver, R. Mackenzie, R. Garcia, P. Welsh, N. Sattar, G. Hamilton, N. Joshi, M.R. Dweck, J.M. Miano, M.W. McBride, D.E. Newby, R.A. McDonald, A.H. Baker, Smooth Muscle Enriched Long Noncoding RNA (SMILR) Regulates Cell Proliferation, Circulation. 133 (2016) 2050. https://doi.org/10.1161/CIRCULATIONAHA.115.021019.

[204] Z. Zhao, T. Liang, S. Feng, Silencing of HAS2-AS1 mediates PI3K/AKT signaling pathway to inhibit cell proliferation, migration, and invasion in glioma, Journal of Cellular Biochemistry. 120 (2019) 11510–11516. https://doi.org/10.1002/JCB.28430.

[205] P. Sun, L. Sun, J. Cui, L. Liu, Q. He, Long noncoding RNA HAS2-AS1 accelerates non-small cell lung cancer chemotherapy resistance by targeting LSD1/EphB3 pathway., American Journal of Translational Research. 12 (2020) 950–958. http://www.ncbi.nlm.nih.gov/pubmed/32269726 (accessed December 2, 2020).

[206] H. Hugo, M.L. Ackland, T. Blick, M.G. Lawrence, J.A. Clements, E.D. Williams, E.W. Thompson, Epithelial—mesenchymal and mesenchymal—epithelial transitions in carcinoma progression, Journal of Cellular Physiology. 213 (2007) 374–383. https://doi.org/10.1002/JCP.21223.

[207] C.M. Nelson, D. Khauv, M.J. Bissell, D.C. Radisky, Change in Cell Shape Is Required for Matrix Metalloproteinase-Induced Epithelial-Mesenchymal Transition of Mammary Epithelial Cells, Journal of Cellular Biochemistry. 105 (2008) 25. https://doi.org/10.1002/JCB.21821.

[208] C.H. Heldin, M. Vanlandewijck, A. Moustakas, Regulation of EMT by TGFβ in cancer, FEBS Letters. 586 (2012) 1959–1970. https://doi.org/10.1016/J.FEBSLET.2012.02.037.

[209] J. Wang, J. Gu, A. You, J. Li, Y. Zhang, G. Rao, X. Ge, K. Zhang, J. Li, X. Liu, Q. Wang, T. Lin, L. Cheng, M. Zhu, X. Wu, D. Wang, The transcription factor USF1 promotes glioma cell invasion and migration by activating lncRNA HAS2-AS1, Bioscience Reports. 40 (2020). https://doi.org/10.1042/BSR20200487.

[210] S. Thuault, U. Valcourt, M. Petersen, G. Manfioletti, C.H. Heldin, A. Moustakas, Transforming growth factor-β employs HMGA2 to elicit epithelial–mesenchymal transition, Journal of Cell Biology. 174 (2006) 175–183. https://doi.org/10.1083/JCB.200512110.

[211] S. Thuault, E.J. Tan, H. Peinado, A. Cano, C.H. Heldin, A. Moustakas, HMGA2 and Smads Co-regulate SNAIL1 Expression during Induction of Epithelial-to-Mesenchymal Transition, Journal of Biological Chemistry. 283 (2008) 33437–33446. https://doi.org/10.1074/JBC.M802016200.

[212] J.M.V. Louderbough, J.A. Schroeder, Understanding the dual nature of CD44 in breast cancer progression, Molecular Cancer Research : MCR. 9 (2011) 1573–1586. https://doi.org/10.1158/1541-7786.MCR-11-0156.

[213] A. Afify, P. Purnell, L. Nguyen, Role of CD44s and CD44v6 on human breast cancer cell adhesion, migration, and invasion, Experimental and Molecular Pathology. 86 (2009) 95–100. https://doi.org/10.1016/J.YEXMP.2008.12.003.

[214] A. Ouhtit, Z.Y. Abd Elmageed, M.E. Abdraboh, T.F. Lioe, M.H.G. Raj, In Vivo Evidence for the Role of CD44s in Promoting Breast Cancer Metastasis to the Liver, The American Journal of Pathology. 171 (2007) 2033. https://doi.org/10.2353/AJPATH.2007.070535.

[215] A. Parnigoni, I. Caon, P. Moretto, M. Viola, E. Karousou, A. Passi, D. Vigetti, The role of the multifaceted long non-coding RNAs: A nuclear-cytosolic interplay to regulate hyaluronan metabolism, Matrix Biology Plus. (2021) 100060. https://doi.org/10.1016/j.mbplus.2021.100060.

[216] R.M. Melero-Fernandez de Mera, U.T. Arasu, R. Kärnä, S. Oikari, K. Rilla, D. Vigetti, A. Passi, P. Heldin, M.I. Tammi, A.J. Deen, Effects of mutations in the post-translational modification sites on the trafficking of hyaluronan synthase 2 (HAS2), Matrix Biology. 80 (2019) 85–103. https://doi.org/10.1016/j.matbio.2018.10.004.

[217] R.H. Tammi, A.G. Passi, K. Rilla, E. Karousou, D. Vigetti, K. Makkonen, M.I. Tammi, Transcriptional and post-translational regulation of hyaluronan synthesis, FEBS Journal. 278 (2011) 1419–1428. https://doi.org/10.1111/j.1742-4658.2011.08070.x.

[218] S. Misra, P. Heldin, V.C. Hascall, N.K. Karamanos, S.S. Skandalis, R.R. Markwald, S. Ghatak, HA/CD44 interactions as potential targets for cancer therapy, The FEBS Journal. 278 (2011) 1429. https://doi.org/10.1111/J.1742-4658.2011.08071.X.

[219] K. Saavalainen, S. Pasonen-Seppänen, T.W. Dunlop, R. Tammi, M.I. Tammi, C. Carlberg, The Human Hyaluronan Synthase 2 Gene Is a Primary Retinoic Acid and Epidermal Growth Factor Responding Gene, Journal of Biological Chemistry. 280 (2005) 14636–14644. https://doi.org/10.1074/JBC.M500206200.

[220] F. Yang, S. Lyu, S. Dong, Y. Liu, X. Zhang, O. Wang, Expression profile analysis of long noncoding RNA in HER-2-enriched subtype breast cancer by next-generation sequencing and bioinformatics, OncoTargets and Therapy. 9 (2016) 761–772. https://doi.org/10.2147/OTT.S97664.

[221] X. Shen, B. Xie, Z. Ma, W. Yu, W. Wang, D. Xu, X. Yan, B. Chen, L. Yu, J. Li, X. Chen, K. Ding, F. Cao, Identification of novel long non-coding RNAs in triple-negative breast cancer, Oncotarget. 6 (2015) 21730. https://doi.org/10.18632/ONCOTARGET.4419.

[222] Y. Yamaguchi, H. Yamamoto, Y. Tobisawa, F. Irie, TMEM2: A missing link in hyaluronan catabolism identified?, Matrix Biology. 78–79 (2019) 139–146. https://doi.org/10.1016/J.MATBIO.2018.03.020.

[223] M. Farooqui, L.R. Bohrer, N.J. Brady, P. Chuntova, S.E. Kemp, C.T. Wardwell, A.C. Nelson, K.L. Schwertfeger, Epiregulin contributes to breast tumorigenesis through regulating matrix metalloproteinase 1 and promoting cell survival, Molecular Cancer. 14 (2015). https://doi.org/10.1186/S12943-015-0408-Z.

[224] S.J. Prest, F.E.B. May, B.R. Westley, The estrogen-regulated protein, TFF1, stimulates migration of human breast cancer cells, The FASEB Journal. 16 (2002) 592–594. https://doi.org/10.1096/FJ.01-0498FJE.

[225] Y. Teng, H. Qin, A. Bahassan, N.G. Bendzunas, E.J. Kennedy, J. Cowell, The WASF3-NCKAP1-CYFIP1 complex is essential for breast cancer metastasis, Cancer Research. 76 (2016) 5133. https://doi.org/10.1158/0008-5472.CAN-16-0562.

[226] Y. Bai, Y. Zhan, B. Yu, W.-W. Wang, L. Wang, J. Zhou, R. Chen, F. Zhang, X. Zhao, W. Duan, Y. Wang, J. Liu, J. Bao, Z.-Y. Zhang, X. Liu, A Novel Tumor-Suppressor, CDH18, Inhibits Glioma Cell Invasiveness Via UQCRC2 and Correlates with the Prognosis of Glioma Patients, Cellular Physiology and Biochemistry. 48 (2018) 1755–1770. https://doi.org/10.1159/000492317.

[227] W. Zhu, L. Wei, H. Zhang, J. Chen, X. Qin, Oncolytic adenovirus armed with IL-24 Inhibits the growth of breast cancer in vitro and in vivo, Journal of Experimental & Clinical Cancer Research : CR. 31 (2012) 51. https://doi.org/10.1186/1756-9966-31-51.

[228] M. Zheng, D. Bocangel, B. Doneske, A. Mhashilkar, R. Ramesh, K.K. Hunt, S. Ekmekcioglu, R.B. Sutton, N. Poindexter, E.A. Grimm, S. Chada, Human interleukin 24 (MDA-7/IL-24) protein kills breast cancer cells via the IL-20 receptor and is antagonized by IL-10, Cancer Immunology, Immunotherapy 2006 56:2. 56 (2006) 205–215. https://doi.org/10.1007/S00262-006-0175-1.

[229] C. Yang, Y. Tong, W. Ni, J. Liu, W. Xu, L. Li, X. Liu, H. Meng, W. Qian, Inhibition of autophagy induced by overexpression of mda-7/interleukin-24 strongly augments the antileukemia activity in vitro and in vivo, Cancer Gene Therapy 2010 17:2. 17 (2009) 109–119. https://doi.org/10.1038/cgt.2009.57.

[230] S. Kohsaka, K. Hinohara, L. Wang, T. Nishimura, M. Urushido, K. Yachi, M. Tsuda, M. Tanino, T. Kimura, H. Nishihara, N. Gotoh, S. Tanaka, Epiregulin enhances tumorigenicity by activating the ERK/MAPK pathway in glioblastoma, Neuro-Oncology. 16 (2014) 960. https://doi.org/10.1093/NEUONC/NOT315.

[231] N. Sunaga, K. Kaira, H. Imai, K. Shimizu, T. Nakano, D.S. Shames, L. Girard, J. Soh, M. Sato, Y. Iwasaki, T. Ishizuka, A.F. Gazdar, J.D. Minna, M. Mori, Oncogenic KRAS-induced epiregulin overexpression contributes to aggressive phenotype and is a promising therapeutic target in non-small-cell lung cancer, Oncogene. 32 (2013) 4034. https://doi.org/10.1038/ONC.2012.402.

[232] D.J. Riese, R.L. Cullum, Epiregulin: Roles in Normal Physiology and Cancer, Seminars in Cell & Developmental Biology. 0 (2014) 49. https://doi.org/10.1016/J.SEMCDB.2014.03.005.

[233] N. Sunaga, K. Kaira, Epiregulin as a therapeutic target in non-small-cell lung cancer, Lung Cancer. 6 (2015) 91. https://doi.org/10.2147/LCTT.S60427.

[234] G. Auf, A. Jabouille, M. Delugin, S. Guérit, R. Pineau, S. North, N. Platonova, M. Maitre, A. Favereaux, P. Vajkoczy, M. Seno, A. Bikfalvi, D. Minchenko, O. Minchenko, M. Moenner, High epiregulin expression in human U87 glioma cells relies on IRE1α and promotes autocrine growth through EGF receptor, BMC Cancer. 13 (2013) 1–12. https://doi.org/10.1186/1471-2407-13-597/FIGURES/7.

[235] L.J. Martin, S.B. Smith, A. Khoutorsky, C.A. Magnussen, A. Samoshkin, R.E. Sorge, C. Cho, N. Yosefpour, S. Sivaselvachandran, S. Tohyama, T. Cole, T.M. Khuong, E. Mir, D.G. Gibson, J.S. Wieskopf, S.G. Sotocinal, J.S. Austin, C.B. Meloto, J.H. Gitt, C. Gkogkas, N. Sonenberg, J.D. Greenspan, R.B. Fillingim, R. Ohrbach, G.D. Slade, C. Knott, R. Dubner, A.G. Nackley, A. Ribeiro-Da-Silva, G.G. Neely, W. Maixner, D. v. Zaykin, J.S. Mogil, L. Diatchenko, Epiregulin and EGFR interactions are involved in pain processing, The Journal of Clinical Investigation. 127 (2017) 3353. https://doi.org/10.1172/JCI87406.

[236] J. Brugarolas, C. Chandrasekaran, J.I. Gordon, D. Beach, T. Jacks, G.J. Hannon, Radiation-induced cell cycle arrest compromised by p21 deficiency, Nature. 377 (1995) 552–557. https://doi.org/10.1038/377552A0.

[237] I.B. Roninson, Oncogenic functions of tumour suppressor p21Waf1/Cip1/Sdi1: association with cell senescence and tumour-promoting activities of stromal fibroblasts, Cancer Letters. 179 (2002) 1–14. https://doi.org/10.1016/S0304-3835(01)00847-3.

[238] K. Yang, M. Hitomi, D.W. Stacey, Variations in cyclin D1 levels through the cell cycle determine the proliferative fate of a cell, Cell Division. 1 (2006) 32. https://doi.org/10.1186/1747-1028-1-32.

[239] M. Dai, A.A. Al-Odaini, N. Fils-Aimé, M.A. Villatoro, J. Guo, A. Arakelian, S.A. Rabbani, S. Ali, J.J. Lebrun, Cyclin D1 cooperates with p21 to regulate TGFβ-mediated breast cancer cell migration and tumor local invasion, Breast Cancer Research : BCR. 15 (2013) R49. https://doi.org/10.1186/BCR3441.

[240] S. Fulda, K.M. Debatin, Extrinsic versus intrinsic apoptosis pathways in anticancer chemotherapy, Oncogene 2006 25:34. 25 (2006) 4798–4811. https://doi.org/10.1038/sj.onc.1209608.

[241] A.C. Crawford, R.B. Riggins, A.N. Shajahan, A. Zwart, R. Clarke, Co-Inhibition of BCL-W and BCL2 Restores Antiestrogen Sensitivity through BECN1 and Promotes an Autophagy-Associated Necrosis, PLoS ONE. 5 (2010) 8604. https://doi.org/10.1371/JOURNAL.PONE.0008604.

[242] A. Crawford, R. Nahta, Targeting Bcl-2 in Herceptin-Resistant Breast Cancer Cell Lines, Current Pharmacogenomics and Personalized Medicine. 9 (2011) 184. https://doi.org/10.2174/187569211796957584.

[243] C. Teixeira, J.C. Reed, M.A.C. Pratt, Estrogen Promotes Chemotherapeutic Drug Resistance by a Mechanism Involving Bcl-2 Proto-Oncogene Expression in Human Breast Cancer Cells, Cancer Research. 55 (1995).

[244] L. Salmena, L. Poliseno, Y. Tay, L. Kats, P.P. Pandolfi, A ceRNA hypothesis: The rosetta stone of a hidden RNA language?, Cell. 146 (2011) 353–358. https://doi.org/10.1016/j.cell.2011.07.014.

[245] Y. Lu, G. Guo, R. Hong, X. Chen, Y. Sun, F. Liu, Z. Zhang, X. Jin, J. Dong, K. Yu, X. Yang, Y. Nan, Q. Huang, LncRNA HAS2-AS1 Promotes Glioblastoma Proliferation by Sponging miR-137, Frontiers in Oncology. 11 (2021) 634893. https://doi.org/10.3389/FONC.2021.634893.

[246] F. Kern, J. Amand, I. Senatorov, A. Isakova, C. Backes, E. Meese, A. Keller, T. Fehlmann, miRSwitch: detecting microRNA arm shift and switch events, Nucleic Acids Research. 48 (2020) W268–W274. https://doi.org/10.1093/NAR/GKAA323.

[247] L. Chen, H. Sun, C. Wang, Y. Yang, M. Zhang, G. Wong, miRNA arm switching identifies novel tumour biomarkers, EBioMedicine. 38 (2018) 37–46. https://doi.org/10.1016/J.EBIOM.2018.11.003.

[248] S.C. Li, Y.L. Liao, M.R. Ho, K.W. Tsai, C.H. Lai, W.C. Lin, MiRNA arm selection and isomiR distribution in gastric cancer, Series on Advances in Bioinformatics and Computational Biology. 13 (2012) 1–10. https://doi.org/10.1186/1471-2164-13-S1-S13/FIGURES/4.

[249] Z. Wang, H.H. Sha, H.J. Li, Functions and mechanisms of miR-186 in human cancer, Biomedicine & Pharmacotherapy. 119 (2019) 109428. https://doi.org/10.1016/J.BIOPHA.2019.109428.

[250] X. Lu, X. Song, X. Hao, X. Liu, X. Zhang, N. Yuan, H. Ma, Z. Zhang, MicroRNA-186-3p attenuates tumorigenesis of cervical cancer by targeting MCM2, Oncology Letters. 22 (2021) 1–12. https://doi.org/10.3892/OL.2021.12800/HTML.

[251] Y. Dong, X. Jin, Z. Sun, Y. Zhao, X. Song, MiR-186 Inhibited Migration of NSCLC via Targeting cdc42 and Effecting EMT Process, Molecules and Cells. 40 (2017) 195. https://doi.org/10.14348/MOLCELLS.2017.2291.

[252] M. He, Q. Jin, C. Chen, Y. Liu, X. Ye, Y. Jiang, F. Ji, H. Qian, D. Gan, S. Yue, W. Zhu, T. Chen, The miR-186-3p/EREG axis orchestrates tamoxifen resistance and aerobic glycolysis in breast cancer cells, Oncogene 2019 38:28. 38 (2019) 5551–5565. https://doi.org/10.1038/s41388-019-0817-3.

LIST OF PUBBLICATIONS

- Parnigoni A, Caon I, Moretto P, Viola M, Karousou E, Passi A, Vigetti D. The role of the multifaceted long non-coding RNAs: A nuclear-cytosolic interplay to regulate hyaluronan metabolism. Matrix Biol Plus. 2021 Mar 4;11:100060.

- Marozzi M*, Parnigoni A*, Negri A*, Viola M, Vigetti D, Passi A, Karousou E, Rizzi F. Inflammation, Extracellular Matrix Remodeling, and Proteostasis in Tumor Microenvironment. Int J Mol Sci. 2021 Jul 28;22(15):8102.

- Caravà E, Moretto P, Caon I, Parnigoni A, Passi A, Karousou E, Vigetti D, Canino J, Canobbio I, Viola M. HA and HS Changes in Endothelial Inflammatory Activation. Biomolecules. 2021 May 29;11(6):809.

- Caon I, D'Angelo ML, Bartolini B, Caravà E, Parnigoni A, Contino F, Cancemi P, Moretto P, Karamanos NK, Passi A, Vigetti D, Karousou E, Viola M. The Secreted Protein C10orf118 Is a New Regulator of Hyaluronan Synthesis Involved in Tumour-Stroma Cross-Talk. Cancers (Basel). 2021 Mar 5;13(5):1105.

- Vitale DL, Caon I, Parnigoni A, Sevic I, Spinelli FM, Icardi A, Passi A, Vigetti D, Alaniz L. Initial Identification of UDP-Glucose Dehydrogenase as a Prognostic Marker in Breast Cancer Patients, Which Facilitates Epirubicin Resistance and Regulates Hyaluronan Synthesis in MDA-MB-231 Cells. Biomolecules. 2021 Feb 9;11(2):246.

- Caon I, Parnigoni A, Viola M, Karousou E, Passi A, Vigetti D. Cell Energy Metabolism and Hyaluronan Synthesis. J Histochem Cytochem. 2021 Jan;69(1):35-47.

- Bartolini B, Caravà E, Caon I, Parnigoni A, Moretto P, Passi A, Vigetti D, Viola M, Karousou E. Heparan Sulfate in the Tumor Microenvironment. Adv Exp Med Biol. 2020;1245:147-161.

- Caon I, Bartolini B, Moretto P, Parnigoni A, Caravà E, Vitale DL, Alaniz L, Viola M, Karousou E, De Luca G, Hascall VC, Passi A, Vigetti D. Sirtuin 1 reduces hyaluronan synthase 2 expression by inhibiting nuclear translocation of NF-κB and expression of the long-noncoding RNA HAS2-AS1. J Biol Chem. 2020 Mar 13;295(11):3485-3496.

- Caon I, Bartolini B, Parnigoni A, Caravà E, Moretto P, Viola M, Karousou E, Vigetti D, Passi A. Revisiting the hallmarks of cancer: The role of hyaluronan. Semin Cancer Biol. 2020 May;62:9-19.